

การสังเคราะห์ไดเมทิลอีเทอร์จากเมทานอลบนตัวเร่งปฏิกิริยา H-ZSM-5

นายศราวุธ ศรีนันทวงษ์

วิทยานิพนธ์นี้เป็นส่วนหนึ่งของการศึกษาตามหลักสูตรปริญญาวิศวกรรมศาสตรมหาบัณฑิต

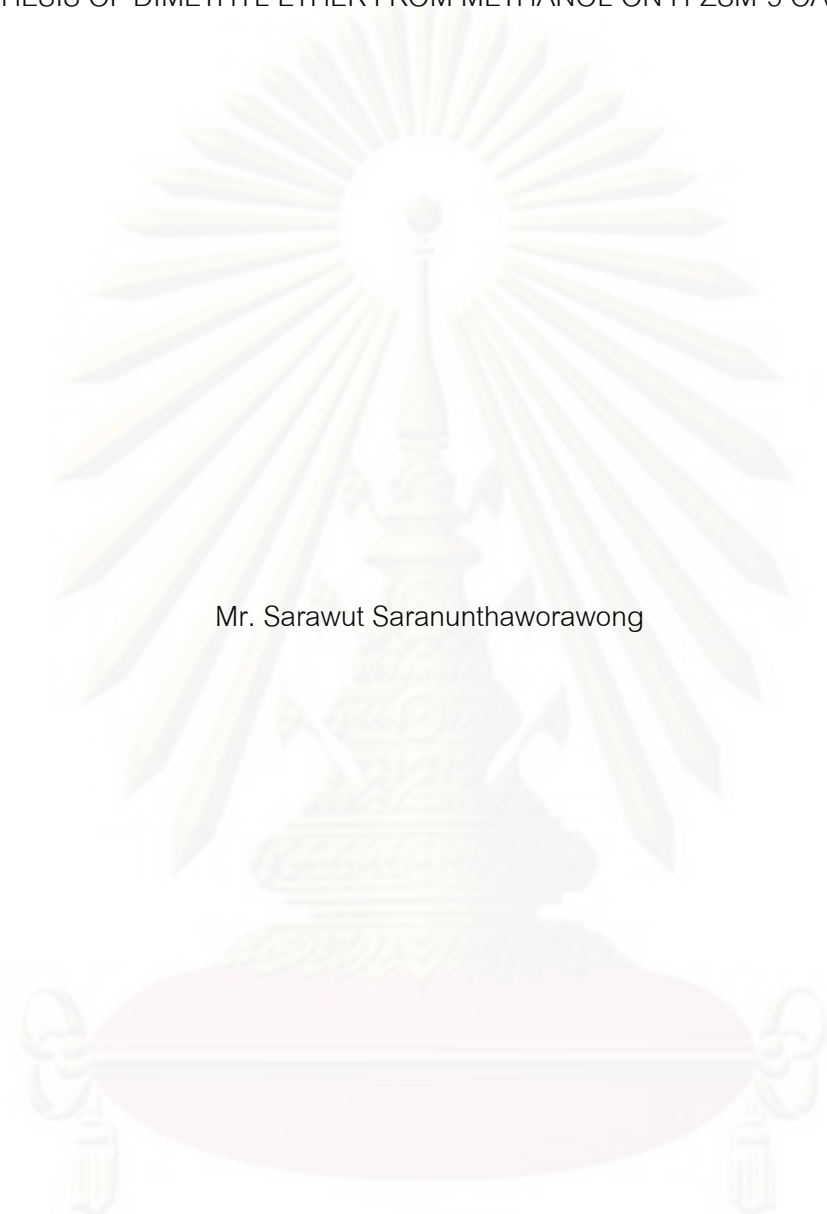
สาขาวิชาวิศวกรรมเคมี ภาควิชาวิศวกรรมเคมี

คณะวิศวกรรมศาสตร์ จุฬาลงกรณ์มหาวิทยาลัย

ปีการศึกษา 2552

ลิขสิทธิ์ของจุฬาลงกรณ์มหาวิทยาลัย

SYNTHESIS OF DIMETHYL ETHER FROM METHANOL ON H-ZSM-5 CATALYST



Mr. Sarawut Saranunthaworawong

A Thesis Submitted in Partial Fulfillment of the Requirements  
for the Degree of Master of Engineering Program in Chemical Engineering

Department of Chemical Engineering

Faculty of Engineering

Chulalongkorn University

Academic Year 2009

Copyright of Chulalongkorn University





ศราวุธ ศรานันทรวงศ์: การสังเคราะห์ไดเมทิลอีเทอร์จากเมทานอลบนตัวเร่งปฏิกิริยา H-ZSM-5 (SYNTHESIS OF DIMETHYL ETHER FROM METHANOL ON H-ZSM-5 CATALYST) อ.ที่ปริกษาวิทยานิพนธ์หลัก: ผศ.ดร. สุพจน์ พัฒนะศรี, 98 หน้า.

งานวิจัยนี้มีวัตถุประสงค์เพื่อศึกษาทำความเข้าใจถึงปฏิกิริยาการขจัดน้ำของเมทานอลเพื่อให้ได้ ไดเมทิลอีเทอร์ โดยมุ่งเน้นในการใช้ตัวเร่งปฏิกิริยาประเภทซีโอไลท์ ในที่นี้คือตัวเร่งปฏิกิริยา ZSM-5 อีกทั้งยังได้ทำการศึกษาถึงผลกระทบของอัตราส่วนซิลิกอนต่ออะลูมิเนียมและขนาดอนุภาคของตัวเร่งปฏิกิริยา ZSM-5 ที่มีต่อประสิทธิภาพของตัวเร่งปฏิกิริยาในการสังเคราะห์ไดเมทิลอีเทอร์ จากการทดสอบปฏิกิริยาการขจัดน้ำของเมทานอลในช่วงอุณหภูมิ 100 - 300 องศาเซลเซียส ที่ความดันบรรยากาศ พบว่าตัวเร่งปฏิกิริยาที่มีค่าอัตราส่วนซิลิกอนต่ออะลูมิเนียมต่ำกว่าจะให้ค่าการเลือกเกิดเป็นไดเมทิลอีเทอร์สูงกว่าตัวเร่งปฏิกิริยาที่มีค่าอัตราส่วนซิลิกอนต่ออะลูมิเนียมสูง ซึ่งจากผลการทดลองเห็นได้ว่าประสิทธิภาพในการผลิตไดเมทิลอีเทอร์นั้นขึ้นอยู่กับความเป็นกรดของตัวเร่งปฏิกิริยา นอกจากนี้พบว่าไดเมทิลอีเทอร์เกิดได้ดีที่อุณหภูมิสูงมากกว่าที่อุณหภูมิต่ำในช่วงอุณหภูมิที่ทำการศึกษา และเมื่อทำการเพิ่มระยะเวลาในการตกผลึกในขั้นตอนการเตรียมตัวเร่งปฏิกิริยาแสดงให้เห็นได้ว่าขนาดอนุภาคของตัวเร่งปฏิกิริยามีขนาดเล็กลง และเมื่อทำการทดสอบปฏิกิริยาการขจัดน้ำของเมทานอลพบว่าตัวเร่งปฏิกิริยาที่มีขนาดอนุภาคเล็กมีประสิทธิภาพสูงกว่าตัวเร่งปฏิกิริยาที่มีขนาดอนุภาคใหญ่ จากนั้นได้ทำการศึกษาผลกระทบของความเป็นผลึกของตัวเร่งปฏิกิริยา ZSM-5 ที่มีต่อปฏิกิริยาการขจัดน้ำของเมทานอล ซึ่งพบว่าตัวเร่งปฏิกิริยา ZSM-5 ที่มีค่าความเป็นผลึกที่เหมาะสมนั้นจะส่งผลดีต่อปฏิกิริยาการขจัดน้ำของเมทานอล

ภาควิชา.....วิศวกรรมเคมี.....ลายมือชื่อนิสิต.....ศราวุธ ศรานันทรวงศ์.....  
 สาขาวิชา.....วิศวกรรมเคมี.....ลายมือชื่อ อ.ที่ปริกษาวิทยานิพนธ์หลัก.....  
 ปีการศึกษา.....2552.....

# # 4970592621 : MAJOR CHEMICAL ENGINEERING

KEYWORDS: ZSM-5 / DME / METHANOL/ DEHYDRATION / Si/Al RATIO/  
PARTICLE SIZE.

SARAWUT SARANUNTHAWORAWONG: SYNTHESIS OF DIMETHYL  
ETHER FROM METHANOL ON H-ZSM-5 CATALYST. THESIS ADVISOR:  
ASST. PROF. SUPHOT PHATANASRI, Ph.D., 98 pp.

The objectives of this work are the study for understanding methanol dehydration reaction for produce dimethyl ether. By emphasize, the usage zeolite catalysts which in this work was ZSM-5 catalyst. Moreover, in this experiment was divided in two parts that the first was effect of Si/Al atomic ratios and second was effect of particle sizes on dimethyl ether generate performance of zeolite catalysts. From methanol dehydration reaction test with in the temperature range 100 – 300 °C and atmospheric pressure, found that, the zeolite catalyst had lower the value of Si/Al ratio that dimethyl ether selectivity was higher than zeolite catalyst had higher the value of Si/Al ratio. The result show that, performance of dimethyl ether generate depend on the acidity of zeolite catalyst. Moreover, found that in temperature range, At the high temperature that dimethyl ether selectivity was higher than low temperature. And then, when expansion the crystallization time of zeolite catalyst preparation that can observed the smaller particle size of zeolite catalyst. When test methanol dehydration reaction, the smaller particle size of zeolite catalyst performance better than the bigger particle size. And then, investigation about effect of crystallinity of ZSM-5 zeolite catalysts on methanol dehydration found that the optimum crystallinity of ZSM-5 zeolite catalyst is beneficial for catalytic performance.

Department:.....Chemical Engineering..... Student's Signature Sarawut Saranunthaworawong

Field of Study:....Chemical Engineering.....Advisor's Signature Suphot Phatanasri

Academic Year : .....2009.....



## ACKNOWLEDGEMENTS

The author would like to express his greatest gratitude to his advisor, Assistant Professor Suphot Phatanasri, for his useful discussion, invaluable suggestions and warm encouragement throughout this study. Moreover, he wishes to give his grateful to Professor Piyasan Prasertdam, as the chairman and Assistant Professor Montree Wongsri, Dr. Pornsawan Assawasaengrat and Assistant Professor Bunjerd Jongsomjit as the member of the thesis committee. Gratefulness for the financial support of the Department of Chemical Engineering of Chulalongkorn University.

Furthermore, the author would like to express his highest gratitude to his parents especially Miss Sasithorn Nugulaur-am-roong who always give her the biggest willpower to the author for all times.

Finally, the author wishes to thankful the members of the Center of Excellence on Catalysis Reaction Engineering, Department of Chemical Engineering, faculty of Engineering, Chulalongkorn University.



ศูนย์วิจัยทรัพยากร  
จุฬาลงกรณ์มหาวิทยาลัย

# CONTENTS

	Page
<b>ABSTRACT (IN THAI)</b> .....	iv
<b>ABSTRACT (IN ENGLISH)</b> .....	v
<b>ACKNOWLEDGEMENTS</b> .....	vi
<b>CONTENTS</b> .....	vii
<b>LIST OF TABLES</b> .....	x
<b>LIST OF FIGURES</b> .....	xi
<b>CHAPTER I INTRODUCTION</b> .....	1
<b>CHAPTER II LITERATURE REVIEWS</b> .....	5
<b>CHAPTER III THEORY</b> .....	7
3.1 Zeolite.....	7
3.2 The structure of zeolite.....	8
3.3 Category of zeolite.....	11
3.4 Zeolite active sites.....	18
3.4.1 Acid sites.....	18
3.4.2 Generation of acid centers.....	19
3.4.3 Acidity of metallosilicate.....	23
3.5 Shape selective.....	23
3.6 Zeolite synthesis.....	25
3.7 Dimethyl ether (DME).....	26
3.8 Olefins.....	27
3.9 Reaction mechanism of methanol to DME and hydrocarbons.....	28
<b>CHAPTER IV EXPERIMENTAL</b> .....	30
4.1 Catalyst preparation.....	30
4.1.1 Chemicals.....	30
4.1.2 Preparation of Na-ZSM-5(MFI).....	30
4.1.2.1 Preparation of gel precipitation and decantation Solution.....	33
4.1.2.2 Crystallization.....	33
4.1.2.3 Calcination.....	34
4.1.2.4 NH <sub>4</sub> - and H- form ZSM-5.....	34

4.2	Pretreatment condition.....	35
4.3	Characterization.....	35
4.3.1	Powder X-ray diffraction analysis (XRD).....	35
4.3.2	X-Ray Fluorescence analysis (XRF).....	36
4.3.3	BET surface area measurement.....	36
4.3.4	Scanning Electron Microscopy (SEM).....	36
4.3.5	Temperature Programmed Adsorptions of Ammonia (NH <sub>3</sub> -TPD).....	37
4.4	Reaction testing.....	37
4.4.1	Chemicals and reagents.....	37
4.4.2	Instruments and apparatus.....	37
4.4.3	Reaction method.....	39
<b>CHAPTER V RESULTS AND DISCUSSION.....</b>		<b>41</b>
5.1	Effect of Si/Al ratios and reaction temperature on methanol dehydration.....	41
5.1.1	Catalyst characterization.....	41
5.1.1.1	X- Ray Diffraction Pattern.....	41
5.1.1.2	Chemical composition.....	44
5.1.1.3	Scanning Electron Microscopy.....	44
5.1.1.4	BET surface area.....	46
5.1.1.5	Temperature Programmed Adsorptions of Ammonia (NH <sub>3</sub> -TPD).....	47
5.1.2	Catalytic reaction.....	48
5.2	Effect of particle size on methanol dehydration.....	52
5.2.1	Catalyst Characterization.....	53
5.2.1.1	X- Ray Diffraction Pattern.....	53
5.2.1.2	Morphology.....	54
5.2.1.3	BET surface area.....	55
5.2.1.4	Temperature Programmed Adsorptions of Ammonia (NH <sub>3</sub> -TPD).....	56
5.2.2	Catalytic reaction.....	57

5.3	Effect of crystallinity of H-ZSM-5 zeolite catalyst on methanol dehydration.....	58
5.3.1	Catalyst characterization.....	59
5.3.1.1	X- Ray Diffraction Pattern.....	59
5.3.1.2	BET surface area.....	62
5.3.1.3	Temperature Programmed Adsorptions of Ammonia (NH <sub>3</sub> -TPD).....	63
5.3.2	Catalytic reaction.....	67
<b>CHAPTER VI CONCLUSIONS AND RECOMMENDATIONS.....</b>		<b>77</b>
6.1	Conclusions.....	77
6.2	Recommendations.....	78
<b>REFERENCES.....</b>		<b>79</b>
<b>APPENDICES.....</b>		<b>82</b>
APPENDIX A. CALCULATION OF Si/Al ATOMIC RATIO FOR ZSM-5.....		83
APPENDIX B. CALCULATION OF GAS VELOCITY.....		84
APPENDIX C. CALCULATION OF TEMPERATURE OF METHANOL.....		85
APPENDIX D. CALCULATION OF Si/Al ATOMIC RATIO.....		86
APPENDIX E. CALCULATION FOR CONVERSION OF METHANOL & SELECTIVITY OF DME.....		87
APPENDIX F. CALCULATION OF % CRYSTALLINITY.....		88
APPENDIX G. CALCULATION FOR PARTICL SIZE.....		89
APPENDIX H. CALIBRATION CURVES.....		90
APPENDIX I. CALCULATION OF ACIDITY.....		96
APPENDIX J. LIST OF PUBLICATION.....		97
<b>VITA.....</b>		<b>98</b>



## LIST OF TABLES

Table	Page
3.1 Structural characteristics of selected zeolites .....	13
4.1 The chemicals used in the catalyst preparation .....	30
4.2 Reagents used for the preparation of Na-ZSM-5: Si/Al = 50.....	31
4.3 Operating condition for gas chromatograph .....	37
5.1 Crystallinity of H-ZSM-5 zeolite catalyst with different Si/Al ratios..	44
5.2 Si/Al ratio of H-ZSM-5 zeolite catalysts .....	44
5.3 Particle sizes of H-ZSM-5 zeolite catalysts.....	45
5.4 BET surface area of various prepared zeolite catalysts .....	46
5.5 The amount of acidity of H-ZSM-5 zeolite catalysts with different Si/Al ratios.....	48
5.6 Crystallinity of H-ZSM-5(40) zeolite catalysts with different particle sizes.....	53
5.7 Particle sizes of H-ZSM-5(40) zeolite catalysts with different crystallization time.....	55
5.8 BET surface area of H-ZSM-5(40) zeolite catalysts with different particle sizes.....	55
5.9 Acidity of H-ZSM-5(40) zeolite catalysts with different particle sizes.....	56
5.10 The effect of particle sizes of H-ZSM-5(40) zeolite catalysts on catalytic performances for synthesis of DME from methanol.....	57
5.11 Crystallinity of H-ZSM-5 zeolite catalyst with different Si/Al ratios..	61
5.12 BET surface area of H-ZSM-5 zeolite catalysts with different crystallinity.....	62
5.13 Acidity of H-ZSM-5 zeolite catalysts with different crystallinity.....	65

## LIST OF FIGURES

Figure	Page
3.1 TO <sub>4</sub> tetrahedra (T=Si or Al) .....	10
3.2 Secondary building units (SBU's) found in zeolite structures .....	10
3.3 Structure of Structure of ZSM-5.....	14
3.4 Structure of Faujasite .....	15
3.5 Structure of beta zeolite.....	16
3.6 Structure of zeolite ZSM-12 .....	16
3.7 Structure of Mordenite.....	17
3.8 Framework structure of MCM-22 .....	18
3.9 Diagram of the surface of a zeolite framework.....	20
3.10 Water molecules co-ordinated to polyvalent cation are dissociated by heat treatment yielding Brønsted acidity.....	21
3.11 Lewis acid site developed by dehydroxylation of Brønsted acid site..	21
3.12 Steam dealumination process in zeolite.....	22
3.13 The enhancement of the acid strength of OH groups by their interaction with dislodged aluminum species.....	22
3.14 Diagram depicting the three type of selectivity .....	24
4.1 The preparation procedure of Na-ZSM-5 by rapid crystallization method.....	32
4.2 Schematic diagram of the reaction apparatus for reaction.....	40
5.1 The X-ray Diffraction pattern of the commercial H-ZSM-5 zeolite catalyst.....	42
5.2 The X-ray Diffraction patterns of the H-ZSM-5 samples with various Si/Al atomic ratio.....	43
5.3 SEM pictures of H-ZSM-5 sample with various Si/Al ratios that following: (a) H-ZSM-5(20), (b) H-ZSM-5(40), (c) H-ZSM-5(80) and (d) H-ZSM-5(160).....	45
5.4 NH <sub>3</sub> -TPD profiles of H-ZSM-5 zeolite catalysts with various Si/Al ratios.....	47

5.5	Dehydration of methanol over H-ZSM-5 zeolite catalysts with various Si/Al ratios. GHSV = 4250 h <sup>-1</sup> , methanol:He = 20:80.....	49
5.6	DME selectivity over H-ZSM-5 zeolite catalysts with various Si/Al ratios.....	50
5.7	DME yield over H-ZSM-5 zeolite catalysts with various Si/Al ratios.....	50
5.8	Hydrocarbons selectivity over H-ZSM-5 zeolite catalysts with various Si/Al ratios.....	51
5.9	The X-ray Diffraction pattern of the H-ZSM-5(40) zeolite catalysts with various particle sizes. ....	53
5.10	SEM image of H-ZSM-5(40) zeolite catalysts with various particle sizes that following: (a) H-ZSM-5(40) 6hr, (b) H-ZSM-5(40) 9hr, (c) H-ZSM-5(40) 12hr.....	54
5.11	TPD profiles of H-ZSM-5(40) zeolite catalysts with different particle sizes.....	56
5.12	The X-ray Diffraction patterns of the H-ZSM-5(20) zeolite catalysts with different crystallinity.....	59
5.13	The X-ray Diffraction patterns of the H-ZSM-5(40) zeolite catalysts with different crystallinity.....	59
5.14	The X-ray Diffraction patterns of the H-ZSM-5(80) zeolite catalysts with different crystallinity.....	60
5.15	The X-ray Diffraction patterns of the H-ZSM-5(160) zeolite catalysts with different crystallinity.....	60
5.16	TPD profiles of H-ZSM-5(20) zeolite catalysts with different crystallinity.....	63
5.17	TPD profiles of H-ZSM-5(40) zeolite catalysts with different crystallinity.....	63
5.18	TPD profiles of H-ZSM-5(80) zeolite catalysts with different crystallinity.....	64
5.19	TPD profiles of H-ZSM-5(160) zeolite catalysts with different crystallinity.....	64

5.20	Dehydration of methanol over H-ZSM-5(20) zeolite catalysts with different crystallinity.....	67
5.21	Dehydration of methanol over H-ZSM-5(40) zeolite catalysts with different crystallinity.....	67
5.22	Dehydration of methanol over H-ZSM-5(80) zeolite catalysts with different crystallinity.....	68
5.23	Dehydration of methanol over H-ZSM-5(160) zeolite catalysts with different crystallinity.....	68
5.24	DME selectivity over H-ZSM-5(20) zeolite catalysts with different crystallinity.....	69
5.25	DME selectivity over H-ZSM-5(40) zeolite catalysts with different crystallinity.....	69
5.26	DME selectivity over H-ZSM-5(80) zeolite catalysts with different crystallinity.....	70
5.27	DME selectivity over H-ZSM-5(160) zeolite catalysts with different crystallinity.....	70
5.28	DME yield over H-ZSM-5(20) zeolite catalysts with different crystallinity.....	71
5.29	DME yield over H-ZSM-5(40) zeolite catalysts with different crystallinity.....	71
5.30	DME yield over H-ZSM-5(80) zeolite catalysts with different crystallinity.....	72
5.31	DME yield over H-ZSM-5(160) zeolite catalysts with different crystallinity.....	72
5.32	Hydrocarbons selectivity over H-ZSM-5(20) zeolite catalysts with different crystallinity.....	73
5.33	Hydrocarbons selectivity over H-ZSM-5(40) zeolite catalysts with different crystallinity.....	73
5.34	Hydrocarbons selectivity over H-ZSM-5(80) zeolite catalysts with different crystallinity.....	74
5.35	Hydrocarbons selectivity over H-ZSM-5(160) zeolite catalysts with different crystallinity.....	74



# CHAPTER I

## INTRODUCTION

### 1.1 Rationale

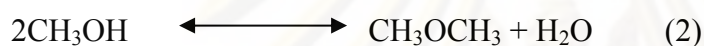
In the future, dimethyl ether (DME) may be a useful fundamental chemical feedstock or chemical intermediate in many processes for making important chemicals such as dimethyl sulfate, methyl acetate, aromatics, light olefins, paraffins and etc. For all reasons, because of it can be produced via natural gas or methanol which in a large quantity. And it is so easy to make a liquidified and efficiently transportation fuel. DME is used as an aerosol propellant in many products such as hair spray and shaving cream because of its environmentally benign properties [1-3].

The rapid development of automotive industry brings about the increase growing rate of fuel consumption. Furthermore, on the world wide, exhaustion of diesel engine give effect to one of the most serious environmental problem is air pollution which their cause come from transportation as trucks, trains and buses exhaust a large amount of  $\text{NO}_x$  and tiny particles and another from industry [4-6]. Now, DME is used as matter to replace for chlorofluorocarbons (CFC) because belief CFC that were to destroy the ozone layer of atmosphere [7]. Because of DME do not have carbon-carbon bonds so tiny particle are not formed when DME is used as a fuel for diesel vehicle [8].

Moreover, recently, DME has been suggested as an alternative fuel for diesel engines. DME has recently received a world wide attention since it has a good performance as a clean alternative fuel for diesel engines because of its engine operation with thermal efficiencies equivalent to traditional diesel fuel, much lower  $\text{NO}_x$  emission, near-zero smoke production and less engine noise [9].

In potential of DME are driving to produce DME in large quantities. But at the present, DME is produced in a little quantities by methanol dehydration over solid acid catalysts such as  $\gamma$ -alumina and zeolite ZSM-5 so many scientists develop and modified solid acid catalysts for adapt activity, stability and selectivity of solid acid

catalysts. While methanol is synthesized from syngas over Cu-based oxide catalysts as CuO/ZnO/Al<sub>2</sub>O<sub>3</sub> that is called methanol synthesis catalyst. In 1980s, syngas to DME process was developed for the direct production of DME from syngas over hybrid catalyst which consists of a methanol synthesis catalyst and an acid solid catalyst [10]. Now a day, only a few solid acid catalysts that were previously said, have been used for methanol dehydration process in DME synthesis. Among a few kinds of solid acids found HZSM-5 zeolite catalyst has been used extensively because of its very high catalytic activity [11,12]. The steps of reactions of the STD process are methanol synthesis, methanol dehydration and water gas shift (WGS)[3,10,11,13,14].



In this study, HZSM-5 zeolite catalyst was synthesized with different Si/Al ratio and crystallite size by rapid crystallization method. And then, characterized in detail for direct synthesis DME from methanol. Investigation of structure, acidity, activity, selectivity of modified HZSM-5 zeolite catalysts. Moreover, we study HZSM-5 zeolite catalyst that is better the performance.

In this my work was divided to six chapters. For Chapter I demonstrated the importance of DME for many processes, environmental problem, its application, an objectives and scope of research.

In Chapter II, involved an overview of DME papers. The literature reviews tell me about knowledge and guide line for my experimental.

And then, the theory were showed in Chapter III, this section demonstrated the basic knowledge of zeolite catalysts as structure, category and acid site etc. The experimental procedure and instrument were used to characterization HZSM-5 zeolite catalysts including reaction testing were described in the Chapter IV.

For Chapter V, the resulted was separated to three sections. The first section showed that the effect of Si/Al ratio on methanol dehydration, The second section that was investigated the effect of particle size on methanol dehydration to DME. Then, termination section studied about the effect of crystallinity on methanol dehydration.

## **1.2 Research objectives**

The objective of this research is to investigate the characteristics and performance of the prepared difference Si/Al ratio, crystallize size and crystallinity of H-ZSM-5 zeolite catalysts on methanol dehydration to dimethyl ether (DME).

## **1.3 Research scopes**

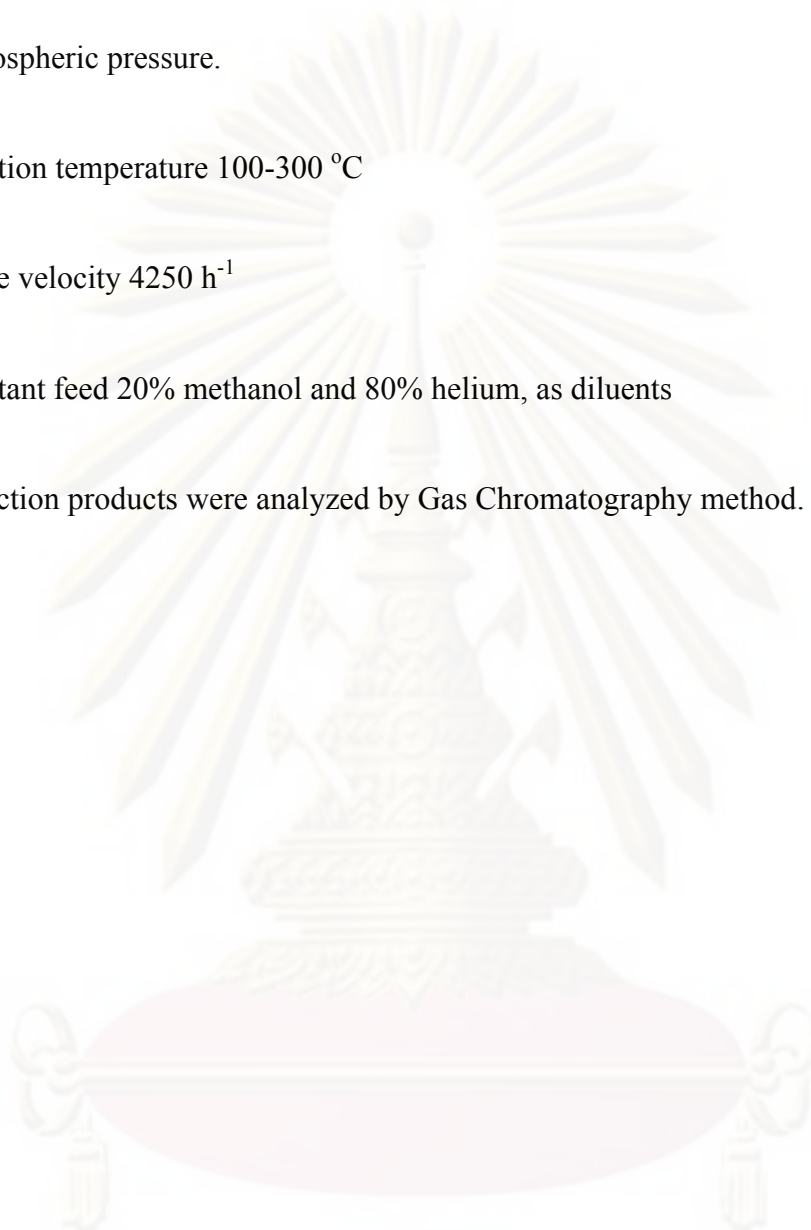
1. Study the method to synthesis and introduction of ZSM-5 zeolite catalyst.
2. Study the catalytic activity and yields of H-ZSM-5 zeolite catalysts having different Si/Al ratios (20,40,80,160) ,crystallize size and crystallinity in methanol dehydration to dimethyl ether.
3. Study the characterization of the prepared catalysts by the following methods.
  - Analyzing structure and crystallinity of catalysts by X-ray diffraction (XRD).
  - Analyzing amount of Si and Al of catalysts by X-ray fluorescence (XRF).
  - Analyzing shape and size of crystallites by Scanning Electron Microscope (SEM).
  - Analyzing surface areas of catalysts by Brunauer-Emmett-Teller (BET) surface areas measurement.
  - Analyzing the acidity of catalysts by NH<sub>3</sub>-TPD



4. Investigate the performance of the prepared catalysts on methanol dehydration to dimethyl ether under the following condition.

- Atmospheric pressure.
- Reaction temperature 100-300 °C
- Space velocity 4250 h<sup>-1</sup>
- Reactant feed 20% methanol and 80% helium, as diluents

The reaction products were analyzed by Gas Chromatography method.



ศูนย์วิจัยทรัพยากร  
จุฬาลงกรณ์มหาวิทยาลัย

## CHAPTER II

### LITERATURE REVIEWS

Dongsen Mao et al. studies about HZSM-5 zeolites modified with various amounts of magnesium oxide that characterized in detail and used as dehydration components of hybrid catalysts for the direct synthesis of DME from syngas. The results showed that both the surface areas and pore volumes decreased monotonically with an increasing amounts of magnesium oxide. However, the modification procedure decreases crystallinity of the HZSM-5 with increasing MgO content. After modification with a suitable amount of magnesium oxide, the result indicated that Bronsted acid sites (especially the strong Bronsted acid sites) decreased and an increased in Lewis acid sites. Hence, the selectivity for DME increased significantly over the hybrid catalyst with the modified HZSM-5 as methanol dehydration component, because of the effective inhibition of the undesirable side reactions that consist of dehydration of DME to lower olefins and their subsequent hydrogenation to the paraffins. Nevertheless, the catalytic activity of HZSM-5 zeolite modified with MgO for methanol dehydration was depend on both the acidity and basicity [15].

Yuchuan Fu et al. studies the nature, strength and number of surface acid sites of HZSM-5, steam de-aluminated H-Y zeolites,  $\gamma$ -Al<sub>2</sub>O<sub>3</sub> and Ti(SO<sub>4</sub>)<sub>2</sub>/  $\gamma$ -Al<sub>2</sub>O<sub>3</sub> catalyst for the dehydration of methanol to DME. The results indicated that the HZSM-5 and SY catalysts possessed strong Bronsted acidity and exhibited high activity for dehydration methanol to DME at relatively low temperatures. The  $\gamma$ -Al<sub>2</sub>O<sub>3</sub> catalyst had a strong Lewis acidity that showed low activity for methanol dehydration because of water was adsorbed on Lewis acid sites and poisoned to the strong Lewis acid sites. Moreover, the modification of  $\gamma$ -Al<sub>2</sub>O<sub>3</sub> by Ti(SO<sub>4</sub>)<sub>2</sub> appear the greatly increased surface Bronsted acidity that is responsible for the greatly increased methanol dehydration activity. In summary, the order of the activities following to HZSM-5 > SDY > Ti(SO<sub>4</sub>)<sub>2</sub>/  $\gamma$ -Al<sub>2</sub>O<sub>3</sub> >  $\gamma$ -Al<sub>2</sub>O<sub>3</sub> [16].

V. Vishwanathan et al. investigated into development of a modified HZSM-5 catalysts by sodium. Researcher expected in modified HZSM-5 catalysts that give high yield and selectivity for synthesis DME by using crude  $\text{CH}_3\text{OH}$  as feedstock. Then, they reported unmodified HZSM-5 catalyst had a higher catalytic activity than  $\gamma\text{-Al}_2\text{O}_3$  over a temperature range from 230 to 320°C. And result were indicated that Na-modified HZSM-5 (Si/Al = 20) catalyst shows a high catalytic performance such as activity, selectivity and stability over a wide range of temperatures (230-340°C). All of various the catalysts, Na<sub>80</sub>-HZSM-5 catalyst demonstrated higher performance in methanol dehydration and resistance for water. The modification procedure of catalysts by Na that eliminated the strong surface acid site, resulting in the prevention of hydrocarbon formation as well as coke [17].

Tatsuya Takeguchi et al. investigated the catalyst which consist of a methanol synthesis catalyst and a silica-rich silica-alumina. And found that at atmospheric pressure, Lewis acid – base pair were major active sites for methanol dehydration. But at higher pressure, water formed by methanol dehydration reaction and then that was strongly adsorbed on Lewis acid sites. Therefore, the DME formation was suppressed. Addition of Pd to the methanol-synthesis catalyst was to enhance the STD activity at low temperatures [18].

Mingting Xu et al. studied in synthesis of DME from methanol over a series of solid-acid catalysts such as  $\gamma\text{-Al}_2\text{O}_3$ , HZSM-5, amorphous silica-alumina as well as titania modified zirconia. For the results showed that all the catalysts was active and selective for DME formation. Moreover, active sites of  $\gamma\text{-Al}_2\text{O}_3$  catalyst was suppressed by water to give effect on the activity of  $\gamma\text{-Al}_2\text{O}_3$  but this effect were not occur over HZSM-5(50) [13].

ศูนย์วิจัยทรัพยากร

จุฬาลงกรณ์มหาวิทยาลัย

## CHAPTER III

### THEORY

#### 3.1 Zeolite

The name of “zeolite” comes from the Greek words zeo (to boil) and lithos (stone). The classical definition of a zeolite is a crystalline, porous aluminosilicate. However, some relatively recent discoveries of materials virtually identical to the classical zeolite, but consisting of oxide structures that have well-defined pore structures due to a high degree of crystallinity in their definition of the zeolite.

In these crystalline materials we call zeolites, the metal atoms (classically, silicon or aluminum) are surrounded by four oxygen anions to form an approximate tetrahedron consisting of a metal cation at the center and oxygen anions at the four apexes. The tetrahedra metals are called T-atoms for short, and these tetrahedral then stack in beautiful, regular arrays such that channels form. The possible way for the stacking to occur is virtually limitless, and hundred of unique structures are known. Graphical depictions of several representative types are given under “Representative Structures”.

The zeolitic channels (pores) are microscopically small, and in fact, have molecular size dimensions such that they are often termed “molecularsieves”. The size and shape of the channels have extraordinary effects on the properties of these materials for adsorption processes, and this property leads to their use in separation processes. Molecules can be separated via shape and size effects related to their possible orientation in the pore, or by differences in strength of adsorption.

Since silicon typically exists in a 4+ oxidation state, the silicon-oxygen tetrahedral are electrically neutral. However, in the zeolites, aluminum typically exists in the 3+ oxidation state so that aluminum-oxygen tetrahedral form centers that are electrically deficient one electron. Thus, zeolite frameworks are typically anionic, and charge-compensating cations populate the pores to maintain electrical neutrality. These cations can participate in ion-exchange processes, and this yields some



important properties for zeolites. When charge-compensating cations are “soft” cations such as sodium, zeolites are excellent water softeners because they can pick up the “hard” magnesium and calcium cations in water leaving behind the soft cations. When the zeolitic cations are protons, the zeolite becomes a strong solid acid. Such solid acids form the foundations of zeolite catalysis applications including the important fluidized bed cat-cracking refinery process. Other types of reactive metal cations can also populate the pores to form catalytic materials with unique properties. Thus, zeolites are also commonly used in catalytic operations and catalysis which zeolites is often called “shape-selective catalysis”

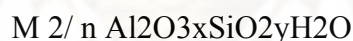
### 3.2 The structure of the zeolite

Zeolite are highly crystalline, hydrated aluminosilicates that upon dehydration develop in the ideal crystal a uniform pore structure having minimum channel diameters(aperture) of from about 0.3 to 1.0 nm. The size depends primarily on the type of zeolites and secondarily on the cations present and the nature of treatments such as calcination, leaching, and various chemical treatments. Zeolites have been of intense interest as catalysts for some three decades because of the high activity and unusual selectivity they provide, mostly in a variety of acid-catalyzed reaction. In many cases, but not all, the unusual selectivity is associated with the extremely fine pore structure, which permits only certain molecules to penetrate into the interior of the catalyst particles, or only certain products to escape from the interior. In some cases unusual selectivity seems to stem instead from constrains that the pore structure sets on allowable transition states, sometimes termed spacio – selectivity.

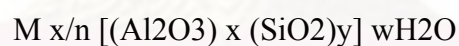
The structure of the zeolite consists of a three-dimensional framework of the  $\text{SiO}_4$  and  $\text{AlO}_4$  tetrahedra as presented in Figure 3.1 [19], each of which contains a silicon or aluminum atom in the center. In 1982, Barrer defined zeolites as the porous tectosilicates [20], that is, three-dimensional networks built up of  $\text{TO}_4^-$  tetrahedra where T is silicon or aluminum. The oxygen atoms are sheared between adjoining tetrahedral, which can be present in various ratios and arrange in a variety of ways. The framework thus obtained pores, channels, and cages, or interconnected voids.

A secondary building unit (SBU) consists of selected geometric groupings of those tetrahedral. There are sixteen such building units, which can be used to describe all of known zeolite structures; for example, 4 (S4R), 6 (S6R), and 8 (S8R) – member single ring, 4-4 (D6R), 8-8 (D8R)-member double rings. The topologies of these units are shown in Figure 3.2 [21]. Also listed are the symbols used to describe them. Most zeolite framework can be generated from several different SBU's. Descriptions of known zeolite structures based on their SBU's [22]. Both ZSM-5 zeolite and Ferrierite are described by their 5-1 building units. Offertile, Zeolite L, Cancrinite, and Erionite are generated using only single 6- member rings. Some zeolite structures can be described by several buildings. The sodalite framework can be built from either the single 6-member ring or the single 4- member ring. Faujasite (type X or type Y) and zeolite be constructed using 4 ring or 6 ring building units. Zeolite a can also be formed using double 4 ring building units, whereas Faujasite cannot.

Zeolites may be represented by the empirical formula:



or by a structural formula:



Where the bracketed term is the crystallographic unit cell. The metal cation (of valence) is present it produces electrical neutrality since for each aluminum tetrahedron in the lattice there is an overall charge of  $-1$ . M is a proton, the zeolite becomes a strong Bronsted acid. Access to the channels is limited by aperture consisting of a ring of oxygen atoms of connected tetrahedra. There may be 4, 5, 6, 8, 10, or 12 oxygen atoms in the ring. In some cases an interior cavity exists of larger diameter in the aperture; in others, the channel is of uniform diameter like a tube [23].

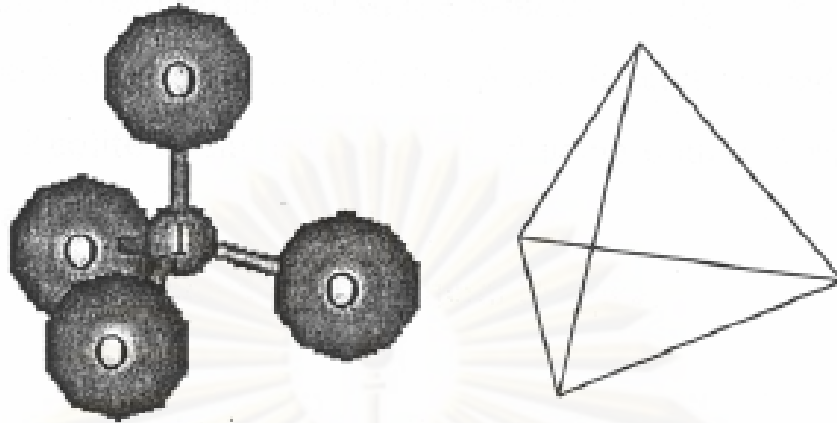


**Figure 3.1** TO<sub>4</sub> tetrahedra (T=Si or Al) [19]

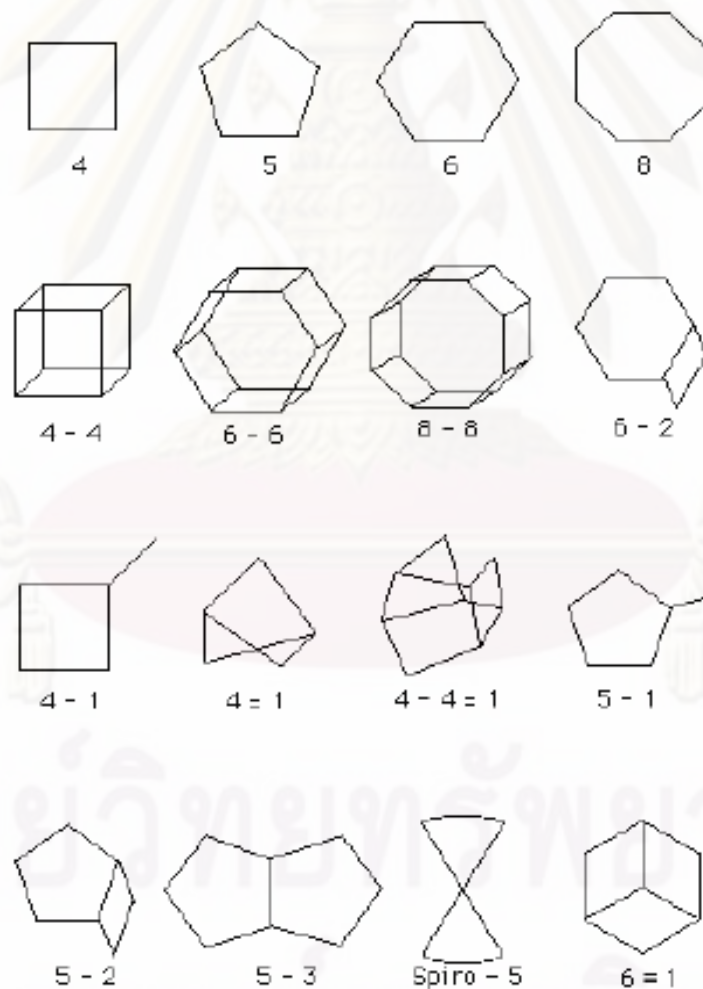


**Figure 3.2** Secondary building units (SBU's) found in zeolite structures[21]



The MFI - type (ZSM-5) zeolite is probably the most useful one. ZSM-5 zeolites with a wide range of  $\text{SiO}_2/\text{Al}_2\text{O}_3$  ratio can easily be synthesized. High siliceous ZSM-5 zeolites are more hydrophobic and hydro thermally stable compared with many other zeolites. Although the first synthetic ZSM-5 zeolite was discovered more than three decades ago (1972) new interesting applications are still emerging to this day. For example, its recent application in  $\text{NO}_x$  reduction, especially in the exhaust of lean-burned engine, has drawn much attention. Among various zeolite catalysts, ZSM-5 zeolite has the greatest number of industrial applications, covering from petrochemical production and refinery processing to environmental treatment.

### 3.3 Category of Zeolite

There are over 40 known natural zeolites and more than 150 synthetic zeolites have been reported [24]. The number of synthetic zeolites with new structure morphologies grows rapidly with time. Based on size of their pore opening, zeolites can be roughly divided into five major categories, namely 8 -, 10 -, and 12- member oxygen ring systems, dual pore systems and mesoporous systems. Their pore structures can be characterized by crystallography, adsorption, measurements and/or through diagnostic reactions. One such diagnostic characterization test is the “constraint index” test. The concept of constraint index was defined as the ratio of the cracking rate constant of n-hexane to 3-methylpentane. The constraint index of a typical medium-pore zeolite usually ranges from 3 to 12 and those of the large-pore zeolites are the range 1-3. For materials with an open porous structure, such as amorphous silica alumina, their constraint indices are normally less than 1. On the index for erionite is 38.

A comprehensive bibliography of zeolite structures has been published by the International Zeolite Association [24]. The structural characteristics of assorted zeolites are summarized in Table 3.2

Zeolite with 10-membered oxygen rings normally possesses a high siliceous framework structure. They are of special interest in industrial applications. In fact, they were the first family of zeolite that was synthesized with organic ammonium salts. With pore openings close to the dimensions of many organic molecules, they are

particularly useful in shape selective catalysis. The 10-membered oxygen ring zeolites also possess other important characteristic properties including high activity, high tolerance to coking and high hydrothermal stability. Among the family of 10-membered oxygen ring zeolites, the MFI - type (ZSM-5) zeolite as presented in Figure 3.3 is probably the most useful one. ZSM-5 zeolite has two types of channel systems of similar sized, one with a straight channel of pore opening  $5.3 \times 5.6 \text{ \AA}$  and the other with a tortuous channel of pore opening  $5.1 \times 5.5 \text{ \AA}$ . Those intersecting channels are perpendicular to each other, generating a three dimensional framework. ZSM-5 zeolites with a wide range of  $\text{SiO}_2/\text{Al}_2\text{O}_3$  ratio can easily be synthesized. High siliceous ZSM-5 zeolites are more hydrophobic and hydro thermally stable compared with many other zeolites. Although the first synthetic ZSM-5 zeolite was discovered more than two decades ago (1972) new interesting applications are still emerging to this day. For example, its recent application in  $\text{NO}_x$  reduction, especially in the exhaust of lean-burned engine, has drawn much attention. Among various zeolite catalysts, ZSM-5 zeolite has the greatest number of industrial applications, covering from petrochemical production and refinery processing to environmental treatment.

**Table 3.1** Structural characteristics of selected zeolites [24]

Zeolite	Number of rings	Pore opening Å	Pore/Channel structure	Void volume (ml/g)	$D_{\text{Frame}}^a$ (g/ml)	$CI^b$
<i>8-membered oxygen ring</i>						
Erionite	8	3.6x5.1	Intersecting	0.35	1.51	38
<i>10-membered oxygen ring</i>						
ZSM-5	10	5.3x5.6 5.1x5.5	Intersecting	0.29	1.79	8.3
ZSM-11	10	5.3x5.4	Intersecting	0.29	1.79	8.7
ZSM-23	10	4.5x5.2	One-dimensional	-	-	9.1
<i>Dual pore system</i>						
Ferrierite (ZSM-35, FU-9)	10,8	4.2x5.4 3.5x4.8	One-dimensional 10:8 intersecting	0.28	1.76	4.5
MCM-22	12	7.1	Capped by 6 rings	-	-	1-3
Mordenite	10	Elliptical				
	12	6.5x7.0	One-dimensional	0.28	1.70	0.5
	8	2.6x5.7	12:8 intersecting			
Omega (ZSM-4)	12	7.4	One-dimensional	-	-	2.3
	8	3.4x5.6	One-dimensional	-	-	0.6
<i>12membered oxygen ring</i>						
ZSM-12	12	5.5x5.9	One-dimensional	-	-	2.3
Beta	12	7.6x6.4 5.5x5.5	Intersecting	-	-	0.6
Faujasite (X,Y)	12	7.4	Intersecting	0.48	1.27	0.4
	12	7.4x6.5	12:12 intersecting			
<i>Mesoporous system</i>						
VPI-5	18	12.1	One-dimensional	-	-	-
MCM41-S	-	16-100	One-dimensional	-	-	-

<sup>a</sup>Framework density<sup>b</sup>Constraint index

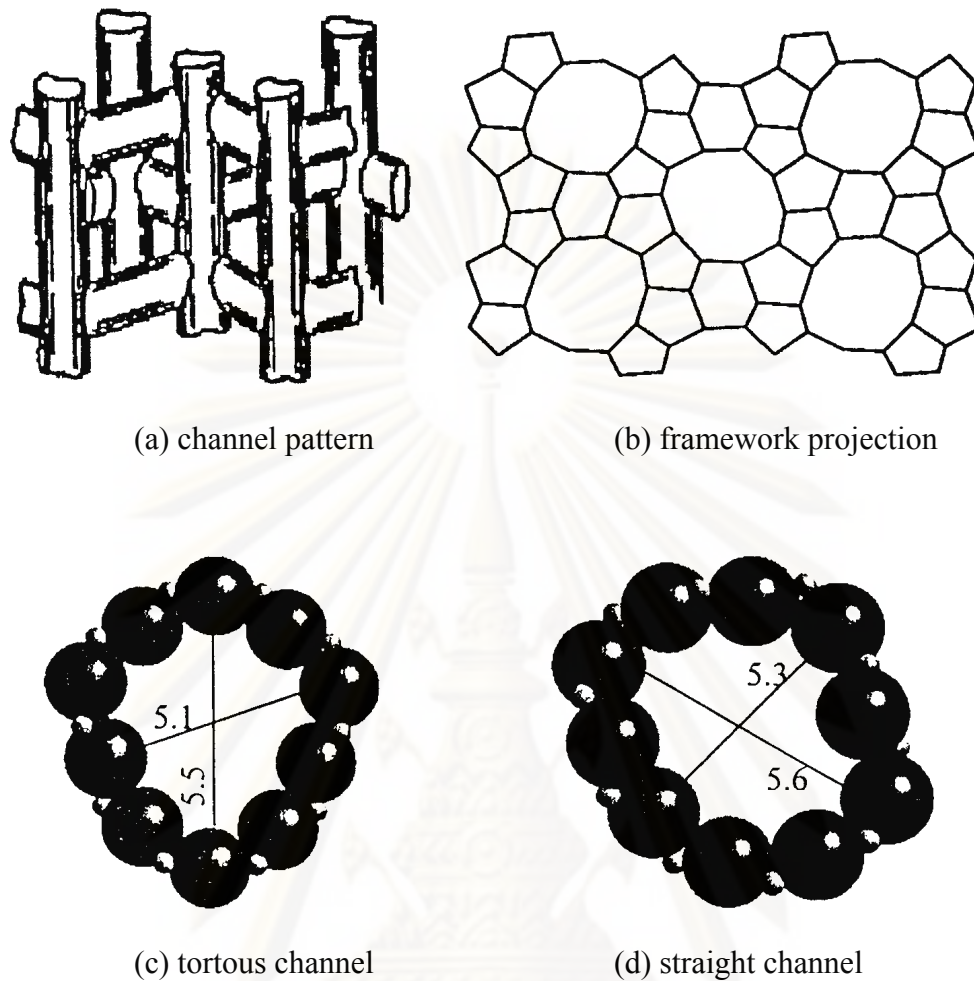


**Figure 3.3** Structure of Structure of ZSM-5 [24].

Although the 10-membered oxygen ring zeolite was found to possess remarkable shape selectivity, catalysis of large molecules may require a zeolite catalyst with a large-pored opening. Typical 12-membered oxygen ring zeolites, such as faujasite-type zeolites, normally have pore opening greater than 5.5 Å and hence are more useful in catalytic applications with large molecules, for example in trimethylbenzene (TMB) conversions. Faujasite (X or Y; Figure 3.4 [24]) zeolites can be synthesized using inorganic salts and have been widely used in catalytic cracking since 1960s. The framework structures of beta zeolite and ZSM-12 are shown in Figure 3.5 and 3.6, respectively.



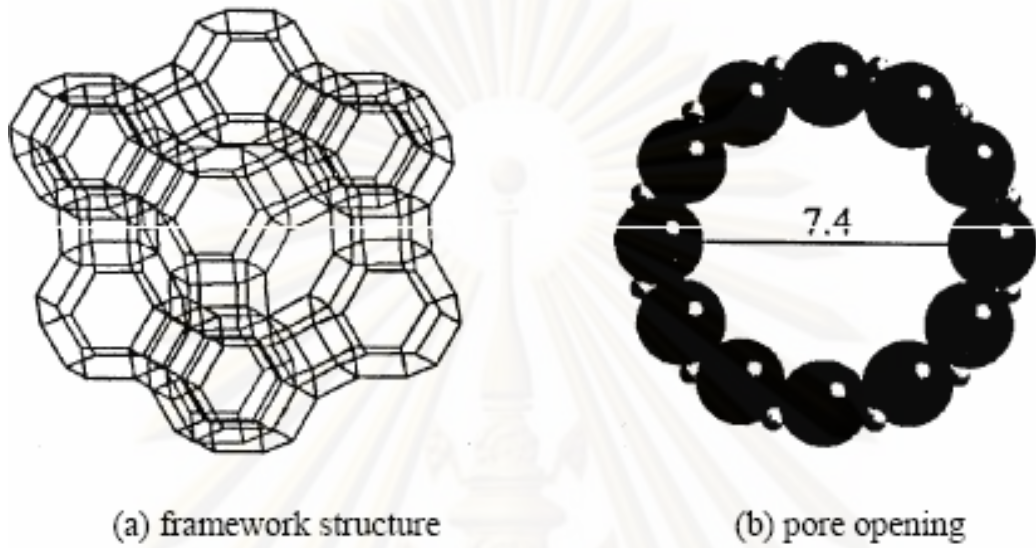


Figure 3.4 Structure of Faujasite [24].

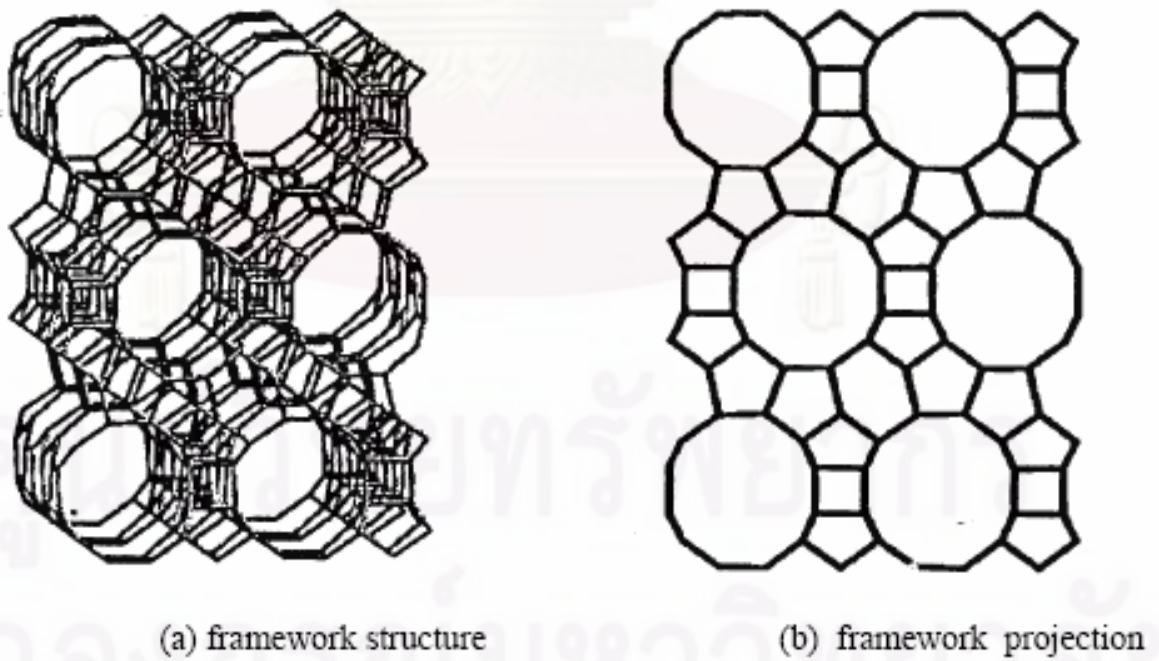


Figure 3.5 Structure of beta zeolite [24].

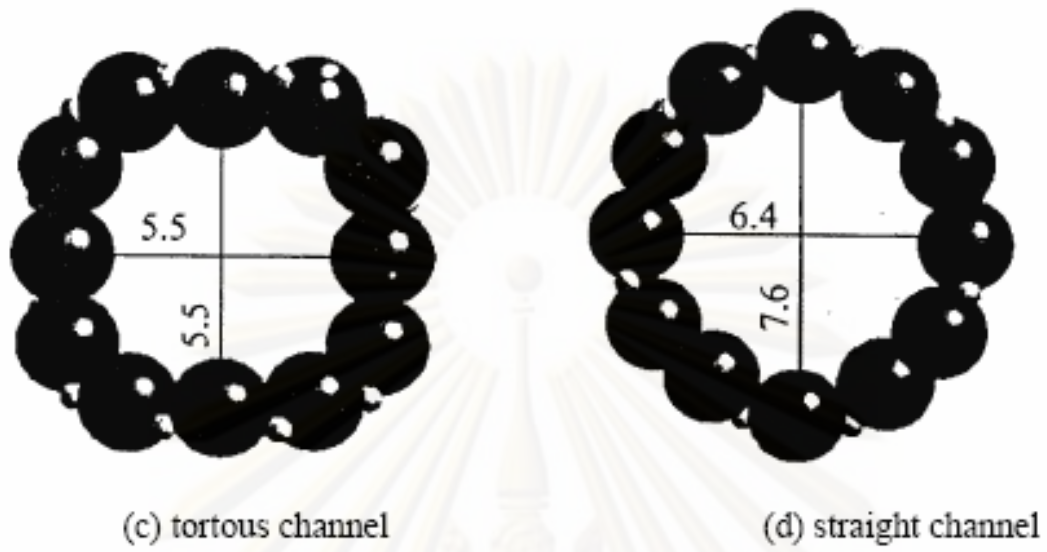


Figure 3.5 Structure of beta zeolite [24].

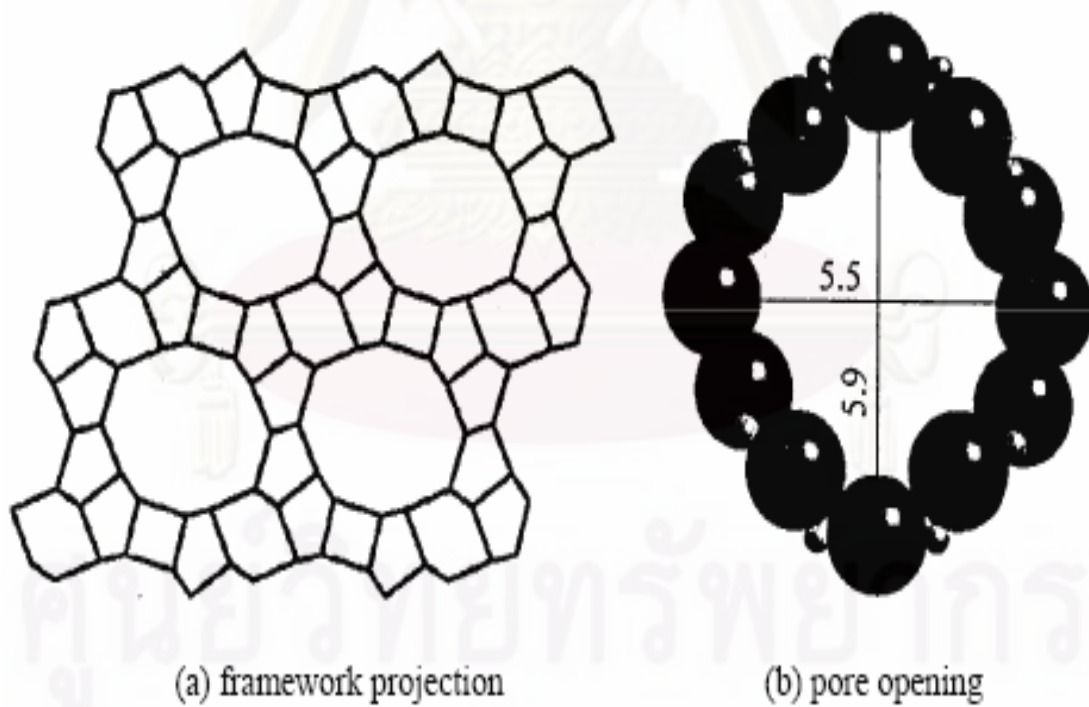
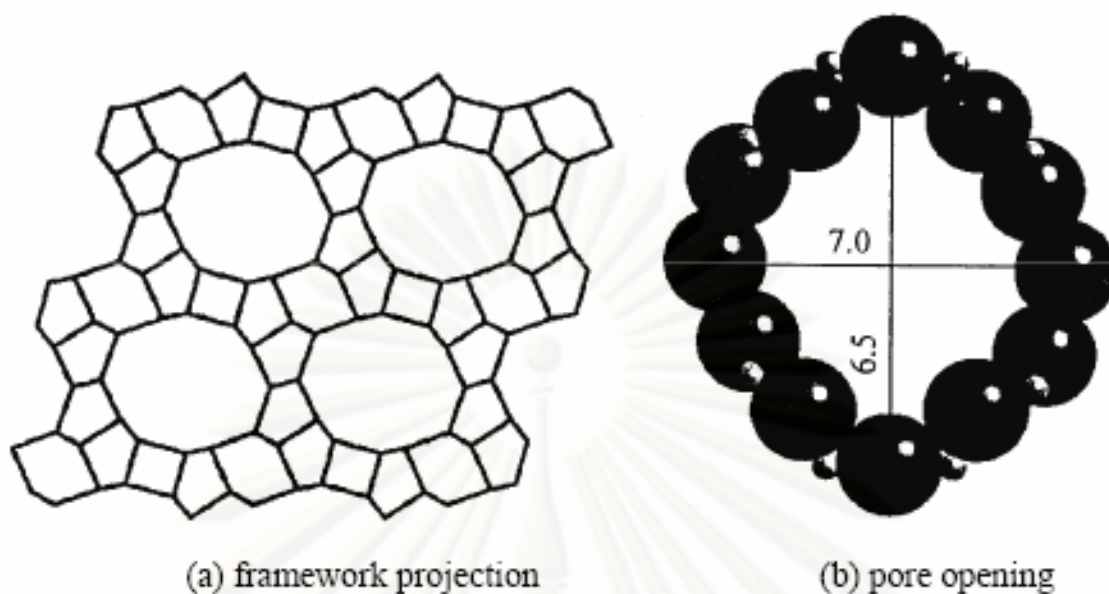


Figure 3.6 Structure of zeolite ZSM-12 [24].



**Figure 3.7** Structure of Mordenite [24].

Zeolites with a dual pore system normally possess interconnecting porechannels with two different pore opening sizes. Mordenite is a well-known dual pore zeolite having a 12-membered oxygen ring channel with pore opening  $6.5 \times 6.7 \text{ \AA}$  which is interconnected to 8-membered oxygen ring channel with opening  $2.6 \times 5.7 \text{ \AA}$  (Figure 3.7 [25]). MCM-22, which was found more than 10 years, also possess a dual pore system. Unlike Mordenite, MCM-22 consists of 10- and 12- membered oxygen rings (Figure 3.8 [24]) and thus shows prominent potential in future applications.

In the past decade, many research efforts in synthetic chemistry have been invested in the discovery of large-pored zeolite with pore diameter greater than 12-membered oxygen rings. The recent discovery of mesoporous materials with controllable pore opening (from 12 to more than  $100 \text{ \AA}$ ) such as VPI-5, MCM-41S undoubtedly will shed new light on future catalyst applications.



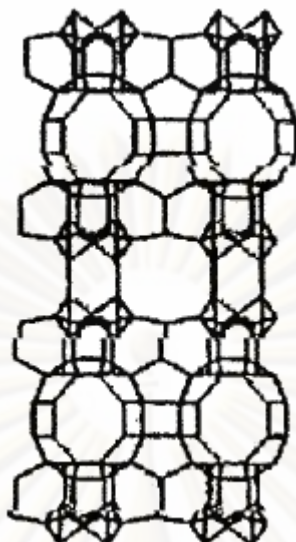


**Figure 3.8** Framework structure of MCM-22 [24].

### 3.4 Zeolite Active sites

#### 3.4.1 Acid sites

Classical Brønsted and Lewis acid models of acidity have been used to classify the active sites on zeolites. Brønsted acidity is proton donor acidity; a tridagonally coordinated alumina atom is an electron deficient and can accept an electron pair, therefore behaves as a Lewis acid [26].

In general, the increase in Si/Al ratio will increase acidic strength and thermal stability of zeolite [27]. Since the numbers of acidic OH groups depend on the number of aluminium in zeolites framework, decrease in Al content is expected to reduce catalytic activity of zeolite. If the effect of increase in the acidic centers, increase in Al content, shall result in enhancement of catalytic activity

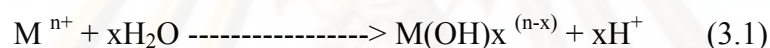
Based on electrostatic consideration, the charge density at a cation site increase with increase Si/Al ratio. It was conceived that these phenomena are related to reduction of electrostatic interaction between framework sites, and possibly to difference in the order of aluminum in zeolite crystal-the location of Al in crystal structure [28].

An improvement in thermal or hydrothermal stability has been ascribed to the lower density of hydroxyl groups, which is parallel to that of Al content [26]. A longer distance between hydroxyl groups decrease the probability of dehydroxylation that generates defects on structure of zeolites.

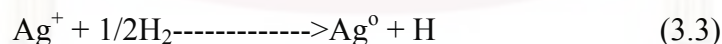
### 3.4.2 Generation of Acid Centers

Protonic acid centers of zeolite are generated in various ways. Figure 3.9 depicts the thermal decomposition of ammonium-exchanged zeolite yielding the hydrogen form [29].

The Brønsted acidity due to water ionization on polyvalent cations, described below, is depicted in Figure 3.10 (Tanaka et al., 1989).



The exchange of monovalent ions by polyvalent cations could improve the catalytic property. Those highly charged cations create very centers by hydrolysis phenomena. Brønsted acid sites are also generated by the reduction of transition metal cations. The concentration of OH groups of zeolite containing transition metals was noted to increase by hydrogen at 275.5 – 723 K to increase with the rise of the reduction temperature [19].



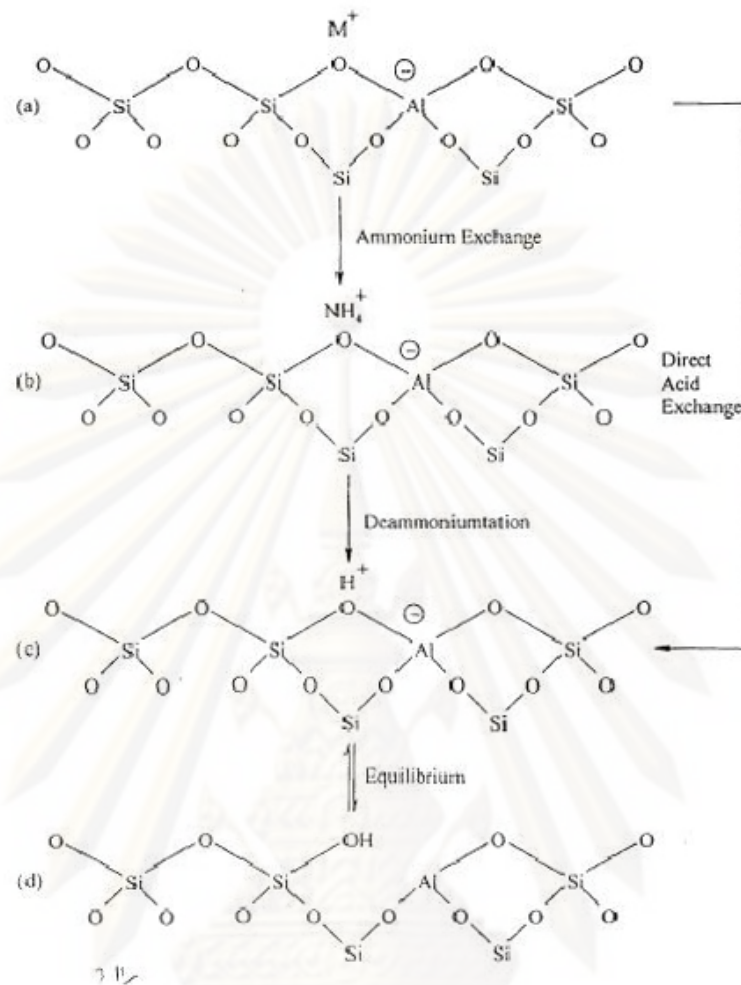


**Figure 3.9** Diagram of the surface of a zeolite framework [22].

- In the as-synthesis form  $M^+$  either an organic cation or an alkali metal cation.
- Ammonium in exchange produces the  $NH_4^+$  exchanged form.
- Thermal treatment is used to remove ammonia, producing the  $H^+$ , acid form.
- The acid form in (c) is in equilibrium with the shown in (d), where is a silanol group adjacent to tricoordinate aluminium.

The formation of Lewis acidity from Brønsted acid sites is depicted in Figure 3.11 [22]. The dehydration reaction decrease the number of protons and increases that of Lewis sites. Brønsted ( $-OH$ ) and Lewis ( $-Al-$ ) sites can be present simultaneously in

the structure of zeolite at high temperature. Dehydroxylation is thought to occur in ZSM-5 zeolite above at 773 K and calcination at 1073 to 1173 K produces irreversible dehydroxylation, which causes deflection in crystal structure of zeolite.

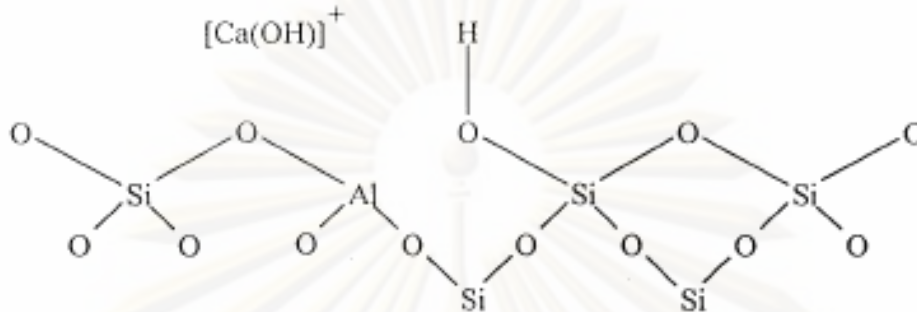


**Figure 3.10** Water molecules co-ordinated to polyvalent cation are dissociated by heat treatment yielding Brønsted acidity [22].

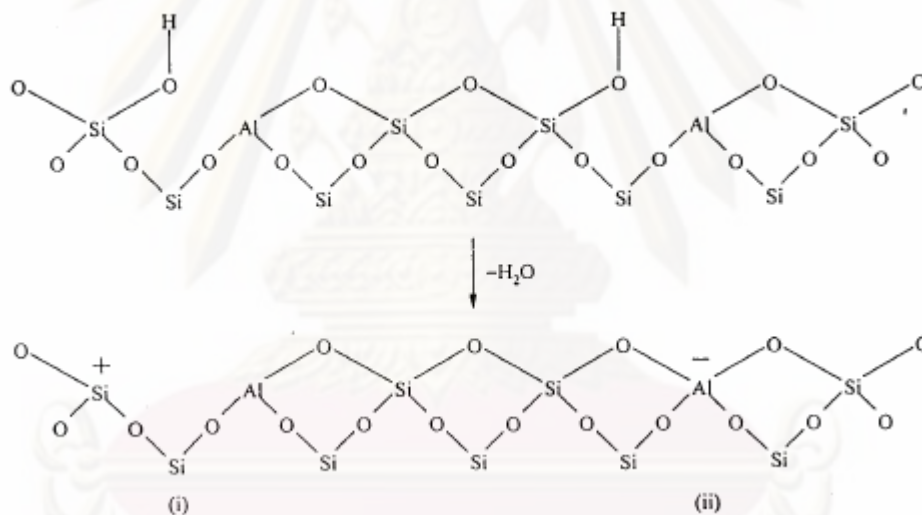


**Figure 3.11** Lewis acid site developed by dehydroxylation of Brønsted acid site [22].

Dealumination is believed to occur during dehydroxylation, which may result from the steam generation within the sample. The dealumination is indicated by an increase in the surface concentration of aluminum on the crystal. The dealumination process is expressed in Figure 3.12 [30]. The extent of dealumination monotonously increases with the partial pressure of steam.



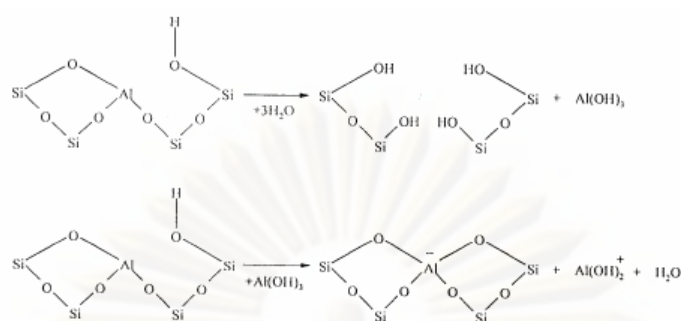


**Figure 3.12** Steam dealumination process in zeolite [30]

The enhancement of the acid strength of OH groups is recently proposed to be pertinent to their interaction with those aluminum species sites tentatively expressed in Figure 3.13 [30]. Partial dealumination might therefore yield a catalyst of higher activity while severe steaming reduces the catalytic activity.

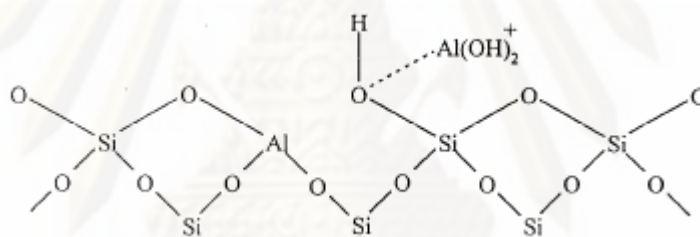


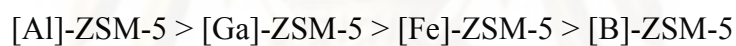
**Figure 3.13** The enhancement of the acid strength of OH groups by their interaction with dislodged aluminum species [30].

### 3.4.3 Basic Sites

In certain instances reactions have been shown to be catalyzed at basic (cation) site in zeolite without any influences from acid sites. The best-characterized example of this is that K-Y which splits n-hexane isomers at 773 K. The potassium cation has been shown to control the unimolecular cracking ( $\beta$ -scission). Free radical mechanisms also contribute to surface catalytic reactions in these studies.

### 3.4.4 Acidity of Metallosilicate

The synthesis of zeolites containing various element such as B, P, or Ge has been carried out for a long time. Since the discovered of ZSM-5 ( aluminosilicate ) and silicate, many attempts have been made to synthesize the metallosilicate with the ZSM-5 structure. The isomorphous substitution of aluminum with other element greatly modifies the acidic properties of the silicate. The elements introduced include, Be, B, Ti, Cr, Fe, Zn, Ga, and V. These elements were usually introduced by adding metal salts as one of the starting materials for the synthesis of the metallosilicate. It is also know that boron can be directly introduced by reacting ZSM-5 with boron trichloride. Metallosilicste with ZSM-5 structure having metal M as a component will be denoted [M]-ZSM-5. Silicate II can be transformed into gallosilicate with its reaction with NaGaO<sub>2</sub> in an aqueous solution. The acid strength of metallosilicate changes in decreasing order as follws:



Weaker acid strength of [B]-ZSM-5 is confirmed also by catalytic reactions. Table 3.4 shows the product distributions of 1-butene reaction over [B]-ZSM-5 and [Al]-ZSM-5 at 773 K. It is clear that there is a great difference in the product dismatic hydrocarbons, while over [B]-ZSM-5, lower alkenes are the m does not proceed over [B]-ZSM-5ain products. This indicates that the hydride transfer reaction from alkenes to carbonium ion. For the same reasons, alkenes are the main products in the conversion of methanol over [b]-ZSM-5, while [Al]-ZSM-5 is a unique catalyst for gasoline production.

### 3.5 Shape Selective

Many reactions involving carbonium intermediates are catalyzed by acidic zeolite. With respects to a chemical standpoint the reaction mechanisms are nor fundamentally different with zeolites or with any the acidic oxides. What zeolite add is shape selectivity effect. The shape selective characteristics of zeolites influence their catalytic phenomena by three modes: shape selectivity, reactants shape

selectivity, products shape selectivity and transition states shape selectivity. These types of selectivity are illustrated in Figure 3.14.

Reactants of charge selectivity results from the limited diffusibility of some of the reactants, which cannot effectively enter and diffuse inside crystal pore structures of the zeolites. Product shape selectivity occurs as slowly diffusing product molecules cannot escape from the crystal and undergo secondary reaction. This reaction path is established by monitoring changes in product distribution as a function of varying contact time.

Restricted transition state shape selectivity is a kinetic effect from local environment around the active site, the rate constant for a certain reaction mechanism is reduced if the space required for formation of necessary transition state is restricted.

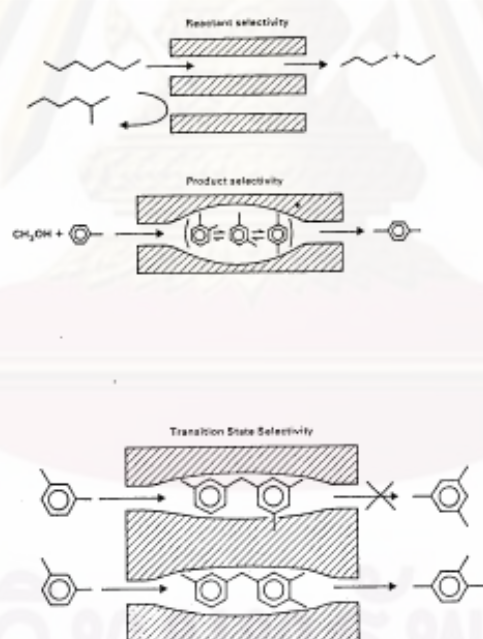


**Figure 3.14** Diagram depicting the three type of selectivity [21].

The critical diameter (as opposed to the length) of the molecules and the pore channel diameter of zeolites are important in predicting shape selective effects. However, molecules are deformable and can pass through opening, which are smaller

than their critical diameters. Hence, not only size but also the dynamics and structure of the molecules must be taken into account.

### 3.6 Zeolite Synthesis

Zeolites are generally synthesized by a hydrothermal process from a source of alumina (e.g., sodium aluminate or aluminium sulfate) and of silica (e.g., a silica sol, fumed silica, or sodium water glass) and an alkali such as NaOH, and/or a quaternary ammonium compound. An inhomogeneous gel is produced which gradually crystallizes, in some cases forming more than one type of zeolite in succession. Nucleation effects can be important, and an initial induction period at near ambient temperature may be followed by crystallization temperature that may range up to 473 K or higher. The pressure is equal to the saturated vapor pressure of the water present.

The final product depends on a complex interplay between many variables including  $\text{SiO}_2/\text{Al}_2\text{O}_3$  ratio in the starting medium, nucleating agents, temperature, pH, water content, aging, stirring, and the presence of various inorganic and organic cations. Much remains to be learned about how the initial reaction mixture forms the precursor species and how these arrange into the final crystalline products. A key concept is that the cations present give rise to a templating action, but clearly the process is more complex.

Bauer and coworkers in the early 1960s developed the use of reaction mixtures containing quaternary ammonium ions or other or other cations to direct the crystallization process. In their work and succeeding studies, a primary motivation was to attempt to synthesize zeolites with large apertures than X and Y. This did not occur, but instead organic species were found to modify the synthesis process in a variety of ways that led to the discovery of many new zeolites, and new methods of synthesizing zeolite with structures similar to previously know zeolite.

The mechanism of action of the organic species is still controversial. It was originally thought to be primarily a templating effect, but later it was found that at least some of zeolites could be synthesized without an organic template. Further, organic species other than quaternary ammonium compounds had directing effects not



readily ascribed to their size or shape. However, an important result was the zeolites of higher  $\text{SiO}_2/\text{Al}_2\text{O}_3$  ratio than before could be synthesized. Previously, only structures with  $\text{SiO}_2/\text{Al}_2\text{O}_3$  ratios of about 10 or less could be directly forms, but with organic additives, zeolites with ratio of 20 to 100 or more can be directly prepared.

After synthesis the zeolite are washed, dried, heated to remove water of crystallization, and calcined in air, e.g., at about 813 K. Organic species are also thus removed. For most catalytic purpose, the zeolite is converted into acidic form. For some zeolites this can be achieved by treatment with aqueous HCl without significantly altering the framework structure. For other zeolites  $\text{Na}^+$  is replaced with  $\text{NH}_4^+$  via an ammonium compound such as  $\text{NH}_4\text{OH}$ ,  $\text{NH}_4\text{Cl}$  or  $\text{NH}_4\text{NO}_3$ . Upon heating  $\text{NH}_3$  is driven off, leaving the zeolite in the acid form. For some reaction a hydrogenation component such as platinum or nickel is introduced by impregnation or ion exchange [29,31].

### 3.7 Dimethyl ether (DME)

The DME is an ether compound that was synthesis from syngas ( $\text{CO}+\text{H}_2$ ) or methanol over hybrid catalysts. The hybrid catalyst composed of methanol synthesis catalyst and solid acid catalyst. DME which is now used as the substitute for chlorofluorocarbons, has high cetane number owing to its low ignition temperature. DME is used as a fuel for diesel engines because of its produced a little  $\text{NO}_x$ , near zero smoke production, less engine noise compared with traditional diesel fuels. As well know DME is a useful chemical intermediate for the production of various important chemicals such as dimethyl sulfate, methyl acetate, and light olefins. Each a day, with increasingly stringent environmental regulations. So DME has recieved a more attention owing to its potential use as a clean alternative fuel for diesel engines. Hence, there is a growing demand to produce a large amount of DME in the near future.

### 3.8 Olefins

The olefin or ethylene series ( type formula  $C_nH_{2n}$  ) is composed of unsaturated hydrocarbon ;i.e., the members of this series are capable of uniting directly with other material such as chlorine, bromine, hydrochloric acid, and sulfuric acid, without displacing a hydrogen atom. The name of these hydrocarbons end in –ene, as ethane(ethylene) , propene (propylene) and butene(butylenes). Unsaturated compounds react with and dissolve in sulfuric acid and may thus be remove from petroleum oils.The low boiling olefin are probably not present in crude petroleum, but they are round in cracked products. Egloff, Schaad, and Lowry have made an excellent study of the literature of the olefin hydrocarbons.

Ethylene is used primarily as an intermediate in the manufacture of other chemicals, especially plastics. Ethylene may be polymerized directly to produce polyethylene (also called polyethylene or polythene), the world's most widely-used plastic. Ethylene can be chlorinated to produce ethylene dichloride (1,2-Dichloroethane), a precursor to the plastic polyvinyl chloride, or combined with benzene to produce ethylbenzene, which is used in the manufacture of polystyrene, another important plastic.

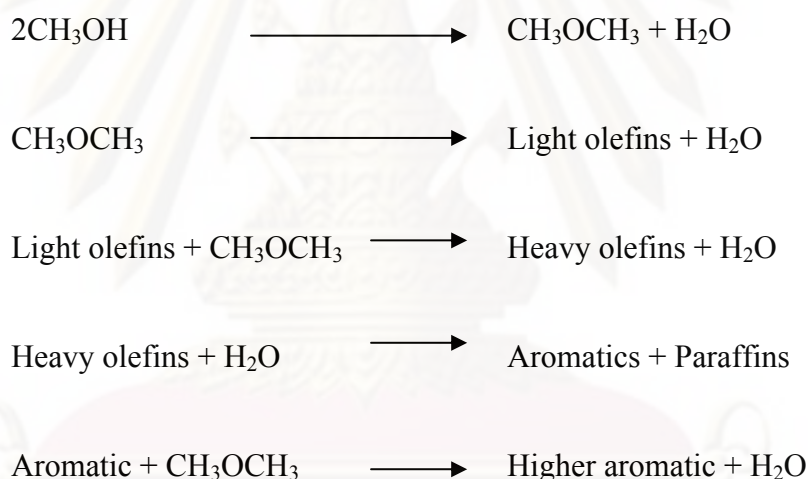
Smaller amounts of ethylene are oxidized to produce chemicals including ethylene oxide, ethanol, and polyvinyl acetate. Global demand for ethylene exceeded 100 million tonnes per year in 2005. Ethylene was once used as an inhaled anesthetic, but it has long since been replaced in this role by nonflammable gases. It has also been hypothesized that ethylene was the catalyst for utterances of the oracle at Delphi in ancient Greece. Ethylene is used in greenhouses and is sprayed on crops to speed ripening. It is also found in many lip gloss products.

Propylene, also known by its IUPAC name propylene, is an organic compound having the chemical formula  $C_3H_6$ . It is the second simplest member of the alkene class of hydrocarbons, ethylene (ethylene) being the simplest. At room temperature and pressure, propylene is a gas. It is colorless, highly flammable, and has an odor similar to garlic.(this smell is added to make it easily detectable, pure propylene, like most simple hydrocarbons, has no natural scent.) It is found in coal gas and can be synthesized by cracking petroleum. Propylene is a major commodity in the

petrochemicals industry. The main use of propylene is as a monomer, mostly for the production of polypropylene. Propylene is also used as a fuel gas for various industrial processes. It has a similar calorific value to propane but a lower mass of combustion products so a higher flame temperature. Propylene also has approximately twice the vapor pressure of propane at room temperature and pressure.

### 3.9 Reaction mechanism of methanol to DME and hydrocarbons

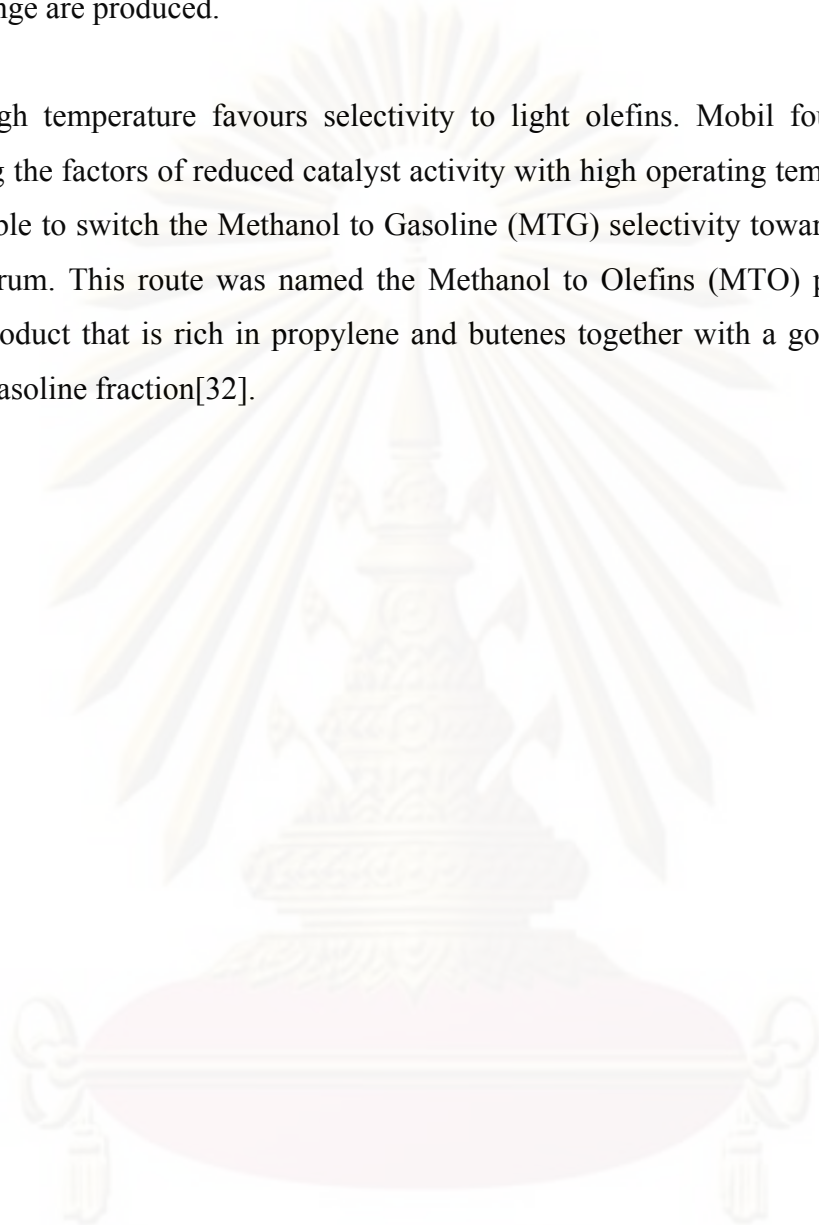
The reaction of methanol to hydrocarbon products is vigorously exothermic, with a theoretical adiabatic temperature rise of about 600°C. The reaction path is believed to pass through a number of series and parallel steps. The mechanism is complex and is discussed elsewhere. A simplified path is given below



Methanol is made from synthesis gas (a mixture of carbon monoxide and hydrogen) which is formed by steam reforming of natural gas or gasification of coal. The first step in the reaction sequence is the dehydration of methanol to an equilibrium mixture of dimethylether (DME), methanol and water. The DME then reacts further to form a mixture of light olefins. As the concentration of DME is depleted, the equilibrium of reaction is disturbed and further dehydration of ethanol take place. The DME alkylates the light olefins (mostly propylene and butanes) to high olefins, which can then further react with one another to form aromatics and paraffins. If any residual DME remains at the point where aromatics form, those aromatics are readily alkylated to higher carbon number of C<sub>10</sub>. The heaviest

component is durene (1,2,4,5-tetraethylbenzene), which lies near the high end of the gasoline boiling range. No components with normal boiling points above the gasoline boiling range are produced.

High temperature favours selectivity to light olefins. Mobil found that by combining the factors of reduced catalyst activity with high operating temperatures, it was possible to switch the Methanol to Gasoline (MTG) selectivity towards an olefin rich spectrum. This route was named the Methanol to Olefins (MTO) process, and gives a product that is rich in propylene and butenes together with a good aromatic rich  $C_5+$  gasoline fraction[32].



ศูนย์วิจัยทรัพยากร  
จุฬาลงกรณ์มหาวิทยาลัย



## CHAPTER IV

### EXPERIMENTAL

#### 4.1 Catalyst Preparation

In this study, four of H-ZSM-5 catalysts, having different Si/Al ratio (20,40,80,160) and particle size. H-ZSM-5 was prepared for methanol dehydration to dimethyl ether. The preparation of H-ZSM-5 was described as follows:

##### 4.1.1 Chemicals

The details of chemicals used in the preparation procedure of ZSM-5 were shown in Table 4.1

**Table 4.1** The chemicals used in the catalyst preparation

Chemical	Supplier
-Tetrapropyl ammonium bromide (TPABr)	Aldrich
-Sodium silicate Solution ( SiO <sub>2</sub> 25.5-28.5)	Merck
-Sodium hydroxide [NaOH]	Merck
-Aluminium chloride [AlCl <sub>3</sub> ]	Aldrich
-Magnesium nitrate [Mg(NO <sub>3</sub> ) <sub>2</sub> ]	Aldrich
-Sodium hydroxide (NaOH)	Merck
-Sulfuric acid (98.08%)	J.T. Baker

##### 4.1.2 Preparation of Na-ZSM-5 ( MFI )

The preparation procedure of Na-ZSM-5 by rapid crystallization method was shown in Figure 4.1, while reagents were shown in table 4.2. This method can advantageously and rapidly prepare the uniform and fine zeolite crystals with the following improvements: (i) the preparation of supernatant liquid was separated from

that of gel, which was important to prepare the uniform crystals, (ii) the precipitated gel was milled before the hydrothermal treatment, which was essential to obtain the uniform and fine crystals, and (iii) the temperature under the hydrothermal treatment was programmed to minimize the time which was necessary for the crystallization. The detail preparation procedures of Na-ZSM-5 were described below.

**Table 4.2** Reagents used for the preparation of Na-ZSM-5: Si/Al = 50

Solution for the gel Preparation	Solution for the decant-solution preparation
<p><u>Solution A1</u></p> <p>AlCl<sub>3</sub> 0.8831g            TPABr 5.72 g            NaCl 11.95 g            De-ionized water 60 ml            H<sub>2</sub>SO<sub>4</sub> 3.4 ml</p>	<p><u>Solution A2</u></p> <p>AlCl<sub>3</sub> 0.8831 g            TPABr 7.53 g            De-ionized water 60 ml            H<sub>2</sub>SO<sub>4</sub> 3.4 ml</p>
<p><u>Solution B1</u></p> <p>De-ionized water 45 ml            Sodium silicate 69 g</p>	<p><u>Solution B2</u></p> <p>De-ionized water 45 ml            Sodium silicate 69 g</p>
<p><u>Solution C1</u></p> <p>TPABr 2.16 g            NaCl 40.59 g            NaOH 2.39 g            De-ionized water 208 ml            H<sub>2</sub>SO<sub>4</sub> 1.55 ml</p>	<p><u>Solution C3</u></p> <p>NaCl 26.27 g            De-ionized water 104 ml</p>

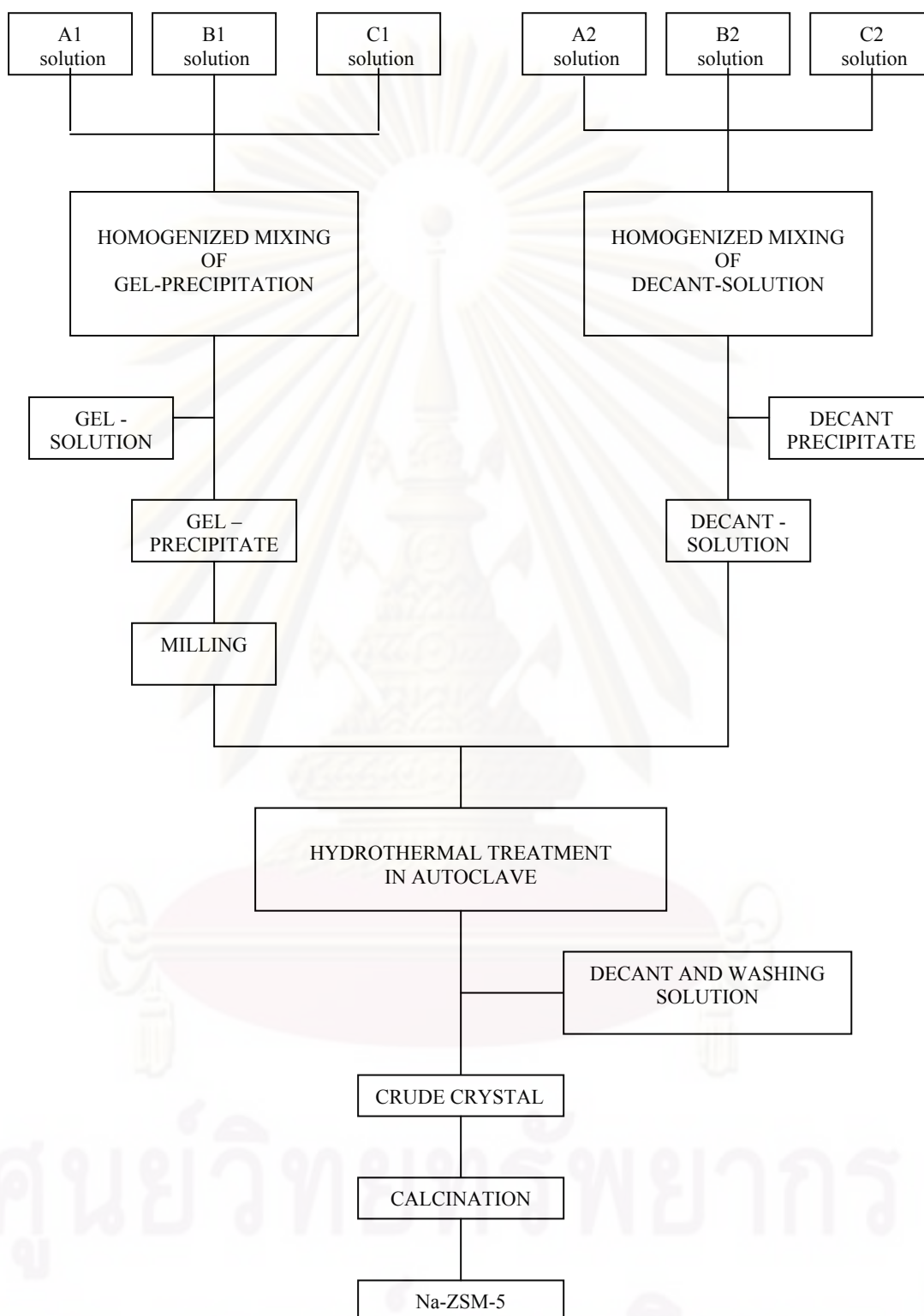


**Figure 4.1** The preparation procedure of Na-ZSM-5 by rapid crystallization method.

#### 4.1.2.1 Preparation of Gel Precipitation and Decantation Solution

A supernatant liquid was separated from the gel, which was important for preparing the uniform crystals. A gel mixture was prepared by adding solution A-1 and solution B-1 into solution C-1 drop wise with vigorous stirring using a magnetic stirrer at room temperature. The pH of the mixed solution was maintained within the range 9-11 because it was expected that this pH range was suitable for precipitation. The gel mixture was separated from the supernatant liquid by a centrifuge. The precipitated gel mixture was milled for 1 h by a powder miller. The milling procedure was as follows: milled 15 min → centrifuge (to remove the liquid out) → milled 15 min → centrifuge → milled 15 min. Milling the gel mixture before the hydrothermal treatment was essential to obtain the uniform, fine crystals.

A decantation solution was prepared by adding solution A-2 and solution B-2 into solution C-2 same as for the preparation of the gel mixture. During the time the supernatant liquid from A-2, B-2, and C-2 is mixing together. The pH of the solution was adjusted to between 9-11.  $\text{H}_2\text{SO}_4$  (conc.) or 1 M NaOH solution were used to adjust pH of the decant mixture to an appropriate level if it is necessary. The colorless supernatant liquid was separated from the mixture by sedimentation and centrifugation.

#### 4.1.2.2 Crystallization

The mixture of the milling precipitate and the supernatant of decant solution was charged in a 500 ml Pyrex glass container. The glass container was placed in a stainless steel autoclave. The atmosphere in the autoclave was replaced by nitrogen gas and pressurized up to 3 kg/cm<sup>2</sup> gauge. Then the mixture in the autoclave was heated from room temperature to 160 °C in 90 min and then up to 210 °C with a constant heating rate of 12 °C/h while being stirred at 60 rpm, followed by cooling of the hot mixture to room temperature in the autoclave overnight. The temperature was programmed to minimize the time necessary for the crystallization. The product crystals were washed with de-ionized water about 8 times using the centrifugal



separator (about 15-20 min. for each time), to remove  $\text{Cl}^-$  from the crystals, and dried in an oven at  $110\text{ }^\circ\text{C}$  for at least 3 h.

#### 4.1.2.3 Calcination

The dry crystals were calcined in an air stream at  $540\text{ }^\circ\text{C}$  for 3.5 h, by heating them from room temperature to  $540\text{ }^\circ\text{C}$  in 1 h, to burn off the organic template and leave the cavities and channels in the crystals. The calcined crystals were finally cooled to room temperature in a desiccator. The obtained Na-MFI was the parent ZSM-5 zeolite which was further transformed to the other appropriate forms for the experiments in this study.

Moreover, the Na-ZSM-5 obtained from each batch was checked by using the X-Ray Diffraction (XRD) analysis to confirm the ZSM-5 structure and crystallinity of sample. If, unfortunately, the XRD pattern could not be acceptable, the sample would be discarded and a new sample has to be made.

#### 4.1.2.4 $\text{NH}_4^-$ and H- form ZSM-5

To make  $\text{NH}_4$ -ZSM-5, the parent Na-ZSM-5 powder was firstly mixed with 1 M  $\text{NH}_4\text{NO}_3$  solution at 30 ml per gram of catalyst. In the procedure, the catalyst amounts did not exceed 5 grams to approach complete exchange. The slurry of zeolite and solution was then stirred and heated on a hot plate, maintained at  $80\text{ }^\circ\text{C}$  by reflux.

After heating the mixture for about 1 h, the mixture was cooled down to room temperature and centrifuged to remove the used solution. The remained crystals were mixed again with  $\text{NH}_4\text{NO}_3$  solution in the same amount. The previous step was repeated. The exchanged catalyst was then washed twice with deionized water by using a centrifugal separator. Then, the ion exchange crystal was dried at  $110\text{ }^\circ\text{C}$  for at least 3 h. in oven. The dried catalyst was obtained the  $\text{NH}_4$ -form of ZSM-5. The  $\text{NH}_4$ / ZSM-5 was converted to H-form ZSM-5 by removing  $\text{NH}_3$  species from the catalyst surface.  $\text{NH}_3$  can be removed by thermal treatment of the  $\text{NH}_4$ -ZSM-5 zeolite. This was done by heating a sample in a furnace from ambient temperature to

540 °C in 1 h and holding the sample at 540 °C for 3.5 h. After this step, the obtained crystals were H-zeolite.

#### 4.1.2.5 Preparation of H-ZSM-5 with various crystallinity.

The H-ZSM-5 zeolite catalyst was calcined in air at room temperature to 600 °C (heating rate 10 °C/min) and then heated that from 600 °C to 850 °C (heating rate 1.67 °C/min) and holding the sample at 850°C for 30 min. The water was filled in saturator glass and bubbling by nitrogen gas. And that was maintained at desire temperature. In this step (hold at 850°C for 30 mins), the as-received sample was pretreated with water 0% and 20% mol.

#### 4.1.2.6 Preparation of H-ZSM-5 with various crystallize size.

The crystallization process, the mixture in the autoclave was heated from room temperature to 160 °C in 90 min. and then up to 210 °C in 4.5, 7.5 and 10.5 hr. In interval temperature (160 °C - 210 °C) was different heating rate. So that, the various crystallize size of H-ZSM-5 zeolite catalyst got from different crytallization time (6, 9 and 12 hr.)

## 4.2 Pretreatment condition

Before reaction, The catalysts(0.2 g) were pretreated by helium in situ at 250°C for 1 h.

## 4.3 Characterization

### 4.3.1 X- Ray Diffraction analysis (XRD)

Crystallinity and X-ray diffraction (XRD) patterns of the catalysts were performed by a X-ray diffractometer SEIMENS D500 connected with a personal computer with Diffract AT version 3.3 program for fully control of the XRD analyzer.

The experiments were carried out by using  $\text{CuK}\alpha$  radiations with Ni filter and the operating condition of measurement are shown as follows:

2 $\theta$ range of detection	:	4 – 50 °
Resolution	:	0.04 °
Number of Scan	:	20

The functions of based line subtraction and smoothing were used in order to get the well formed XRD spectra.

#### 4.3.2 X-Ray Fluorescence analysis (XRF)

Quantities of  $\text{SiO}_2/\text{Al}_2\text{O}_3$  in the sample were determined by atomic absorption spectroscopy using Oxford Modle ED 2000 at the Scientific and Technological Research Equipment Centre, Chulalongkorn University (STREC) was used for this purpose.

#### 4.3.3 BET surface area measurement

The surface area ( $A_{\text{BET}}$ ) of the samples was calculated using BET technique, Micromeritics ASAP 2020.

#### 4.3.4 Scanning Electron Microscopy (SEM)

Scanning Electron Microscopy was employed for including the shape and size of the prepared zeolite crystal. The JEOL JSM-35 CF model at the Scientific and Technological Research Equipment Centre, Chulalongkorn University (STREC) was used for this purpose

#### 4.3.5 Temperature Programmed Adsorptions of Ammonia (NH<sub>3</sub>-TPD)

The acid properties were observed by Temperature programmed desorption (TPD) equipment by using micromeritics chemisorb 2750 Pulse Chemisorption System.

### 4.4 Reaction Testing

#### 4.4.1 Chemicals and Reagents

Methanol was available from MERCK, 99.9 % for methanol conversion.

#### 4.4.2 Instruments and Apparatus

(a) Reactor: The reactor was a conventional micro reactor made from a glass tube with 6 mm inside diameter. The reaction was carried out under He gas flow and atmospheric pressure.

(b) Automatic Temperature Controller: This unit consists of a magnetic switch connected to a variable voltage transformer and a RKC temperature controller connected to a thermocouple attached to the catalyst bed in reactor. A dial setting established a set point at any temperatures within the range between 100°C to 300°C.

(c) Electric Furnace: This supply the required heated to the reactor for reaction. The reactor could be operated from room temperature up to 700° C at maximum voltage of 220 volt.

(d) Gas Controlling Systems: Helium was equipped with pressure regulator (0-120 psig), an on-off valve and a needle valve were used to adjust flow rate of gas.

(e) Gas Chromatographs: Operating conditions were shown in Table 4.3.



**Table 4.3** Operating condition for gas chromatograph

Gas chromatograph	Shimadzu GC8ATP
Detector	TCD
Column	Porapack-N
Carrier gas	He (99.999%)
Carrier gas flow	50 ml./min.
Column temperature	
- Initial	100°C
- Final	100°C
Detector temperature	100°C
Injector temperature	100°C
Current	80 mA
Analyzed gas	Methanol DME

Gas chromatograph	Shimadzu GC
Detector	FID
Column	
Carrier gas	N <sub>2</sub> , H <sub>2</sub> , air (99.999%)
Carrier gas flow	50 ml./min.
Column temperature	
- Initial	75°C
- Final	75°C
Detector temperature	150°C
Injector temperature	100°C
Current	80 mA
Analyzed gas	C <sub>1</sub> -C <sub>4</sub>

#### 4.4.3 Reaction Method

The methanol conversion was carried out by using a conventional flow as shown in Figure 4.2. A 0.2 portion of the catalyst was packed in the glass tubular reactor of 6 mm inner diameter. Helium gas was supplied from a cylinder to control methanol partial pressure and flow rate of the system. Methanol conversion reaction was carried out under the following conditions:

Total pressure, 1 atm; methanol composition 20%; balance gas, helium; GHSV, 4250 h<sup>-1</sup>; reaction temperature 100-300 °C

The procedure used to operate this reactor was follows;

- 1) Adjust the pressure of helium gas to 1 kg/cm<sup>2</sup>, and allow the gas to flow through a Rota meter, measure the outlet gas flow rate by using a bubble flow meter.
- 2) Heat up the reactor (under He flow) by raising the temperature from room temperature to 250° C and then hold at this temperature about 60 min for preheating catalyst.
- 3) Put methanol 20 ml in saturator and set the temperature of water bath at 29°C at this temperature. The concentrations of methanol in saturator were 20% mol.
- 4) Start to run the reaction by adjusting three way valves to allow helium gas to pass through reactants inside saturator in water bath.
- 5) Take sample for analyzed by gas chromatograph after the reaction ran for 30 min.

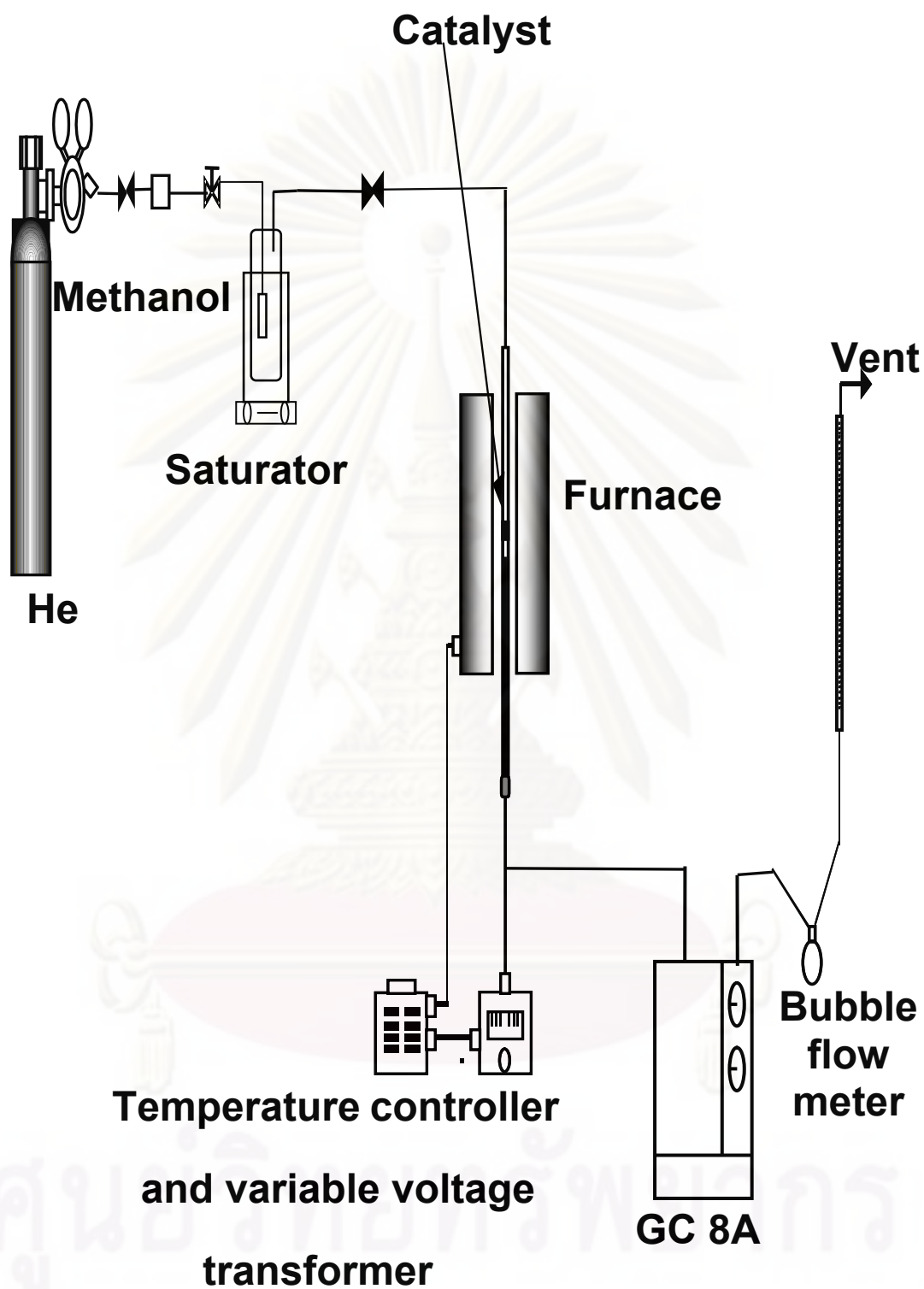


**Figure 4.2** Schematic diagram of the reaction apparatus for reaction.

## CHAPTER V

### RESULTS AND DISCUSSION

In this Chapter described the results and discussion of this experimental. That are divided in three sections. The first part is effect of Si/Al atomic ratios and reaction temperatures on synthesis of dimethyl ether from methanol. This part consist of, characterization of the H-ZSM-5 that various of Si/Al atomic ratio (20 , 40 , 80 and 160) by following :

- X- Ray Diffraction analysis (XRD)
- X-Ray Fluorescence analysis (XRF)
- Scanning Electron Microscopy (SEM)
- BET surface area measurement
- Temperature Programmed Adsorptions of Ammonia (NH<sub>3</sub>-TPD)

and catalytic reaction is represented into the temperature range with studied ( 100 – 300 °C ). These data are describe in section 5.1.

Secondly, this part is investigated in effect of particle sizes on methanol dehydration to synthesize dimethyl ether. The details of this part are composed of characterization (same above method) and reaction test with temperature in the range which data is explained in section 5.2.

At the last part is researched about effect of crystallinity of H-ZSM-5(Si/Al = 40) zeolite catalyst on synthesis of dimethyl ether from methanol. The particulars of this section are composed of data of characterization and reaction testing respectively that is showed in section 5.3.



## 5.1 Effect of Si/Al ratios and reaction temperature on methanol dehydration.

### 5.1.1 Catalyst characterization

#### 5.1.1.1 X- Ray Diffraction Pattern

From Figure 5.1 show that the X-Ray Diffraction pattern of the commercial H-ZSM-5 zeolite catalyst. The characteristic peak of this pattern indicated the MFI structure which its had six prominent points as follows at  $2\theta$  as 8, 8.8, 14.8, 23.1, 24, 29.5 that reported by Zhoao et al. Moreover, the characteristic peak use to check the prepared zeolite catalyst that its was identical reference zeolite catalyst or not.

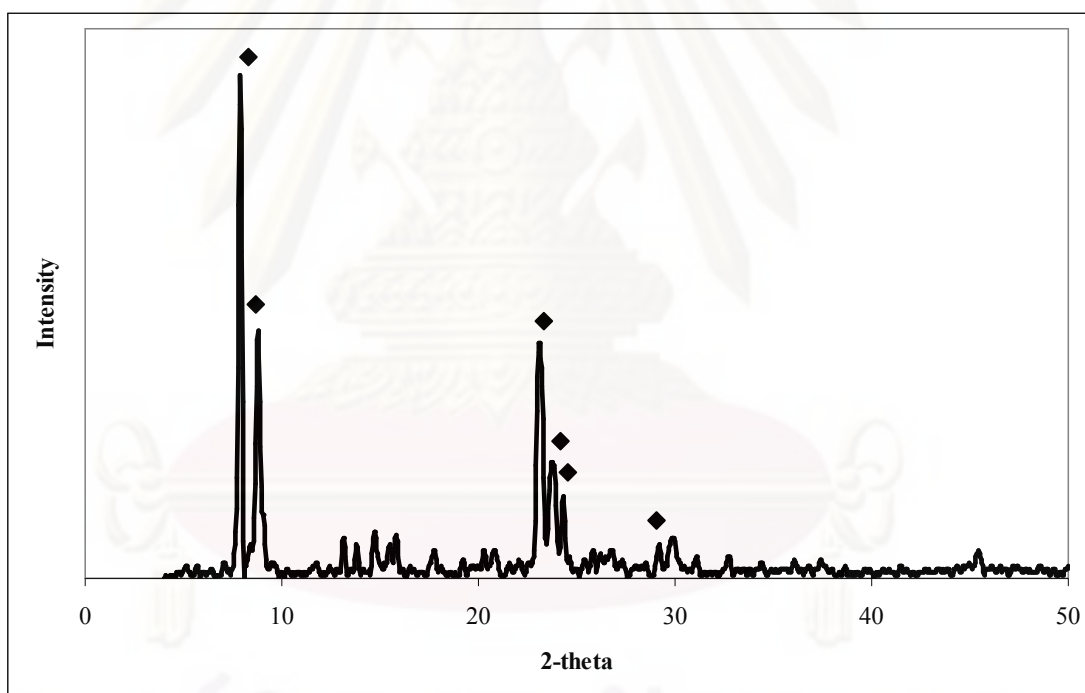


**Figure 5.1** The X-ray Diffraction pattern of the commercial H-ZSM-5 zeolite catalyst.

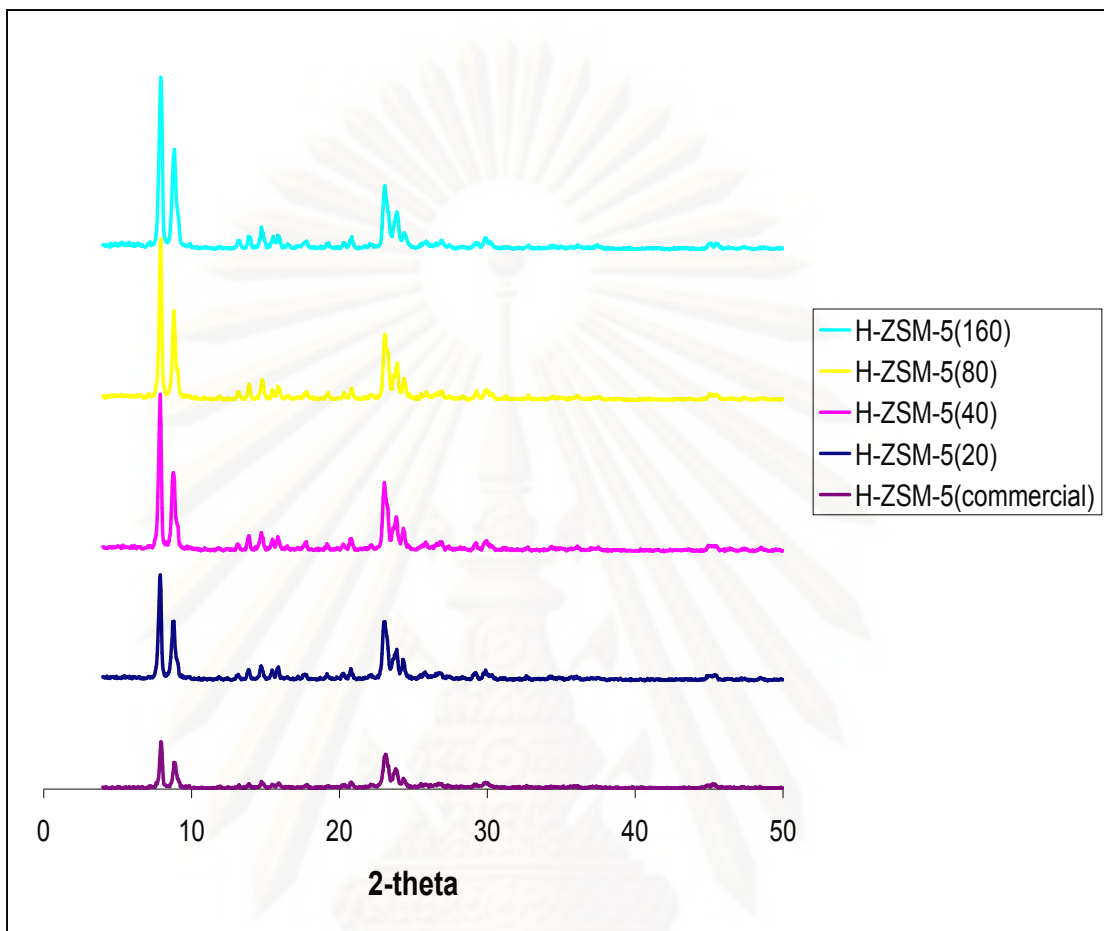


**Figure 5.2** The X-ray Diffraction patterns of the H-ZSM-5 samples with various Si/Al atomic ratio.

X-ray Diffraction patterns of the H-ZSM-5 samples with various Si/Al atomic ratio are compared in Figure 5.2. It can be seen that all the XRD pattern of prepared zeolite catalysts are nice correspond to the XRD pattern of reference zeolite. So, demonstration as variousness Si/Al atomic ratio of zeolite catalysts do not affect on MFI or ZSM-5 structure. From Table 5.1, indicated that the Si/Al ratio increasing that cause of increasing in XRD crystallinity of zeolite catalysts[33,34]. So that the prepared zeolite catalysts were investigated in the next step.

**Table 5.1** Crystallinity of H-ZSM-5 zeolite catalyst with different Si/Al ratios.

Zeolite catalysts	% Crystallinity <sup>a</sup>
H-ZSM-5 (20)	70.7
H-ZSM-5 (40)	96.8
H-ZSM-5 (80)	98.5
H-ZSM-5 (160)	100

a = base on XRD measurement of H-ZSM-5(160).

#### 5.1.1.2 Chemical composition

XRF is used to analyze for chemical composition which this work want to know the quantity of silicon and aluminium in prepared zeolite catalysts. Because of quantity of chemical composition has an affect on catalytic performance. The ratios of silicon and aluminium are demonstrated in Table 5.2.

**Table 5.2** Si/Al ratio of H-ZSM-5 zeolite catalysts.

Zeolite catalysts	Si/Al ratio loaded	Si/Al ratio observed
H-ZSM-5 (20)	20	35.9
H-ZSM-5 (40)	40	56.9
H-ZSM-5 (80)	80	93.4
H-ZSM-5 (160)	160	152.6

From Table 5.2, showed that the Si/Al ratios loaded was nearly composition with Si/Al ratio observed which that corresponding to our expectation. Further, I were investigated in other characteristic of H-ZSM-5 zeolite catalysts.

#### 5.1.1.3 Scanning Electron Microscopy

In this work, Scanning Electron Microscopy or SEM is used to examine in the particle size of prepared H-ZSM-5 zeolite catalysts. From other research work investigated the crystallite size of H-ZSM-5 zeolite had effect on

catalytic performance. So, I verify its by SEM which the data picture are showed in below.

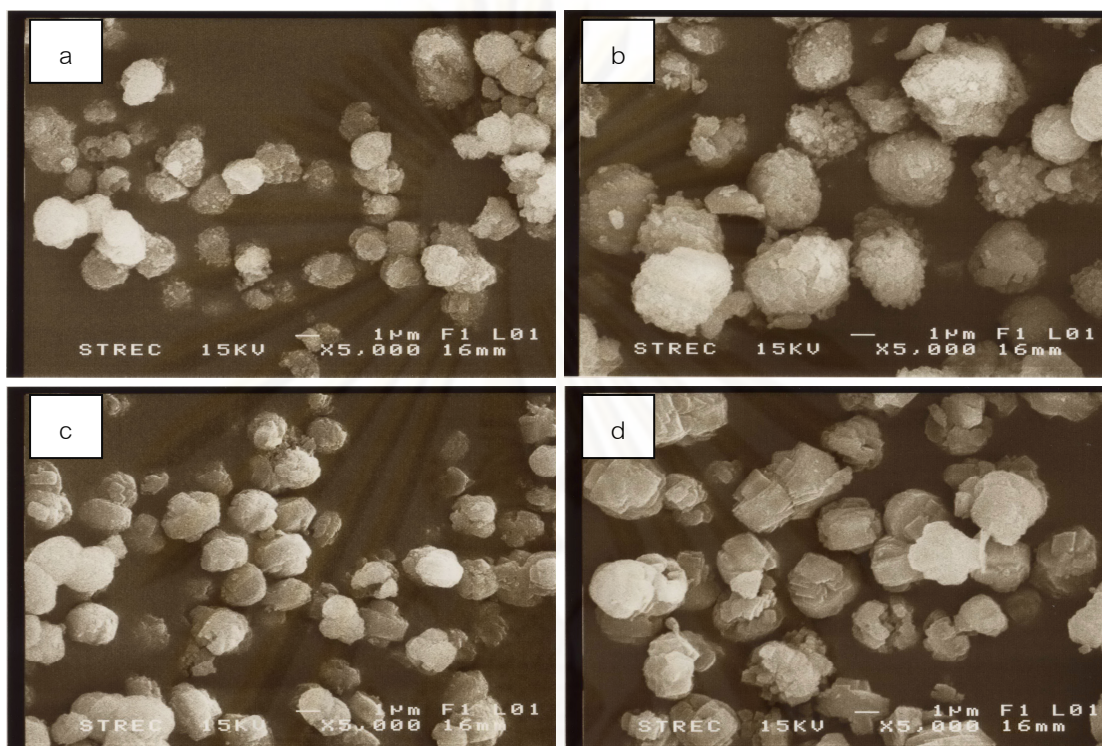


**Figure 5.3** SEM pictures of H-ZSM-5 sample with various Si/Al ratios that following: (a) H-ZSM-5(20), (b) H-ZSM-5(40), (c) H-ZSM-5(80) and (d) H-ZSM-5(160).

**Table 5.3** Particle sizes of H-ZSM-5 zeolite catalysts.

Zeolite catalysts	Particle size( $\mu\text{m}$ )
H-ZSM-5 (20)	1.5
H-ZSM-5 (40)	3.2
H-ZSM-5 (80)	2.2
H-ZSM-5 (160)	2.9

In addition, the SEM pictures of H-ZSM-5 sample with various Si/Al ratios in Figure 5.3 shows that the average crystallite sizes of microcrystalline H-ZSM-5 zeolites used in this work. And then, from Figure 5.3 that can calculated of crystallite sizes of prepared H-ZSM-5 zeolites which are showed in Table 5.3 that



demonstrated the prepared H-ZSM-5 zeolite catalysts are average particle size within the range 1.5 - 3.2  $\mu\text{m}$ . And find out that H-ZSM-5(20) zeolite catalyst has smallest particle size (1.5  $\mu\text{m}$ .) Moreover, the largest particle size are H-ZSM-5(40) zeolite catalyst (3.2  $\mu\text{m}$ ).

From XRD patterns of prepared H-ZSM-5 zeolite catalyst in Figure 5.2 showed that the sample H-ZSM-5(20) zeolite catalyst has a much lower intensity or lowest in crystallinity which is probably due to the much smaller crystals size and thus to higher number of framework defects with respect to larger crystals size[34].

#### 5.1.1.4 BET surface area

Table 5.4 is described BET surface area of various prepared zeolite catalysts.

**Table 5.4** BET surface area of various prepared zeolite catalysts.

Zeolite catalysts	BET surface area ( $\text{m}^2/\text{g}$ of catalysts)
H-ZSM-5 (20)	330.4
H-ZSM-5 (40)	368.9
H-ZSM-5 (80)	369.8
H-ZSM-5 (160)	373.7

\* prepared by rapid crystallization

From Table 5.4, The surface area of various prepared zeolite catalysts are nearly value. However, the value of Si/Al ratio increase but BET surface area is similarity. So, indicate that the Si/Al ratio has no obvious effect on BET surface area.

#### 5.1.1.4 Temperature Programmed Adsorptions of Ammonia (NH<sub>3</sub>-TPD)

This part is observed the acid properties of prepared H-ZSM-5 zeolite catalysts.

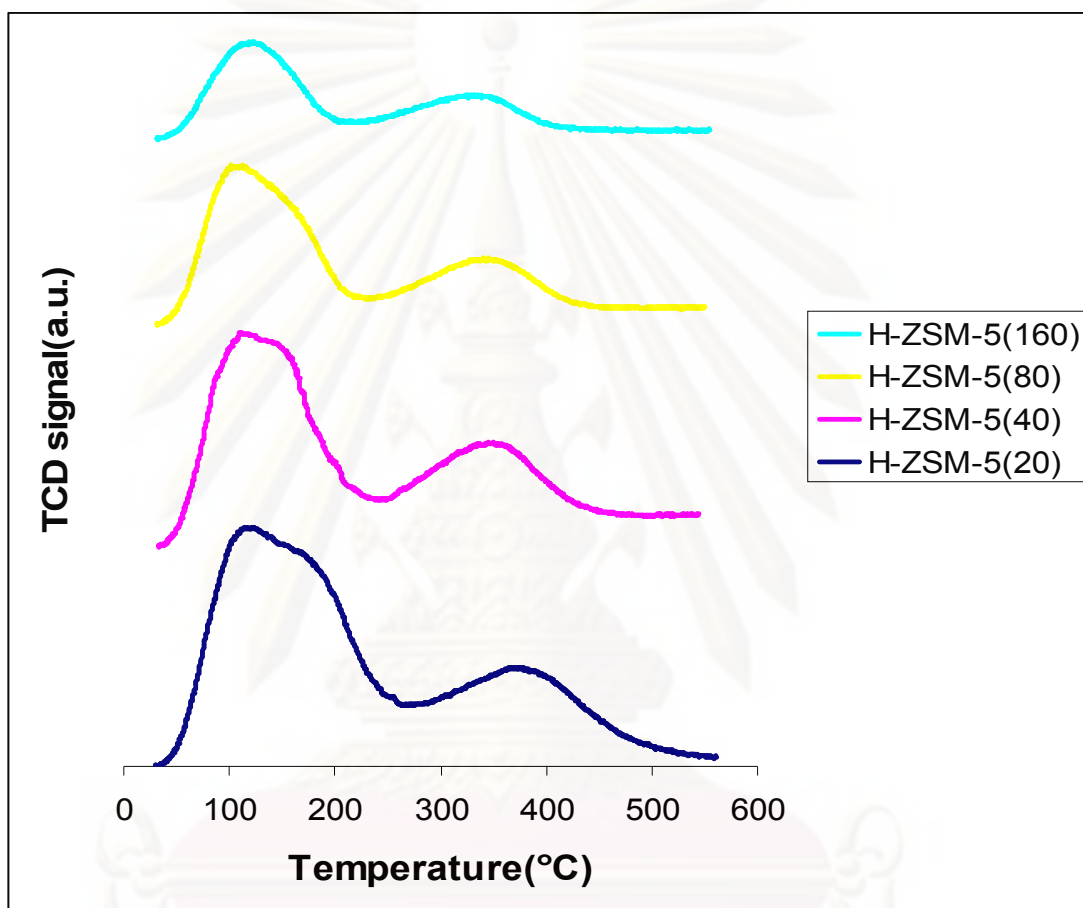


**Figure 5.4** NH<sub>3</sub>-TPD profiles of H-ZSM-5 zeolite catalysts with various Si/Al ratios.

**Table 5.5** The amount of acidity of H-ZSM-5 zeolite catalysts with different Si/Al ratios.

Zeolite catalysts	Weak acidity ( $\mu\text{mol}$ $\text{NH}_3/\text{g.catalyst}$ )	Strong acidity ( $\mu\text{mol}$ $\text{NH}_3/\text{g.catalyst}$ )	Total acidity ( $\mu\text{mol}$ $\text{NH}_3/\text{g.catalyst}$ )
H-ZSM-5(20)	2316.1	654.0	2970.1
H-ZSM-5(40)	1563.8	511.1	2074.9
H-ZSM-5(80)	1186.1	343.2	1529.3
H-ZSM-5(160)	615.5	217.3	832.8

From Figure 5.4 represents the  $\text{NH}_3$ -TPD profiles of H-ZSM-5 zeolite catalysts with different Si/Al ratios. There are two desorption peaks for the H-ZSM-5 zeolite catalysts that it is prominent. The one center in 110 - 120 °C and the other in 330 – 380 °C. These two outstanding peaks are the weak acid sites and strong acid sites, respectively. When increasing the Si/Al ratio of the H-ZSM-5 zeolite catalysts, the amount of both strong and weak acid sites of the H-ZSM-5 represented decreasing. The quantity of acidity of sample H-ZSM-5 zeolite catalysts is showed in Table 5.5, demonstrated the Si/Al increase with decrease total acidity. And then, H-ZSM-5(20) is highest total acidity. Moreover, the position of weak acid sites were not much changed when increasing the Si/Al ratio. But the another desorption peak or strong acid sites shifted to a lower temperature when Si/Al ratio of H-ZSM-5 zeolite catalysts increased. From this the data indicating that the acid strength of H-ZSM-5 zeolite catalysts decreases with a increase in the Si/Al ratio that corresponding to previous research of Ji-Hyun Kim et al[35].

### 5.1.2 Catalytic reaction

In this section is investigated the catalytic performance of the H-ZSM-5 zeolite catalysts by methanol dehydration reaction. Methanol dehydration was carried out in a glass reactor (6 mm.) that fixed bed type. In this experiment each catalyst (0.2 g.) was loaded in the reactor. The methanol was introduced to the reaction zone by

bubbling He (99.9%) through a glass saturator filled with methanol maintain at 29°C. The feed composition was maintained methanol:He = 20:80 and GHSV was 4250 h<sup>-1</sup>. The reaction was carried out at atmospheric pressure and reaction temperature with in the range 100 – 300 °C. The effluent gas was analyzed on-line by GC with FID and TCD detector. The gas line was maintained at 120 °C to prevent condensation of the reactant and products.

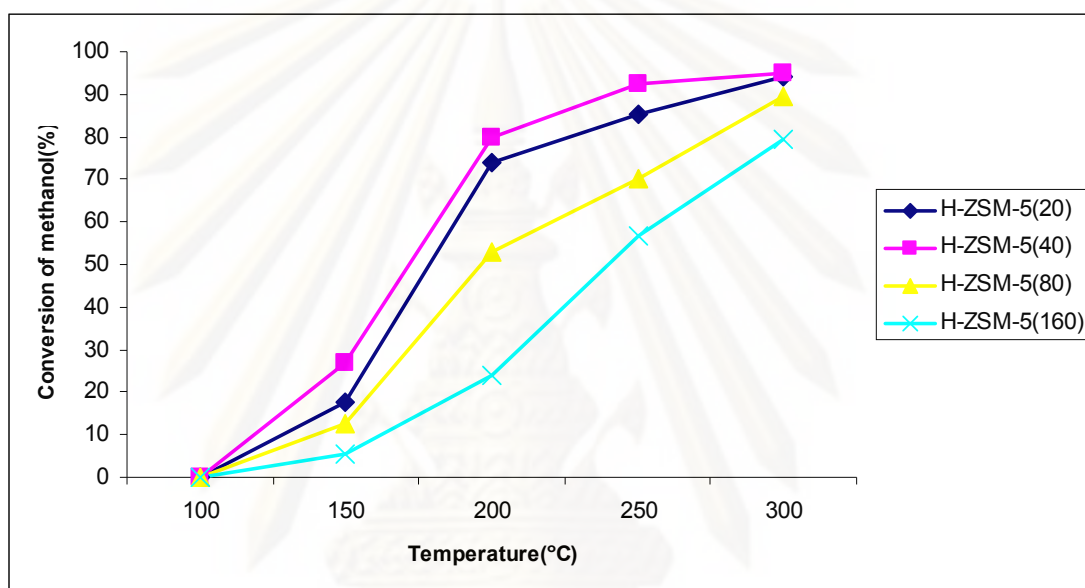


**Figure 5.5** Dehydration of methanol over H-ZSM-5 zeolite catalysts with various Si/Al ratios. GHSV = 4250 h<sup>-1</sup>, methanol:He = 20:80.



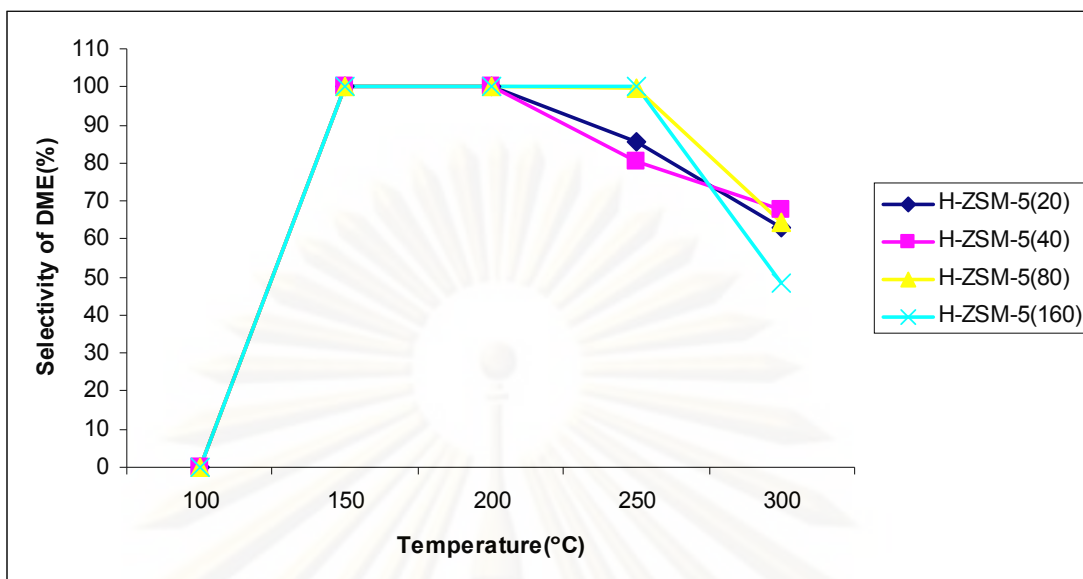


Figure 5.6 DME selectivity over H-ZSM-5 zeolite catalysts with various Si/Al ratios.

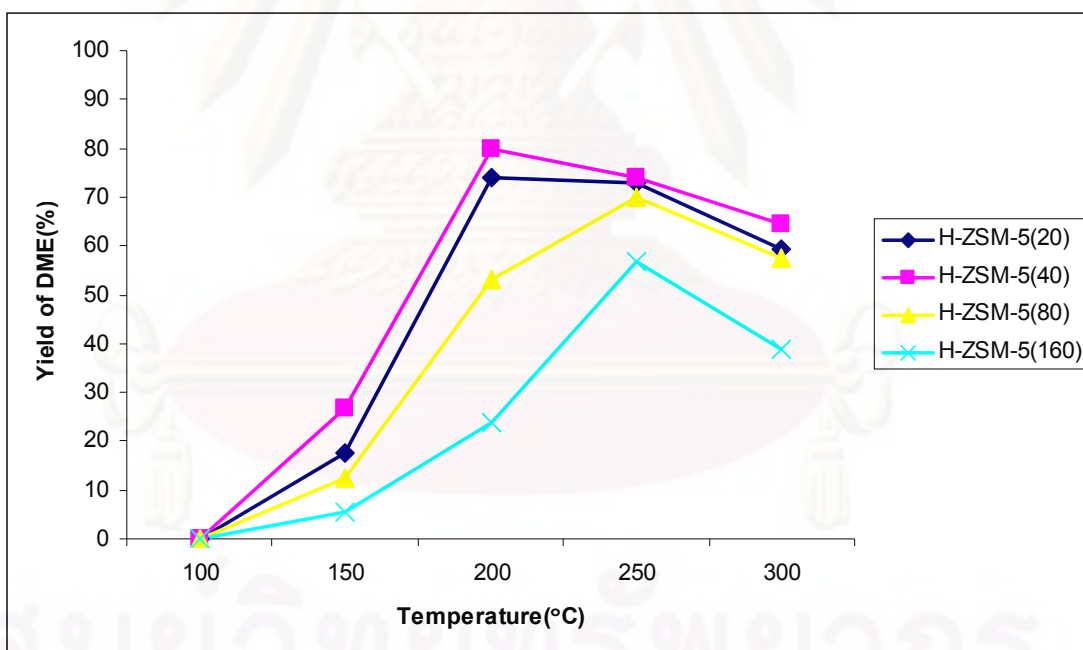
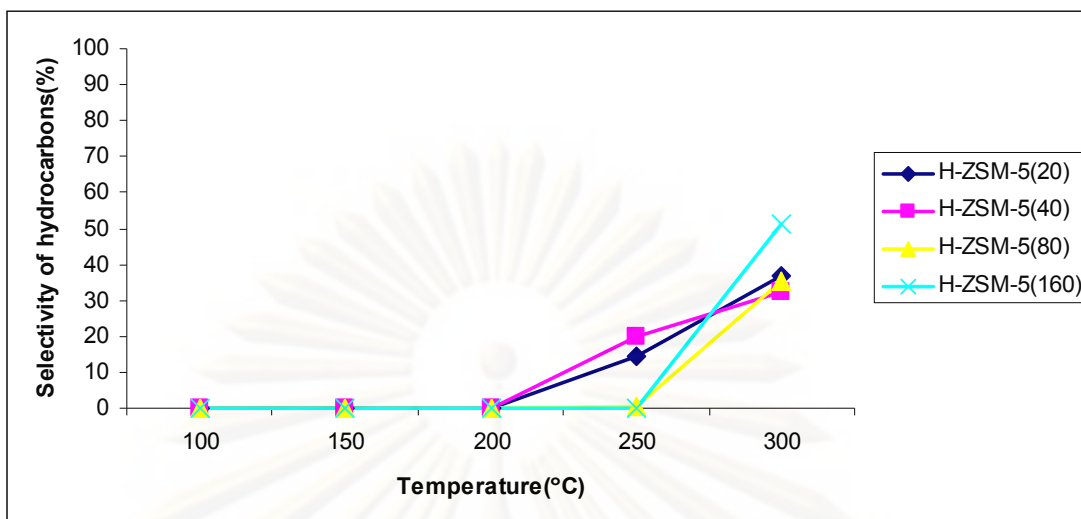


Figure 5.7 DME yield over H-ZSM-5 zeolite catalysts with various Si/Al ratios.



**Figure 5.8** Hydrocarbons selectivity over H-ZSM-5 zeolite catalysts with various Si/Al ratios.

Methanol conversion are showed as in Figure 5.5 with various Si/Al ratios of H-ZSM-5 zeolite catalysts and temperature. The results for the dehydration of methanol to DME over the different zeolite catalysts show that the activity follow the order of H-ZSM-5(40)>H-ZSM-5(20)>H-ZSM-5(80)>H-ZSM-5(160). Moreover, the methanol conversion of each prepared zeolite catalysts increase with increase in temperature reaction.

In the past, the methanol dehydration reaction was used acid solid catalysts, other researcher investigated regarding activity for methanol dehydration on various Si/Al ratios of H-ZSM-5 zeolite catalyst and found that the methanol dehydration rate was dependent on the acidity of the solid acid catalysts. So the activity for methanol dehydration of H-ZSM-5 zeolite catalysts must increased with a decreased in the Si/Al ratio[35]. Further, in this work found that H-ZSM-5(20) was higher acidity than other zeolite catalyst but its not highest catalytic performance. From Figure 5.5 showed that H-ZSM-5(40) zeolite catalyst was highest activity for methanol dehydration even though H-ZSM-5(40) was lower in acidity than H-ZSM-5(20) zeolite catalyst.

The result of DME selectivity over different zeolite catalysts as showed in Figure 5.6. Found that, at begin the temperature 100°C that no occurred DME in the products. The selectivity of methanol to DME was up to 100% with in the temperature range 150-200°C and then DME selectivity was reduced when increasing the temperature. At temperature is 250°C, the selectivity of DME on H-ZSM-5(80) and H-ZSM-5(160) zeolite catalysts was much higher than H-ZSM-5(20) and H-ZSM-5(40) zeolite catalysts. Due to the strong acid site of H-ZSM-5(80) and H-ZSM-5(160) zeolite catalysts was lower than H-ZSM-5(20) and H-ZSM-5(40) zeolite catalysts so that cause the selectivity of hydrocarbons on H-ZSM-5(80) and H-ZSM-5(160) zeolite catalysts was much lower than H-ZSM-5(20) and H-ZSM-5(40) zeolite catalysts that can see in Figure 5.8, showed that in the temperature range 100-150°C that not occurred hydrocarbons in the product. For each Si/Al ratio of H-ZSM- zeolite catalyst, when increasing the temperature reaction, the selectivity of hydrocarbons increasing. The strong acid site of H-ZSM-5 zeolite catalyst promote the generation of secondary products like hydrocarbons, resulting in low selectivity for DME[13,31].

From Figure 5.7, showed that the H-ZSM-5(40) zeolite catalyst was highest on catalytic performance. Moreover, DME occurred highest for yield of DME( $\approx$  80%) at 200°C. On the other hand, the optimum reaction temperature that synthesis of DME was 200°C.

## **5.2 Effect of particle size of H-ZSM-5(40) zeolite catalysts on methanol dehydration**

From previous study at above, H-ZSM-5(40) zeolite catalyst was highest on catalytic performance. So this section I selected the H-ZSM-5(40) zeolite catalyst which investigated about effect of crystallite size on methanol dehydration. Through this work synthesized H-ZSM-5(40) zeolite catalyst that had the smaller particle size.

## 5.2.1 Catalyst Characterization

### 5.2.1.1 X- Ray Diffraction Pattern

Figure 5.9 is the XRD patterns of the different particle size of H-ZSM-5(40) zeolite catalyst which indicated that reducing in particle size does not effect on H-ZSM-5 crystal structures.

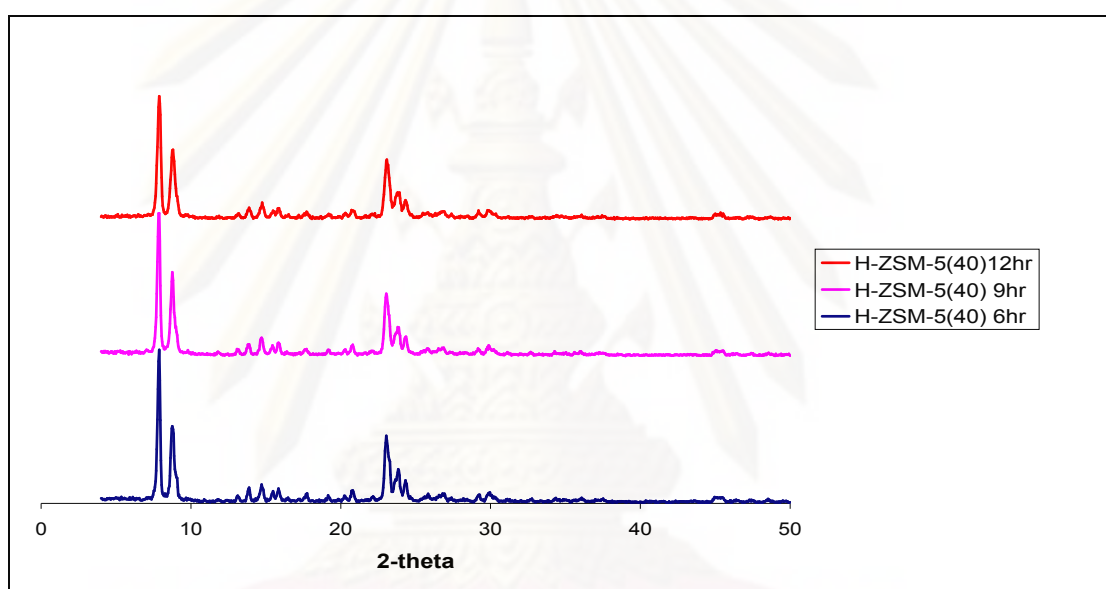


**Figure 5.9** The X-ray Diffraction pattern of the H-ZSM-5(40) zeolite catalysts with various particle sizes.

**Table 5.6** Crystallinity of H-ZSM-5(40) zeolite catalysts with different particle sizes.

Zeolite catalysts	% Crystallinity <sup>a</sup>
H-ZSM-5(40) 6hr.	96.8
H-ZSM-5(40) 9hr.	83.1
H-ZSM-5(40) 12hr.	78.8

a = base on XRD measurement of H-ZSM-5(160).



From Figure 5.9 and Table 5.6 indicated that when increasing the crystallization time in the range 6-9 hr. that make to reduced crystallinity of H-ZSM-5(40) zeolite catalysts from 96.8% to 78.8%.

### 5.2.1.2 Morphology

SEM technique is used to investigated surface of catalyst. In this work, usability this technique for calculated the particle size of zeolite catalysts. The SEM image of different particle size of H-ZSM-5(40) zeolite catalysts as showed in Figure 5.10.

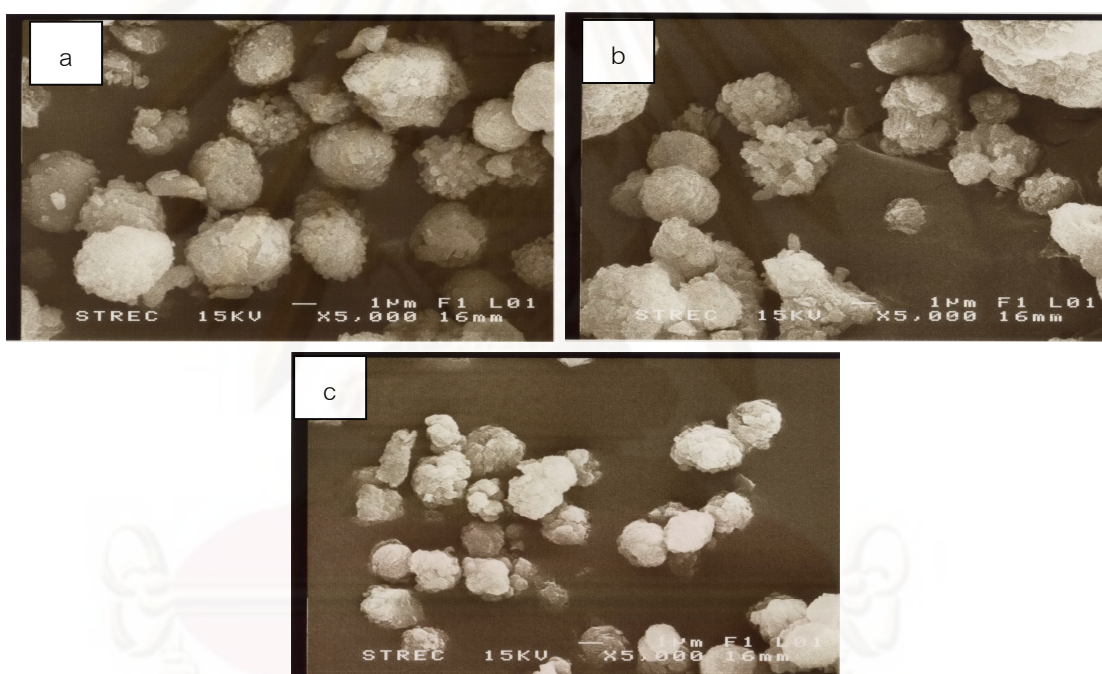


**Figure 5.10** SEM image of H-ZSM-5(40) zeolite catalysts with various particle sizes that following: (a) H-ZSM-5(40) 6hr, (b) H-ZSM-5(40) 9hr, (c) H-ZSM-5(40) 12hr.

**Table 5.7** Particle sizes of H-ZSM-5(40) zeolite catalysts with different crystallization time.

Zeolite catalysts	Particle size( $\mu\text{m}$ )
H-ZSM-5(40) 6hr.	3.8
H-ZSM-5(40) 9hr.	3.1
H-ZSM-5(40) 12hr.	1.9

Crystallite sizes of the H-ZSM-5(40) zeolite catalysts with different crystallization times are compared in Figure 5.10 and Table 5.7. It can be seen that the crystallite size of H-ZSM-5(40) zeolite catalysts decreased with increasing the crystallization time that from 3.8  $\mu\text{m}$  to 1.8  $\mu\text{m}$  which corresponding to previous study of K.Suzuki et al[36].

From XRD patterns of H-ZSM-5(40) zeolite catalysts in Figure 5.9 showed that the H-ZSM-5(40) 12hr zeolite catalyst had lowest the crystallinity because of the much smaller crystals size and thus to higher number of framework defects with respect to larger crystals size[34]. That same as the reason for described about crystallinity of H-ZSM-5 zeolite catalyst in section 5.1.

#### 5.2.1.3 BET surface area

From data of Table 5.8 found that, the BET surface area increase a little with decrease particle size.

**Table 5.8** BET surface area of H-ZSM-5(40) zeolite catalysts with different particle sizes.

Zeolite catalysts	BET surface area ( $\text{m}^2/\text{g}$ of catalysts)
H-ZSM-5(40) 6hr.	368.9
H-ZSM-5(40) 9hr.	377.0
H-ZSM-5(40) 12hr.	391.9

#### 5.2.1.4 Temperature Programmed Adsorptions of Ammonia (NH<sub>3</sub>-TPD)

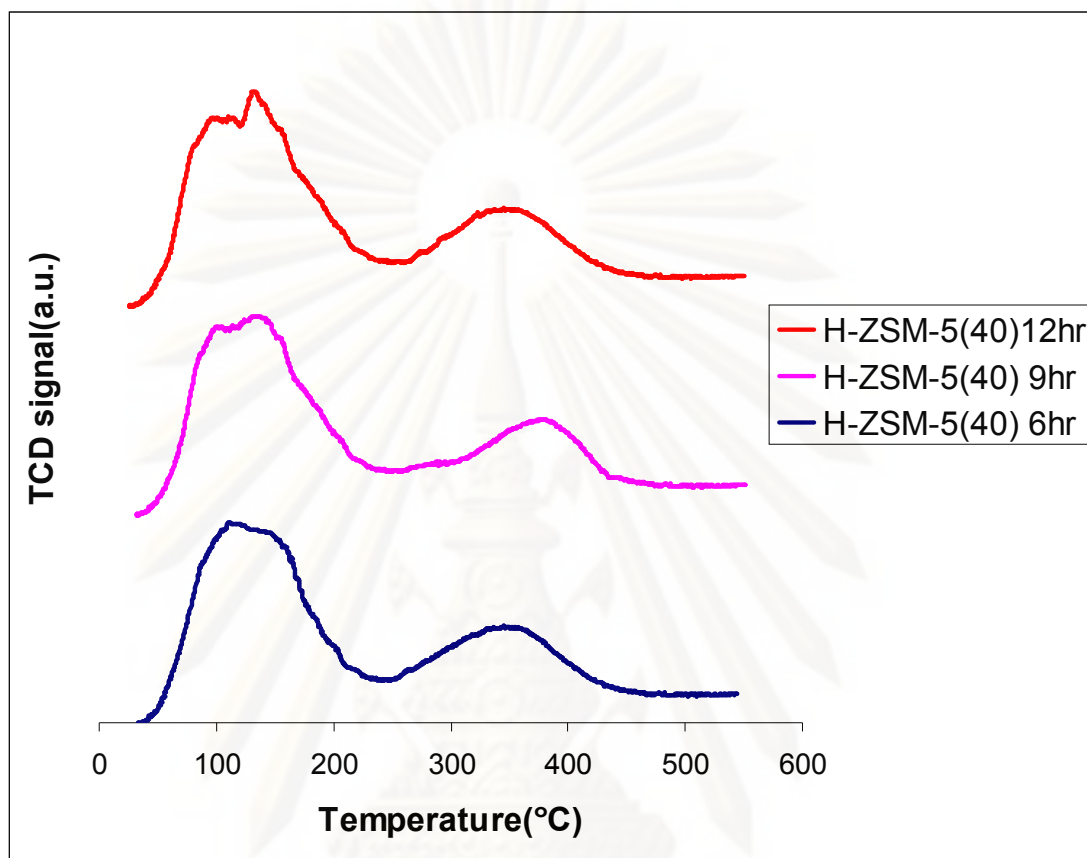


**Figure 5.11** TPD profiles of H-ZSM-5(40) zeolite catalysts with different particle sizes.

**Table 5.9** Acidity of H-ZSM-5(40) zeolite catalysts with different particle sizes.

Zeolite catalysts	Weak acidity ( $\mu\text{mol}$ $\text{NH}_3/\text{g.catalyst}$ )	Strong acidity ( $\mu\text{mol}$ $\text{NH}_3/\text{g.catalyst}$ )	Total acidity ( $\mu\text{mol}$ $\text{NH}_3/\text{g.catalyst}$ )
H-ZSM-5(40) 6hr.	1563.8	511.1	2074.9
H-ZSM-5(40) 9hr.	1648.0	503.3	2151.3
H-ZSM-5(40) 12hr.	1713.5	462.2	2175.7

From Figure 5.11 and Table 5.9 indicated that the weak acidity increased and strong acidity decreased when increasing the crystallization time of H-ZSM-5(40) zeolite catalysts. Thus total acidity increased a little with increasing the crystallization time.

### 5.2.2 Catalytic reaction

This section, comparison the catalytic performance among particle size of H-ZSM-5(40) zeolite catalysts 3.8  $\mu\text{m}$ ., 3.4  $\mu\text{m}$ . and 1.9  $\mu\text{m}$ . In this part selected the reaction temperature equal to 200°C because of its was optimum temperature that from above data in section 5.1. The results are showed in Table 5.10.

**Table 5.10** The effect of particle sizes of H-ZSM-5(40) zeolite catalysts on catalytic performances for synthesis of DME from methanol.

Time of crystallization (hr)	methanol conversion(%)	selectivity(%)		DME yield(%)
		DME	hydrocarbons	
H-ZSM-5(40) 6hr	71.37	99.96	0.04	71.35
H-ZSM-5(40) 9hr	74.92	99.99	0.01	74.91
H-ZSM-5(40) 12hr	81.43	99.99	0.005	81.43

Catalyst 0.2 g; Reaction conditions: T=200°C, P=1atm; methanol 20%; He 80%; flow rate 75 ml/min.

The result of catalytic performances as showed in Table 5.10, it can see that methanol conversion, DME selectivity and DME yield increased with decreasing the particle size of zeolite catalyst because of effect of diffusional resistances. The smaller particle size is made the residence time of DME inside the crystal decrease, thus the DME to be unconverted to hydrocarbons in secondary reaction steps[37]. That's cause increasing the selectivity and yield of DME.



The result from section 5.1 at above, I interested about activity of H-ZSM-5(20) and H-ZSM-5(40) zeolite catalysts. The activity for methanol dehydration of H-ZSM-5 zeolite catalysts must increased with a decreased in the Si/Al ratio[35]. Moreover, in this work found that H-ZSM-5(20) was higher acidity than other zeolite catalyst but its not highest catalytic performance. From Figure 5.5 showed that H-ZSM-5(40) zeolite catalyst was highest activity for methanol dehydration even though H-ZSM-5(40) was lower in acidity than H-ZSM-5(20) zeolite catalyst.

When I considered the result, found that the acidity of H-ZSM-5(20) and H-ZSM-5(40) zeolite catalyst had an adjacent value. Further, the crystal size of H-ZSM-5(20) zeolite catalyst was much smaller than H-ZSM-5(40) zeolite catalysts so in fact H-ZSM-5(20) zeolite catalyst was higher activity than H-ZSM-5(40). But found that once thing, the crystallinity of H-ZSM-5(20) zeolite catalyst was much lower than H-ZSM-5(40).

Thus, I set up the hypothesis of the last section, while the prepared H-ZSM-5 zeolite catalysts had a nearly acidity that the crystallinity may be effect more than crystal sizes on methanol dehydration. Which investigation on the later.

### **5.3 Effect of crystallinity of H-ZSM-5 zeolite catalysts on methanol dehydration**

From the previous section, I set up the hypothesis while the prepared H-ZSM-5 zeolite catalysts had a nearly acidity that effect of crystallinity may be more than crystal sizes on methanol dehydration so I searched the paper for effect of crystallinity of H-ZSM-5 on other reaction. In the past, other researcher studied Influence of crystallinity of zeolite Pd/H-ZSM-5 on catalytic performance in the dehydroalkylation of toluene with ethane. And Arne Bressel et al found that A high crystallinity of the zeolite is beneficial for the catalytic performance in the dehydroalkylation of toluene with ethane. Lower crystallinities result in a reduced time-on-stream stability of the catalyst.

In this section, I synthesized H-ZSM-5 zeolite catalysts that same as in acidity and crystal size but different in the crystallinity for testing my hypothesis.

### 5.3.1 Catalyst Characterization

#### 5.3.1.1 X- Ray Diffraction Pattern

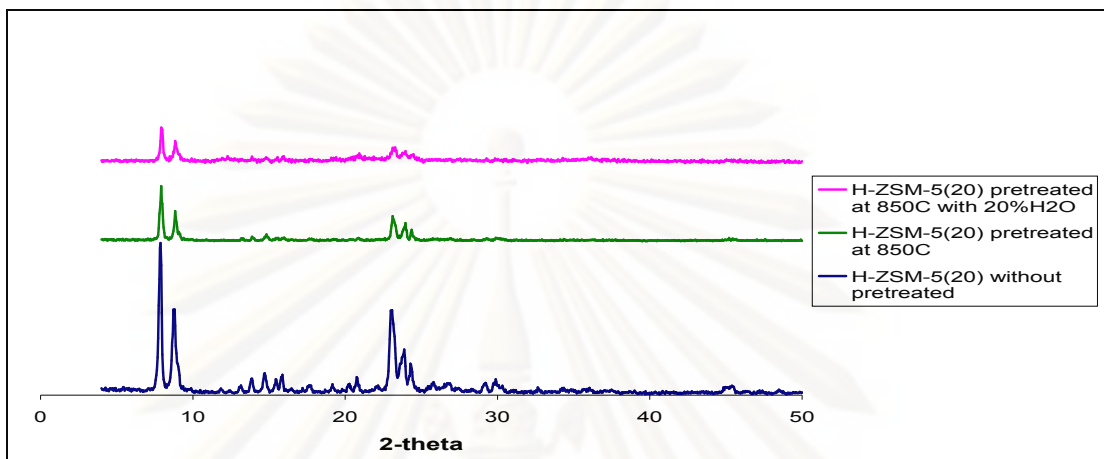


**Figure 5.12** The X-ray Diffraction patterns of the H-ZSM-5(20) zeolite catalysts with different crystallinity.

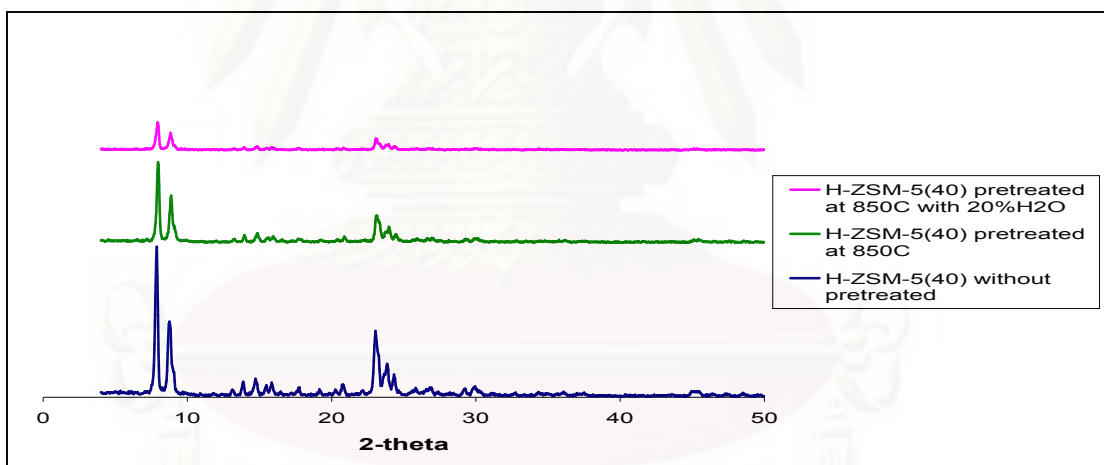


**Figure 5.13** The X-ray Diffraction patterns of the H-ZSM-5(40) zeolite catalysts with different crystallinity.

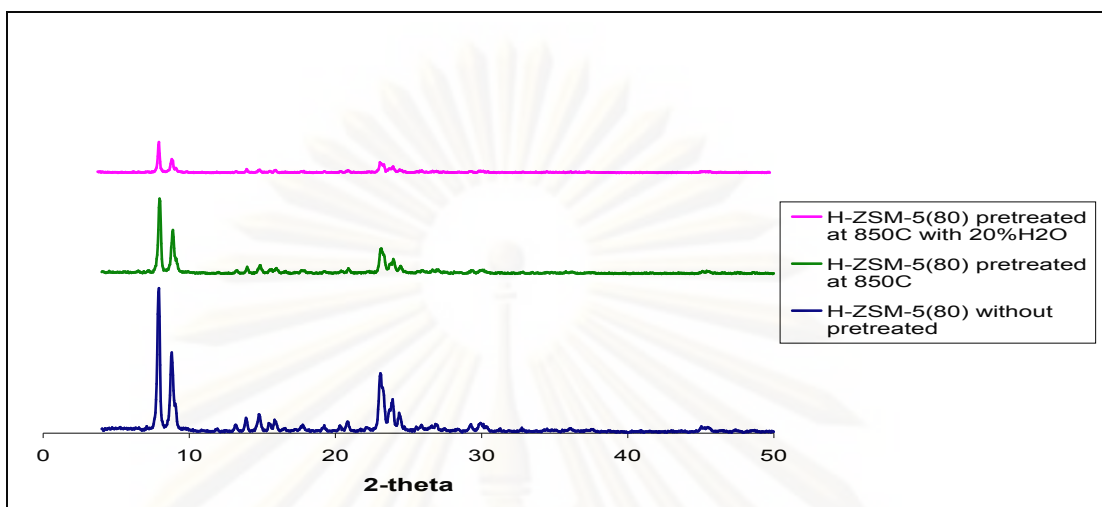


**Figure 5.14** The X-ray Diffraction patterns of the H-ZSM-5(80) zeolite catalysts with different crystallinity.

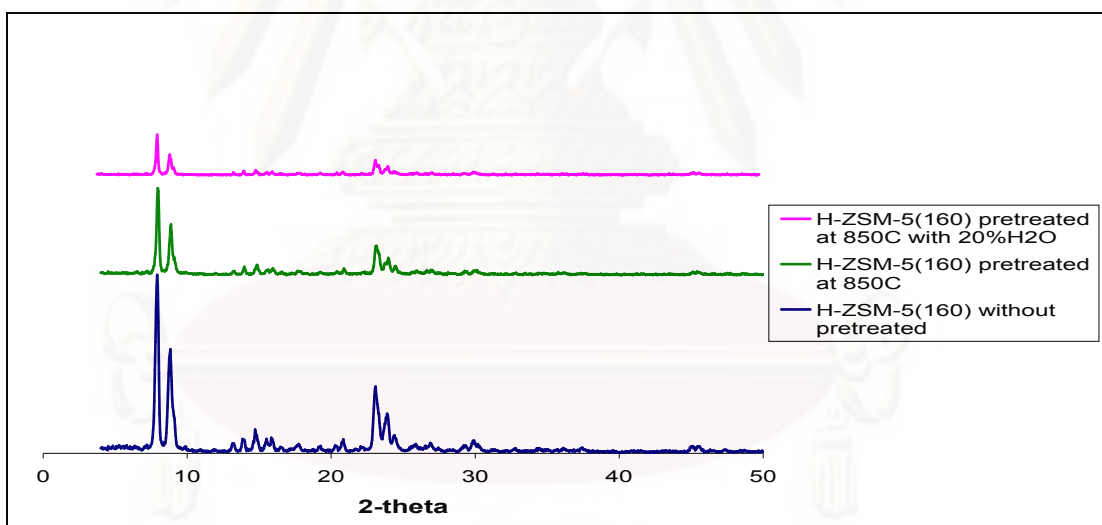


**Figure 5.15** The X-ray Diffraction patterns of the H-ZSM-5(160) zeolite catalysts with different crystallinity.

**Table 5.11** Crystallinity of H-ZSM-5 zeolite catalyst with different Si/Al ratios.

Zeolite catalysts	% Crystallinity <sup>a</sup>
H-ZSM-5(20) without pretreated	70.7
H-ZSM-5(20) pretreated at 850°C	22.1
H-ZSM-5(20) pretreated at 850°C with 20% H <sub>2</sub> O	12.4
H-ZSM-5(40) without pretreated	96.8
H-ZSM-5(40) pretreated at 850°C	43.1
H-ZSM-5(40) pretreated at 850°C with 20% H <sub>2</sub> O	14.5
H-ZSM-5(80) without pretreated	98.5
H-ZSM-5(80) pretreated at 850°C	42.9
H-ZSM-5(80) pretreated at 850°C with 20% H <sub>2</sub> O	13.4
H-ZSM-5(160) without pretreated	100
H-ZSM-5(160) pretreated at 850°C	43.3
H-ZSM-5(160) pretreated at 850°C with 20% H <sub>2</sub> O	15.7

a = base on XRD measurement of H-ZSM-5(160).

Figure 5.12-5.15, It can be seen that all the XRD pattern of prepared zeolite catalysts are correspond to the XRD pattern of ZSM-5 structure. So, demonstration that H-ZSM-5 zeolite catalysts were pretreated do not effect on MFI structure. Moreover , the H-ZSM-5 zeolite catalysts were thermal and hydrothermal treated that Its decreasing in crystallinity[38]. The loss of crystallinity of the H-ZSM-5 zeolite catalysts over hydrothermal treatment more than thermal treatment due to the MFI structure was destroyed by water steam or MFI structure was to collapse.



## 5.3.1.2 BET surface area

**Table 5.12** BET surface area of H-ZSM-5 zeolite catalysts with different crystallinity.

Zeolite catalysts	BET surface area (m <sup>2</sup> /g of catalysts)
H-ZSM-5(20) without pretreated	330.4
H-ZSM-5(20) pretreated at 850°C	322.5
H-ZSM-5(20) pretreated at 850°C with 20% H <sub>2</sub> O	316.5
H-ZSM-5(40) without pretreated	368.9
H-ZSM-5(40) pretreated at 850°C	341.2
H-ZSM-5(40) pretreated at 850°C with 20% H <sub>2</sub> O	335.7
H-ZSM-5(80) without pretreated	369.8
H-ZSM-5(80) pretreated at 850°C	366.8
H-ZSM-5(80) pretreated at 850°C with 20% H <sub>2</sub> O	360.3
H-ZSM-5(160) without pretreated	373.7
H-ZSM-5(160) pretreated at 850°C	354.3
H-ZSM-5(160) pretreated at 850°C with 20% H <sub>2</sub> O	354.3

The BET surface area of H-ZSM-5 zeolite catalysts with different crystallinity are compared in Table 5.12. It can be seen that the both thermal and hydrothermal treatment cause to loss of BET surface area from parent H-ZSM-5 zeolite catalyst. The BET surface area of H-ZSM-5 zeolite catalysts in each Si/Al ratios over hydrothermal treatment was lower than thermal treatment.

### 5.3.1.3 Temperature Programmed Adsorptions of Ammonia (NH<sub>3</sub>-TPD)

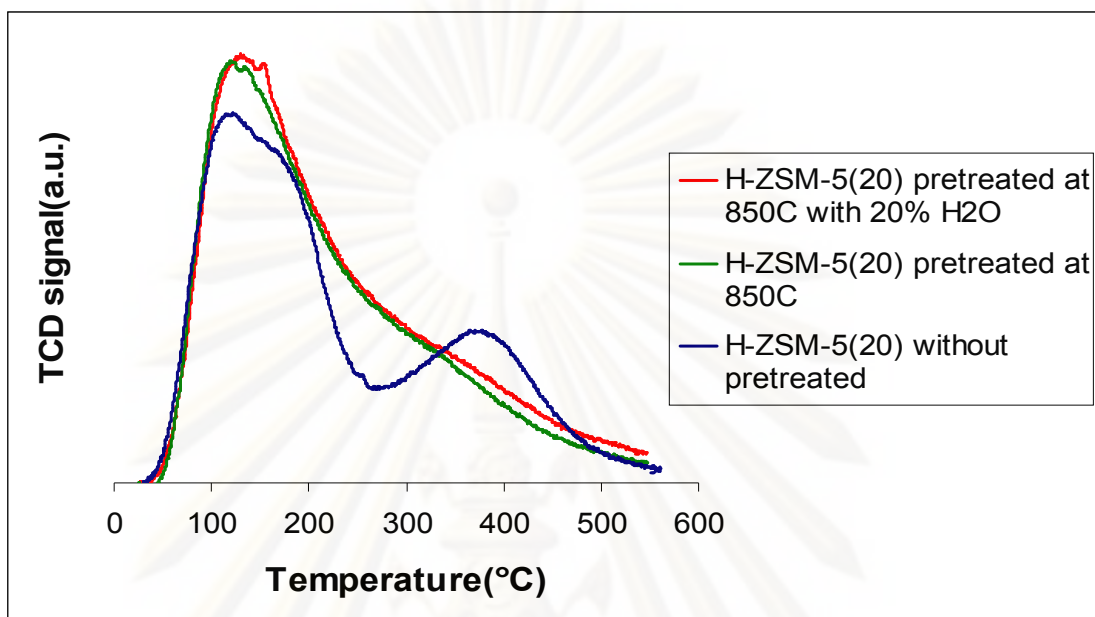


Figure 5.16 TPD profiles of H-ZSM-5(20) zeolite catalysts with different crystallinity

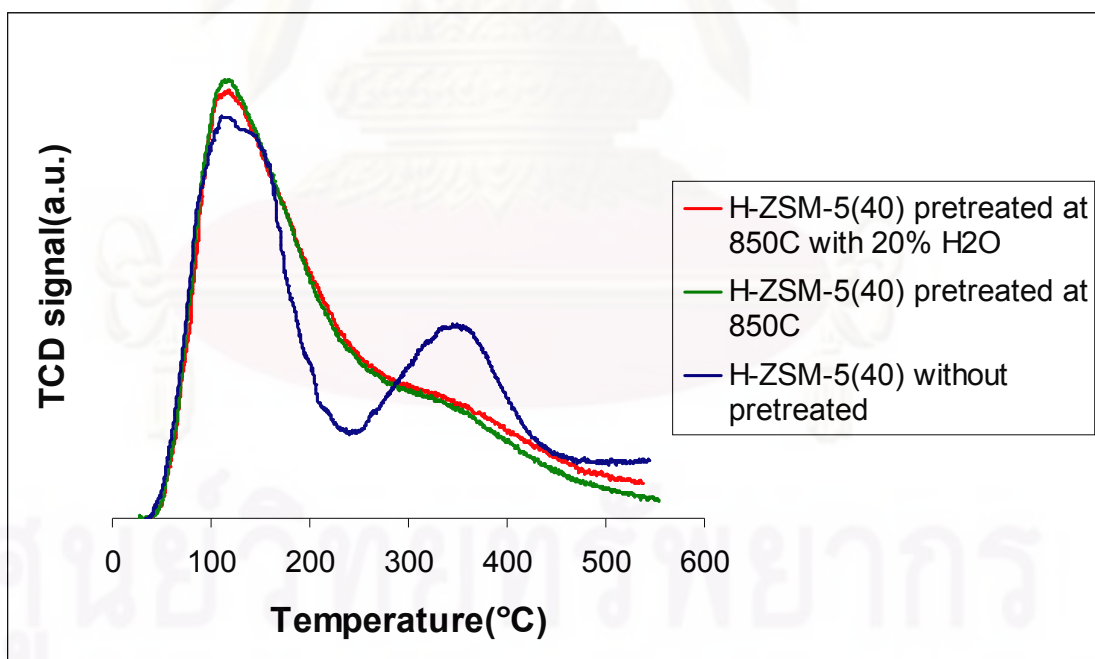
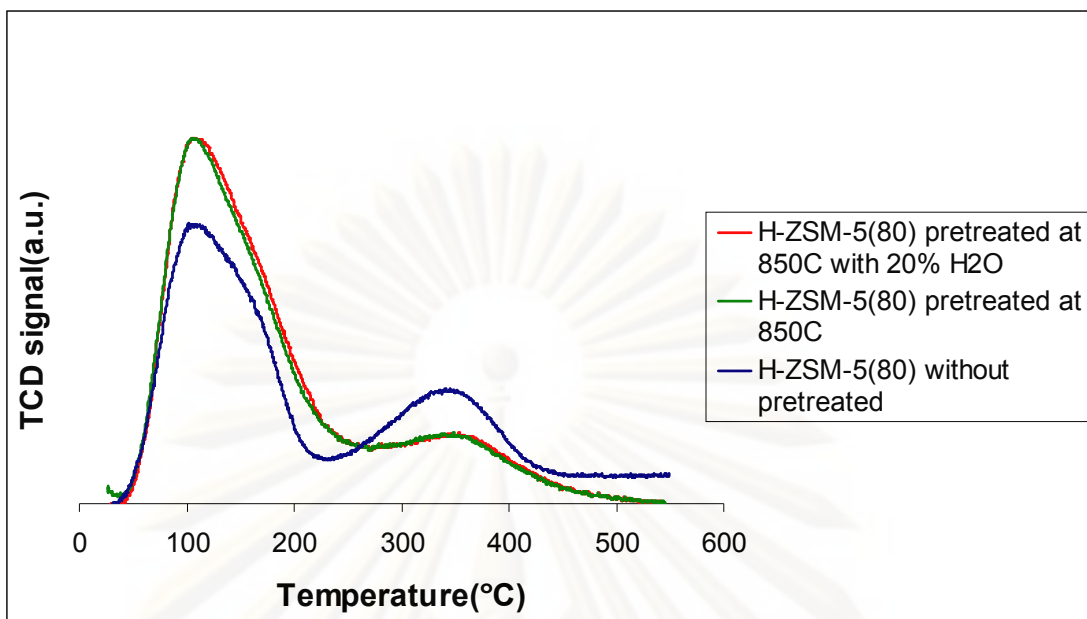
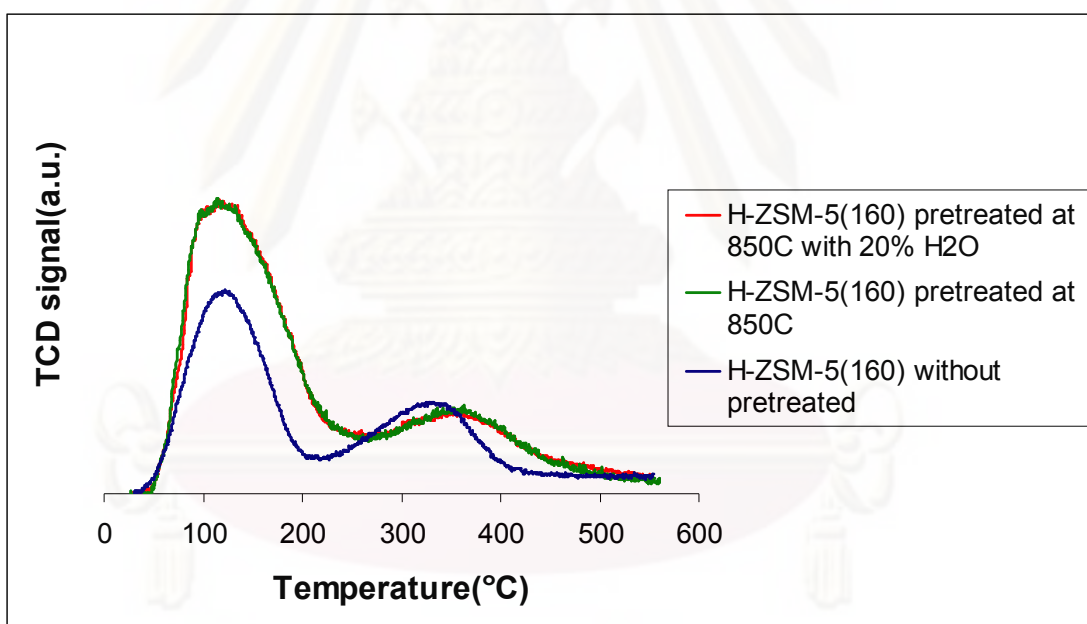


Figure 5.17 TPD profiles of H-ZSM-5(40) zeolite catalysts with different crystallinity



**Figure 5.18** TPD profiles of H-ZSM-5(80) zeolite catalysts with different crystallinity



**Figure 5.19** TPD profiles of H-ZSM-5(160) zeolite catalysts with different crystallinity

**Table 5.13** Acidity of H-ZSM-5 zeolite catalysts with different crystallinity.

Zeolite catalysts	Weak acidity ( $\mu\text{mol}$ $\text{NH}_3/\text{g.catalyst}$ )	Strong acidity ( $\mu\text{mol}$ $\text{NH}_3/\text{g.catalyst}$ )	Total acidity ( $\mu\text{mol}$ $\text{NH}_3/\text{g.catalyst}$ )
H-ZSM-5(20) without pretreated	2316.1	654.0	2970.1
H-ZSM-5(20) pretreated at 850°C	2336.3	33.1	2369.4
H-ZSM-5(20) pretreated at 850°C with 20% H <sub>2</sub> O	2330.9	29.3	2360.2
H-ZSM-5(40) without pretreated	1563.8	511.1	2074.9
H-ZSM-5(40) pretreated at 850°C	1823.5	49.8	1873.3
H-ZSM-5(40) pretreated at 850°C with 20% H <sub>2</sub> O	1852.7	49.1	1901.8
H-ZSM-5(80) without pretreated	1186.1	343.2	1529.3
H-ZSM-5(80) pretreated at 850°C	1557.5	129.8	1687.3
H-ZSM-5(80) pretreated at 850°C with 20% H <sub>2</sub> O	1611.4	137.1	1748.5
H-ZSM-5(160) without pretreated	615.5	217.3	832.8
H-ZSM-5(160) pretreated at 850°C	1133.7	147.5	1281.2
H-ZSM-5(160) pretreated at 850°C with 20% H <sub>2</sub> O	1085.6	141.9	1227.5



Acidity of the all H-ZSM-5 zeolite catalysts with different crystallinity are compared in Figure 5.16-5.19 and Table 5.13. It can be seen that for each Si/Al ratio of H-ZSM-5 zeolite catalysts, The H-ZSM-5 zeolite catalysts were pretreated with thermal and hydrothermal method which the weak acidity was increased but strong acidity was decreased when compared them with the parent H-ZSM-5 zeolite catalysts[38]. Especially, H-ZSM-5(20) and H-ZSM-5(40) had a higher acidity that can see the weak acidity of them were much more decreased.

In the past, Other resech studied about thermal and hydrothermal treatment and found that crystallite size of H-ZSM-5 zeolite catalyst grow up to the treatment temperature. In this work, I choose the treatment temperature equal to 200 °C

And then the TPD profiles indicated that the total acidity of H-ZSM-5 zeolite catalysts(for each Si/Al ratio) were treatment over thermal and hydrothermal was nearly quantity. Therefore, the synthesized H-ZSM-5 zeolite catalysts was same as total acidity and crystallite size.

### 5.3.2 Catalytic reaction

In this part, I testing the pretreated H-ZSM-5 zeolite catalysts with methanol dehydration reaction. Investigation for effect of crystallinity of H-ZSM-5 zeolite catalyst on catalytic performance in methanol dehydration to DME.

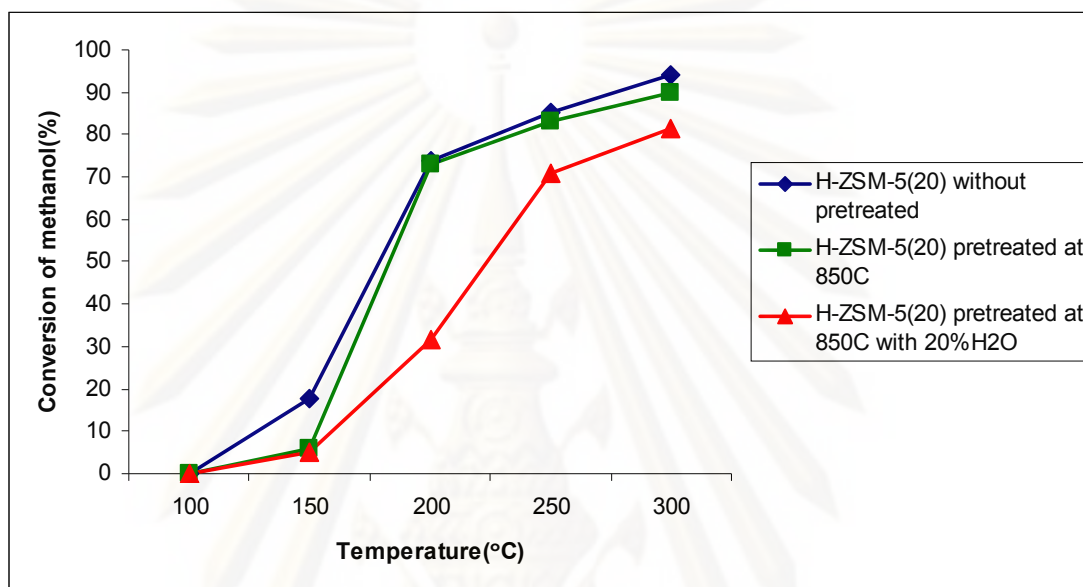


**Figure 5.20** Dehydration of methanol over H-ZSM-5(20) zeolite catalysts with different crystallinity.

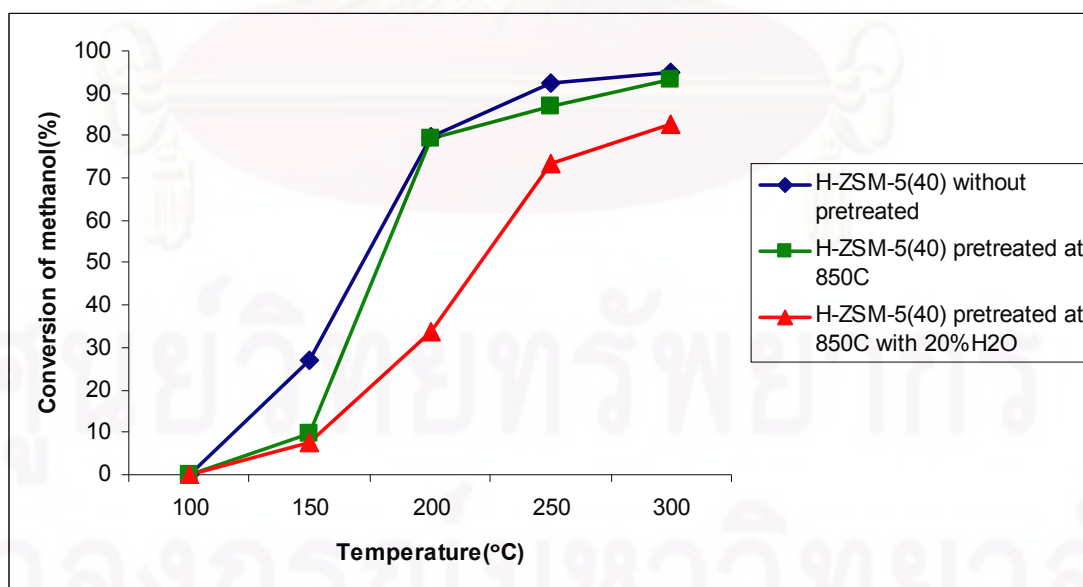


**Figure 5.21** Dehydration of methanol over H-ZSM-5(40) zeolite catalysts with different crystallinity.

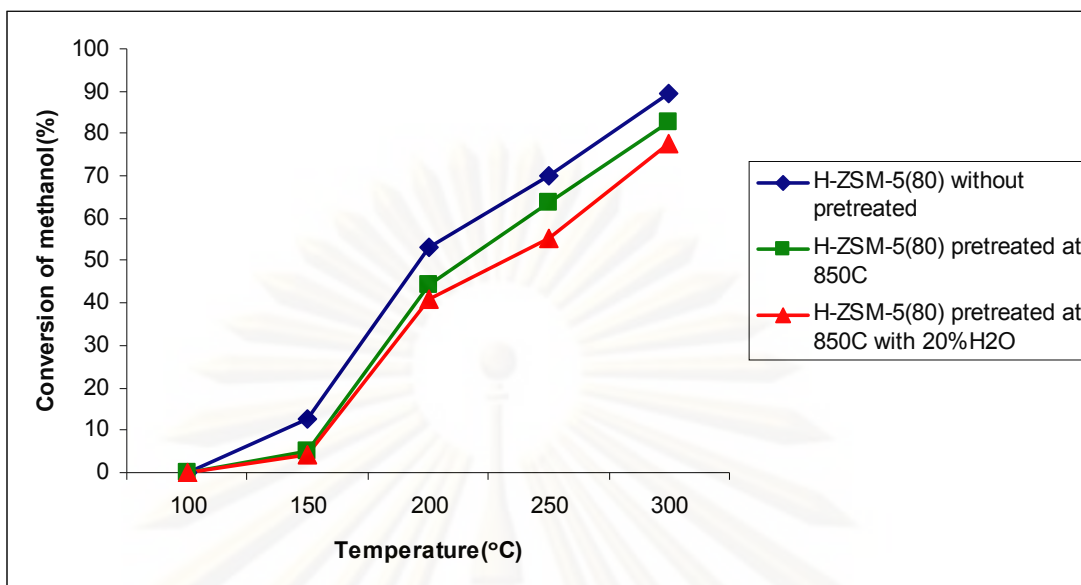


**Figure 5.22** Dehydration of methanol over H-ZSM-5(80) zeolite catalysts with different crystallinity.

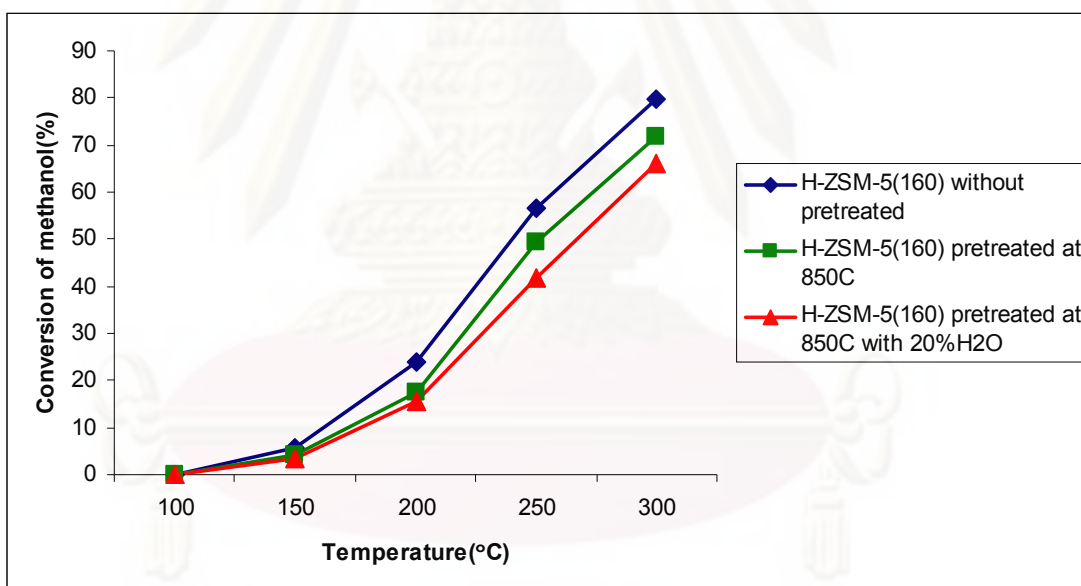


**Figure 5.23** Dehydration of methanol over H-ZSM-5(160) zeolite catalysts with different crystallinity.

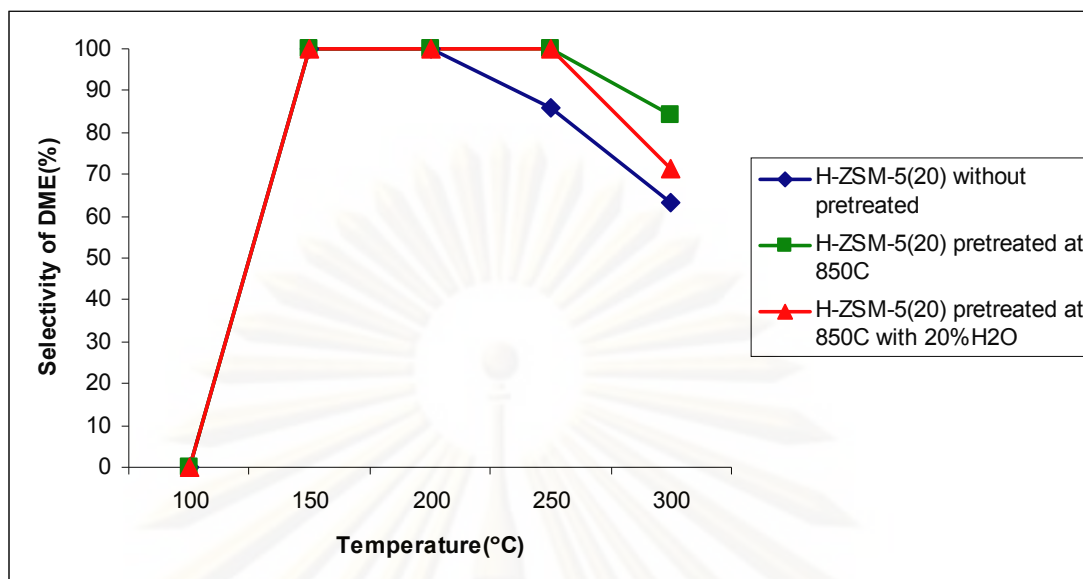


**Figure 5.24** DME selectivity over H-ZSM-5(20) zeolite catalysts with different crystallinity.

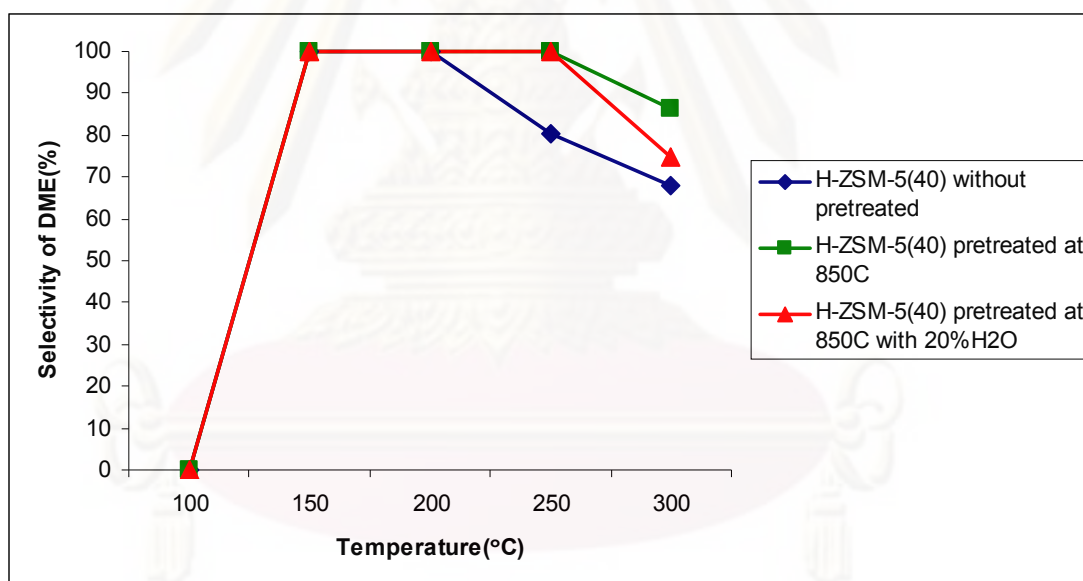


**Figure 5.25** DME selectivity over H-ZSM-5(40) zeolite catalysts with different crystallinity.



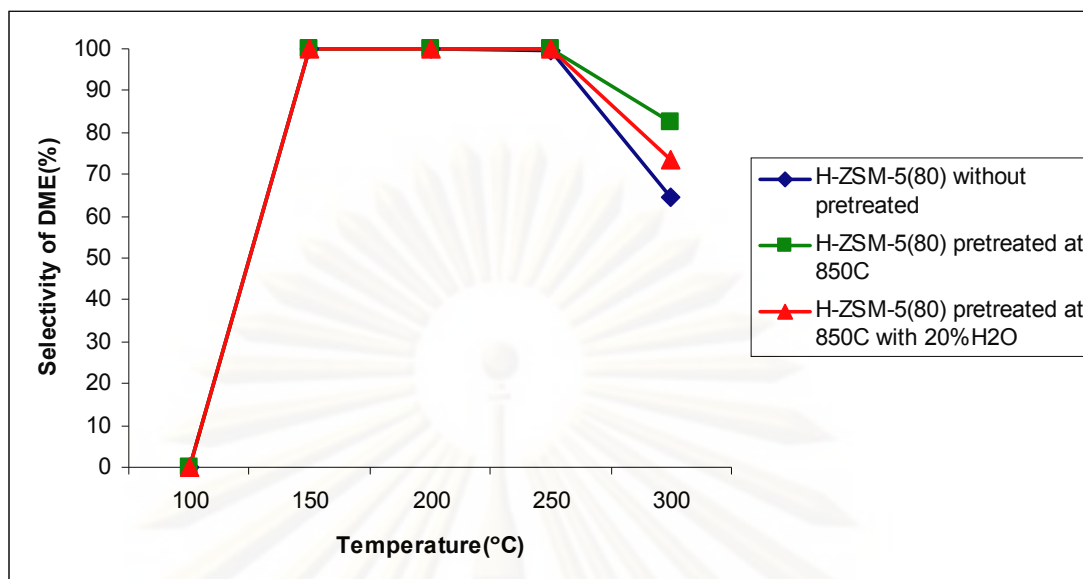


**Figure 5.26** DME selectivity over H-ZSM-5(80) zeolite catalysts with different crystallinity.

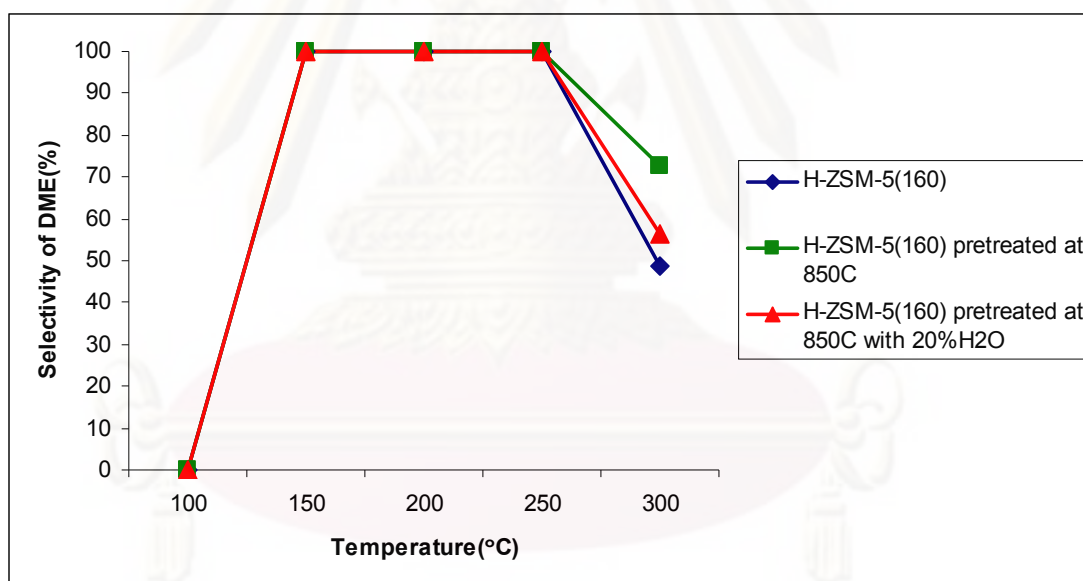


**Figure 5.27** DME selectivity over H-ZSM-5(160) zeolite catalysts with different crystallinity.

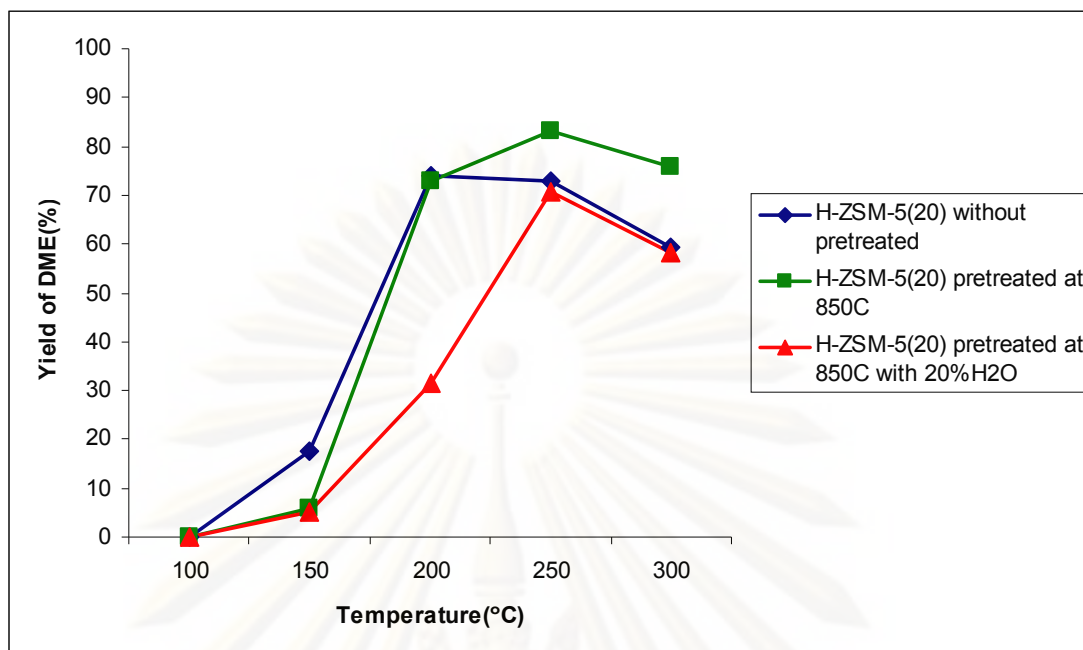


**Figure 5.28** DME yield over H-ZSM-5(20) zeolite catalysts with different crystallinity.

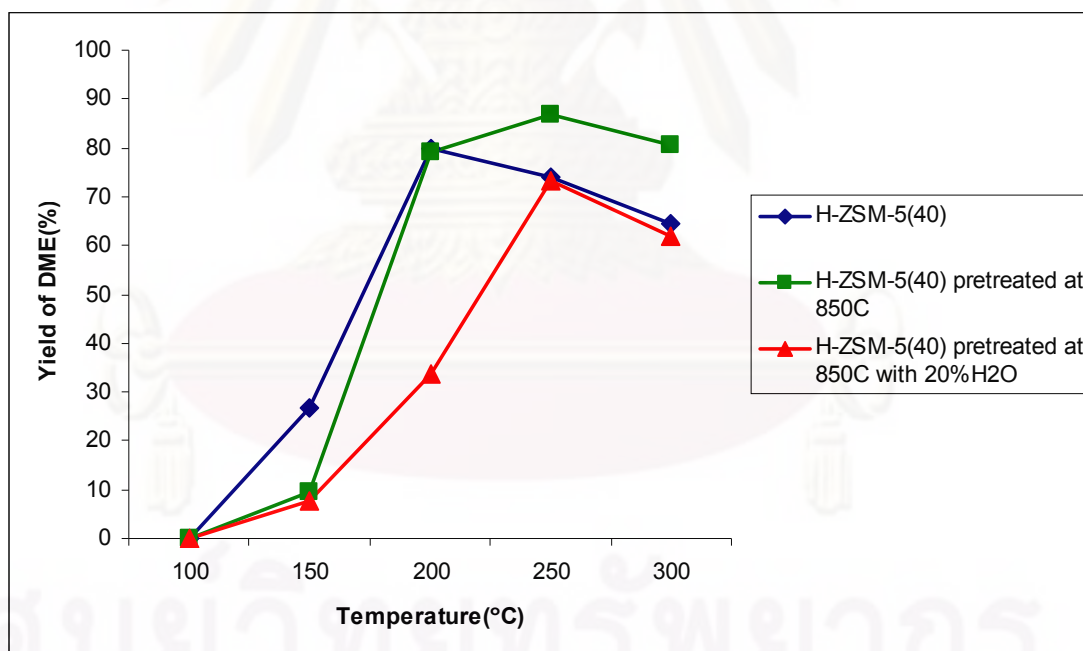


**Figure 5.29** DME yield over H-ZSM-5(40) zeolite catalysts with different crystallinity.

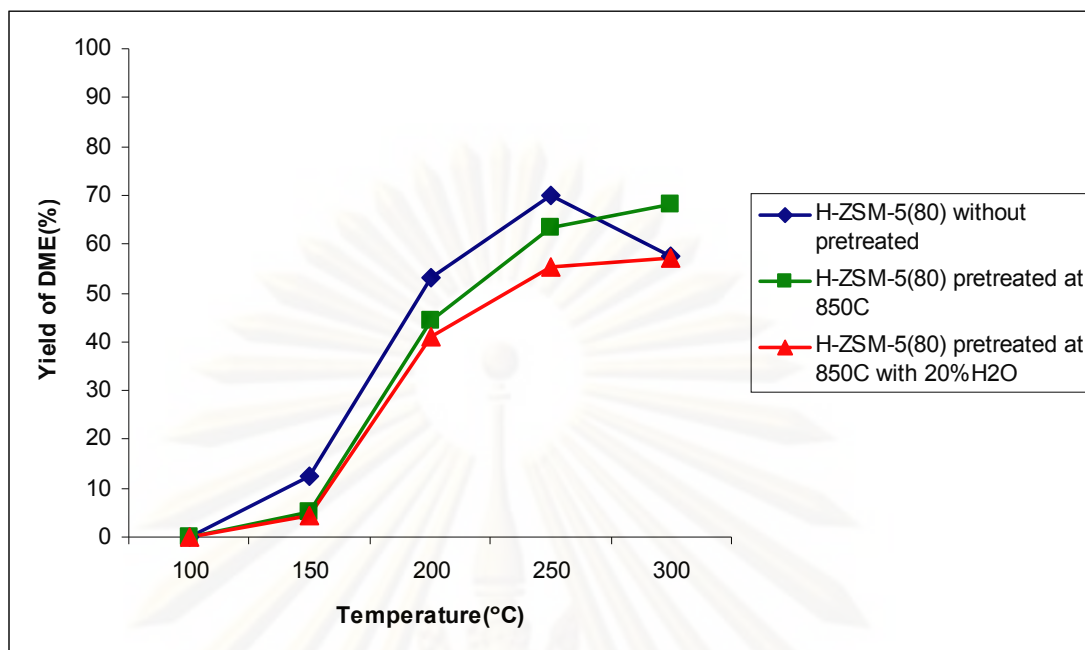


**Figure 5.30** DME yield over H-ZSM-5(80) zeolite catalysts with different crystallinity.

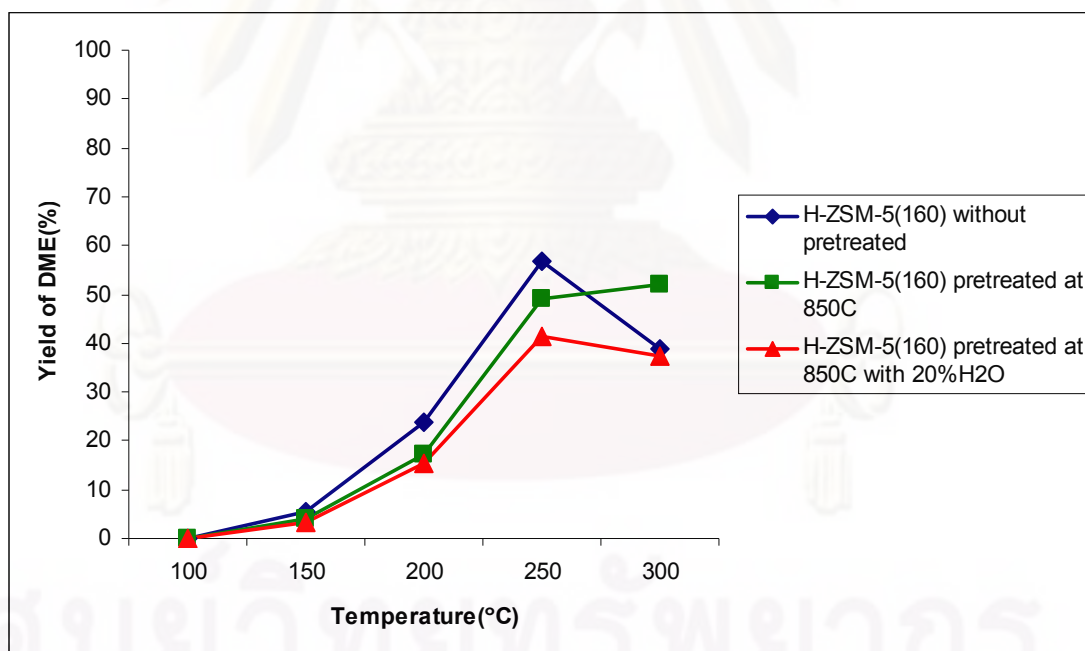


**Figure 5.31** DME yield over H-ZSM-5(160) zeolite catalysts with different crystallinity.

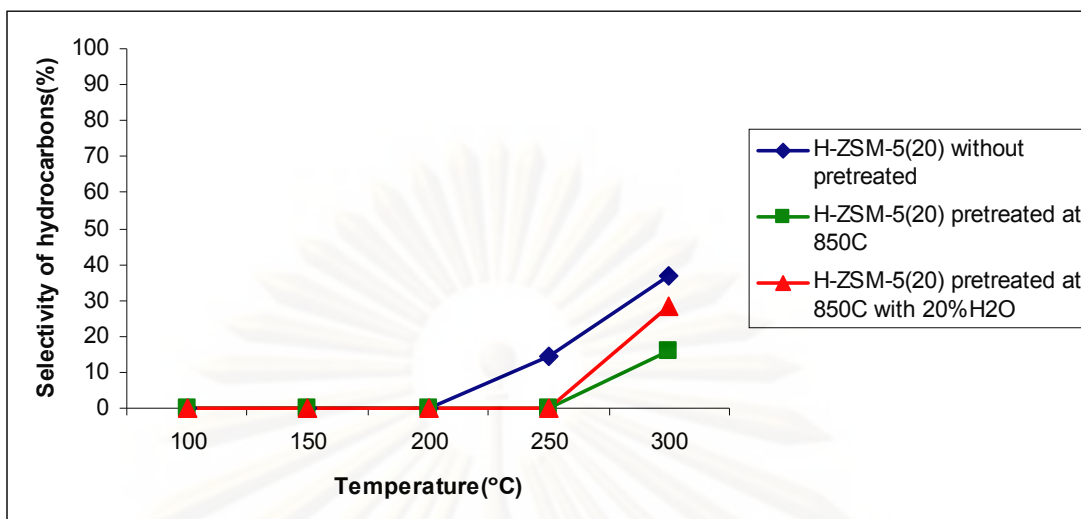


**Figure 5.32** Hydrocarbons selectivity over H-ZSM-5(20) zeolite catalysts with different crystallinity.

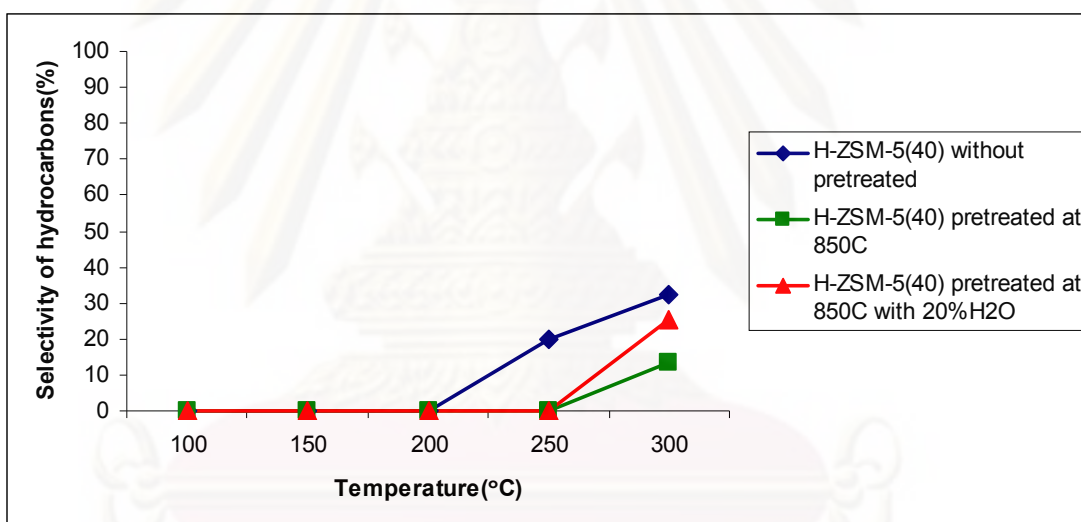


**Figure 5.33** Hydrocarbons selectivity over H-ZSM-5(40) zeolite catalysts with different crystallinity.



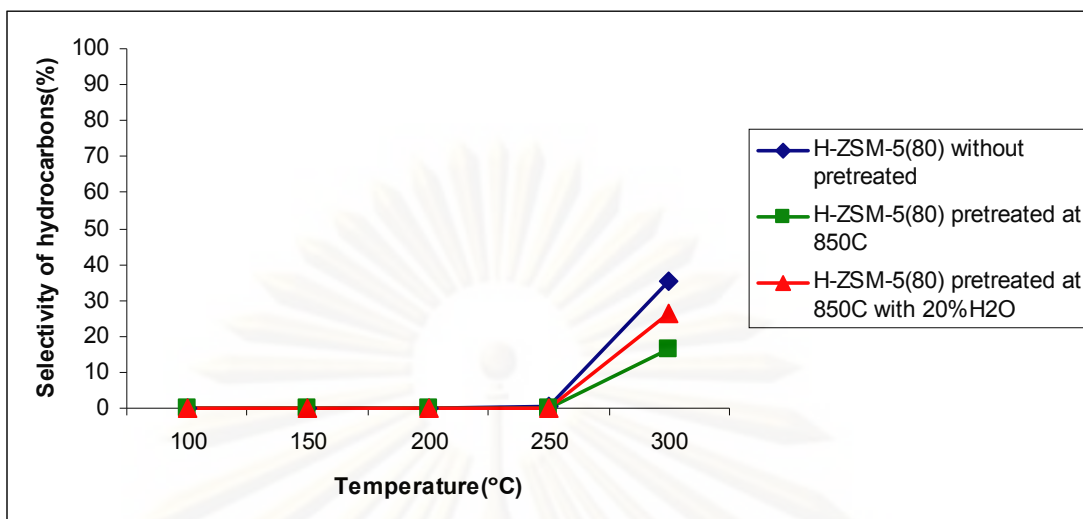


**Figure 5.34** Hydrocarbons selectivity over H-ZSM-5(80) zeolite catalysts with different crystallinity.

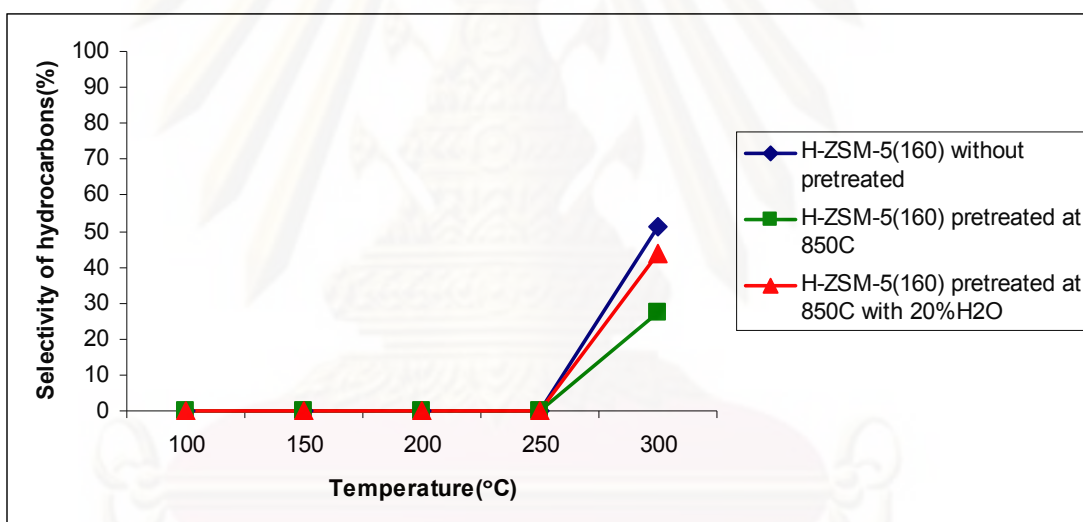


**Figure 5.35** Hydrocarbons selectivity over H-ZSM-5(160) zeolite catalysts with different crystallinity.

From Figure 5.12-5.15 indicated that, the loss of crystallinity of the H-ZSM-5 zeolite catalysts over hydrothermal treatment more than thermal treatment. When testing the pretreated H-ZSM-5 zeolite catalysts by run methanol dehydration reaction. When compared activity of thermal and hydrothermal H-ZSM-5 zeolite catalyst, which them same as in total acidity and crystal size, found that for each Si/Al ratio of H-ZSM-5 zeolite catalyst that the activity of H-ZSM-5 pretreated at 850 °C was higher than H-ZSM-5 pretreated at 850°C with 20% H<sub>2</sub>O because of the crystallinity of H-ZSM-5 pretreated at 850°C was higher than H-ZSM-5 pretreated at 850°C with 20% H<sub>2</sub>O[33]. Nevertheless, the activity of the both of pretreated H-ZSM-5 zeolite catalysts were lower than H-ZSM-5 without pretreated as showed in Figure 5.20-5.23. Hence the crystallinity do effective to methanol dehydration.

The increase in crystallinity was found to increase the conversion of methanol. This is consistent with the rise in conversion of the dehydroalkylation of toluene with ethane at higher crystallinity found by Arne Bressel et al.[33].

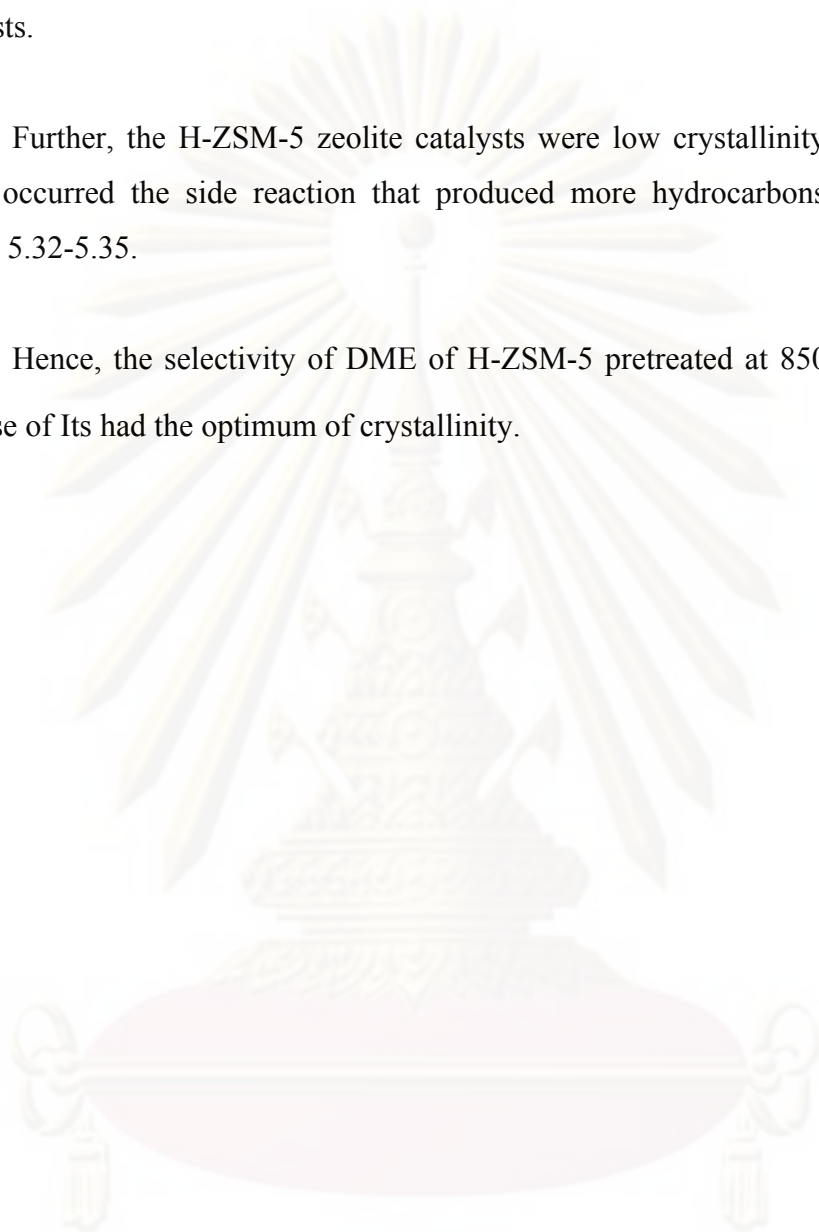
From Figure 5.24-5.27, the experimental results show that for each Si/Al ratio, The selectivity of DME over the pretreated H-ZSM-5 zeolite catalysts show that follow the order of H-ZSM-5 pretreated at 850°C > H-ZSM-5 pretreated at 850°C with 20% H<sub>2</sub>O > H-ZSM-5 without pretreated in the all over temperature range 100-300°C due to the crystallinity of H-ZSM-5 pretreated at 850°C was higher than H-ZSM-5 pretreated at 850°C with 20% H<sub>2</sub>O. The comparison both thermal and hydrothermal zeolite catalysts with the parent H-ZSM-5 found that the DME selectivity of pretreated H-ZSM-5 zeolite catalysts was higher than H-ZSM-5 without pretreated because of the crystallinity of pretreated H-ZSM-5 zeolite catalysts was lower than parent H-ZSM-5 zeolite catalyst.

Moreover, the decreasing the crystallinity of H-ZSM-5 catalyst cause decreasing in strong acidity so that inhibited the generation of secondary products like hydrocarbons, resulting in high selectivity for DME[35]. The optimum crystallinity of H-ZSM-5 zeolite catalyst is beneficial for catalytic performance. As the crystallinity of H-ZSM-5 pretreated at 850°C with 20% H<sub>2</sub>O was lower than H-ZSM-5 pretreated at

850°C but the selectivity and yield of DME of H-ZSM-5 pretreated at 850°C with 20% zeolite catalysts were not increased more than H-ZSM-5 pretreated at 850°C zeolite catalysts.

Further, the H-ZSM-5 zeolite catalysts were low crystallinity too much that cause occurred the side reaction that produced more hydrocarbons as showed in Figure 5.32-5.35.

Hence, the selectivity of DME of H-ZSM-5 pretreated at 850°C was highest because of Its had the optimum of crystallinity.



ศูนย์วิจัยทรัพยากร  
จุฬาลงกรณ์มหาวิทยาลัย

## CHAPTER VI

### CONCLUSIONS AND RECOMMENDATIONS

From previous Chapter, researcher can sum up main issue of this experiment as follows:

#### 6.1 Conclusions

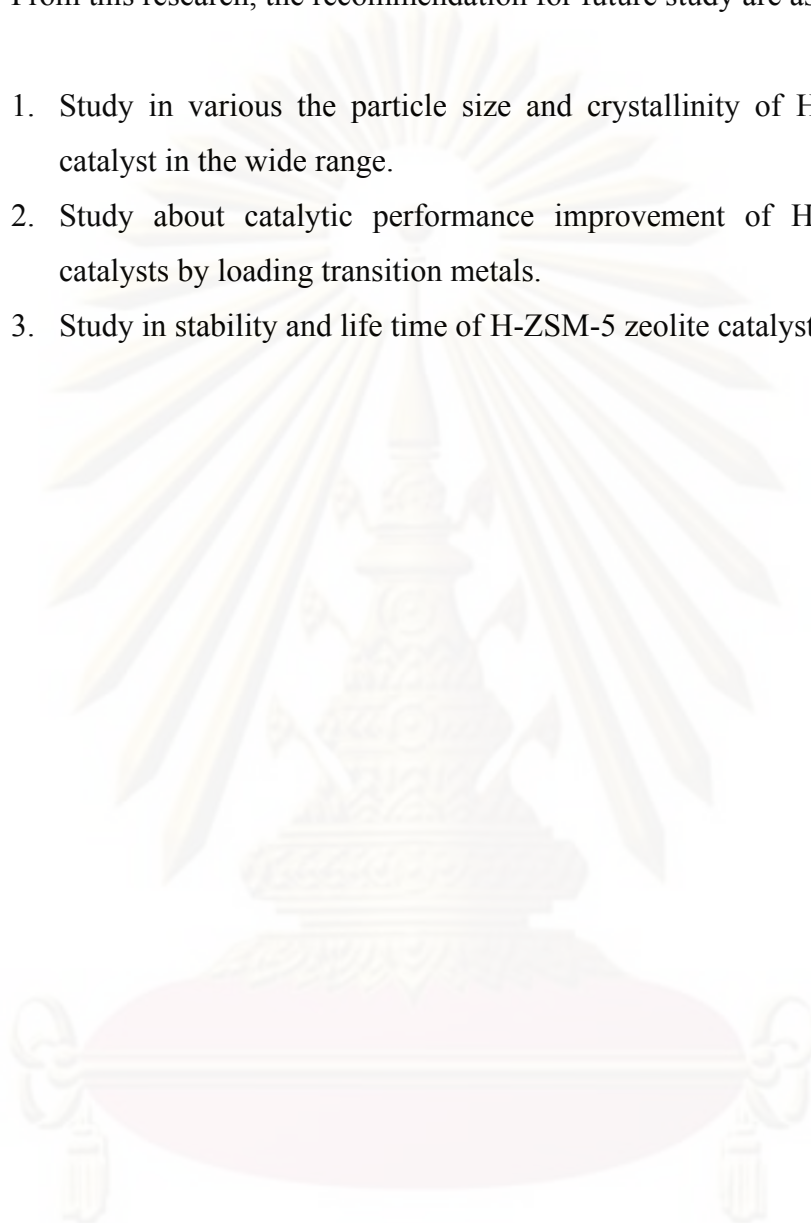
1. The crystallinity of zeolite catalysts increased with increasing in the Si/Al ratio.
2. When increasing the Si/Al ratio of the H-ZSM-5 zeolite catalysts, the amount of both strong and weak acid sites of the H-ZSM-5 decreased.
3. The H-ZSM-5(40) zeolite catalyst exhibited the best catalytic performance for methanol dehydration to DME and methanol conversion.
4. The optimum reaction condition for methanol dehydration to DME was 200°C and atmospheric pressure.
5. The smaller crystallize size and optimum crystallinity of zeolite is beneficial for the catalytic performance in the methanol dehydration to DME, whereas inhibiting the generation of secondary products like hydrocarbons, resulting in high selectivity for DME
6. The higher crystallinity of zeolite gave the better methanol conversion.



## 6.2 Recommendations

From this research, the recommendation for future study are as follows:

1. Study in various the particle size and crystallinity of H-ZSM-5 zeolite catalyst in the wide range.
2. Study about catalytic performance improvement of H-ZSM-5 zeolite catalysts by loading transition metals.
3. Study in stability and life time of H-ZSM-5 zeolite catalyst.



ศูนย์วิจัยทรัพยากร  
จุฬาลงกรณ์มหาวิทยาลัย

## REFERENCES

- [1] Shikada, T., and others. Vapor phase carbonylation of DME and methyl acetate with nickel-active carbon catalysts. Applied Catalysis 7 (1983): 361-368.
- [2] Chang, C.D. Hydrocarbons from methanol. Catalysis Reviews-Science and Engineering 25 (1983): 1-19.
- [3] Cai, G., and others. Light alkenes from syngas via dimethyl ether. Applied Catalysis A: General 125 (1995): 29-38.
- [4] Zhang, P., and others. Study of the performance of modified nano-scale ZSM-5 zeolite on olefins reduction in FCC gasoline. Journal of Molecular Catalysis A: Chemical 261 (2006): 139-146.
- [5] Rouhi, A.M. Olefin metathesis: Big-deal reaction. Chemical and Engineering News 80 (1995): 29-83.
- [6] Sorenson, C.C., and others. Performance and emissions of a 0.273 liter direct injection diesel engine fuelled with neat dimethyl ether. SAE Paper 9 (1995): 950064-950068.
- [7] Hansen, J.B., and Oishi, T. Dimethyl ether (DME) as clean fuel for diesel engines. Petrotech 20 (1997): 823-831.
- [8] Sorenson, S.C. Dimethyl ether in diesel engines: progress and perspectives. Journal of Engineering for Gas Turbines and Power 123 (2008): 652-659.
- [9] Inoue, N., and Ohno, Y. A view of future synthetic fuel oil-5. Dimethyl ether synthesis technology. Petrotech 24 (2001): 319-329.
- [10] Fujimoto, K., and others. Selective synthesis of dimethyl ether from synthesis gas. Chemistry Letter 12 (1984): 2051-2504.
- [11] Hansen, J.B., and Joensen, F. High conversion of synthesis gas into oxygenates. Studies in Surface Science and Catalysis 61 (1991): 457-467.
- [12] Takeguchi, T., and others. Effect of the property of solid acid upon syngas-to-dimethyl ether conversion on the hybrid catalysts composed of Cu-Zn-Ga and solid acids. Applied Catalysis A: General 192 (2000): 201-209.
- [13] Xu, M., and others. Synthesis of dimethyl ether from methanol over solid-acid catalysts. Applied Catalysis A: General 149 (1997): 289-301.
- [14] Li, J.-L., and others. Improvement in the catalyst activity for direct synthesis of DME from synthesis gas through enhancing the dispersion of CuO/ZnO/ $\gamma$ -Al<sub>2</sub>O<sub>3</sub> in hybrid catalysts. Applied Catalysis A: General 147 (1996): 23-33.

- [15] Mao, D., and others. Highly effective hybrid catalyst for the direct synthesis of DME from syngas with magnesium oxide-modified H-ZSM-5 as a dehydration component. Journal of Catalysis 230 (2005): 140-149.
- [16] Fu, Y., and others. Surface acidity and the dehydration of methanol to dimethyl ether. Thermochimica Acta 434 (2005): 22-26.
- [17] Vishwanathan, V., and others. Vapour phase dehydration of crude methanol to DME over Na-modified H-ZSM-5 catalysts. Applied Catalysis A: General 276 (2004): 251-255.
- [18] Takeguchi, T., and others. Effect of the property of solid acid upon syngas-to-dimethyl ether conversion on the hybrid catalysts composed of Cu-Zn-Ga and solid acids. Applied Catalysis A: General 192 (2000): 201-209.
- [19] Kawabata, T., and others. Steam reforming of DME over ZSM-5 coupled with Cu/ZnO/ $\gamma$ -Al<sub>2</sub>O<sub>3</sub> catalyst prepared by homogeneous precipitation. Applied Catalysis A: General 308 (2006): 82-90.
- [20] Barrer, R. Hydrothermal chemistry of zeolites. London: Academic Press, 1982.
- [21] Bekkum, H.V., and others. STM image of silicalite-1 pore structure. Studies in Surface Science and Catalysis 48 (1991): 578-585.
- [22] Asami, K., and others. Semi-indirect synthesis of LPG from syngas: Conversion of DME into LPG. Catalysis Today 106 (2005): 247-251.
- [23] Satterfield, C.N. Heterogeneous catalysis in industrial practice. New York: McGraw-Hill, 1991.
- [24] Meier, W.M. and Olson, D.H. Atlas of zeolite structure types. Boston: Butterworth-Heinemann, 1992.
- [25] Chen, D., and others. The effect of crystal size of SAPO-34 on the selectivity and deactivation of the MTO reaction. Microporous and Mesoporous Material 29 (1999): 191-201.
- [26] Barthoment, D. Acidic catalysts with zeolites. New York: The Hange, 1984.
- [27] Sano, T., and others. High stream stability if H-ZSM-5 type zeolite containing alkaline eart metals catalyst deactivation. Amsterdam: Elsevier, 1987.
- [28] Ashton, A.G., and others. Catalysis by acid-bases. Amsterdam: Elsevir, 1985.
- [29] Sun, K., and others. Low-temperature synthesis of DME from CO<sub>2</sub>/H<sub>2</sub> over Pd-modified CuO-ZnO-Al<sub>2</sub>O<sub>3</sub>-ZrO<sub>2</sub>/H-ZSM-5 catalysts. Catalysis Communication 5 (2004): 367-370.
- [30] Tanake, K. New solid acids and bases. Tokyo: Elsevier, 1989.

- [31] Szoztak, R. Molecular sieve principle of synthesis and identification. New York: Van Nostrand Reingold, 1989.
- [32] Jutharat Khom-in. Synthesis of dimethyl ether (DME) from dehydration of methanol using  $\gamma$ - $\text{Al}_2\text{O}_3$  and  $\gamma\cdot\gamma$ - $\text{Al}_2\text{O}_3$  catalysts. Master's Thesis, Department of Chemical Engineering Faculty of Engineering Chulalongkorn University, 2007.
- [33] Bressel, A., and others. Influence of aluminum content, crystallinity and crystallite size of zeolite Pd/H-ZSM-5 on the catalytic performance in the dehydroalkylation of toluene with ethane. Microporous and Mesoporous Materials 109 (2008): 278-286.
- [34] Armaroli, T., and others. Effects of crystal size and Si/Al ratio on the surface properties of H-ZSM-5. Applied Catalysis A: General 306 (2006): 78-84.
- [35] Kim, J.H., and others. DME synthesis from synthesis gas on the admixed catalysts of Cu/ZnO/ $\text{Al}_2\text{O}_3$  and ZSM-5. Applied Catalysis A: General 264 (2004): 37-41.
- [36] Suzuki, K., and others. Effect of crystallization time on the physicochemical and catalytic properties of a ZSM-5 type zeolite. Applied Catalysis 42 (1988): 35-45.
- [37] Moller, K.P., and others. The use of a jet loop reactor to study the effect of crystal size and the co-feeding of olefins and water on the conversion of methanol over H-ZSM-5. Microporous and Mesoporous Materials 29 (1999): 127-144.
- [38] Li, Y., and others., Thermal and hydrothermal stabilities of the alkali-treated H-ZSM-5 zeolites. Journal of Natural Gas Chemistry 17 (2008): 69-74.





**APPENDICES**

ศูนย์วิทยทรัพยากร  
จุฬาลงกรณ์มหาวิทยาลัย

## APPENDIX A

### CALCULATION OF Si/Al ATOMIC RATIO FOR ZSM-5

The calculation is based on weight of Sodium Silicate( $\text{Na}_2\text{O}\cdot\text{SiO}_2\cdot\text{H}_2\text{O}$ ) in B1 and B2 solutions (Topic 4.1.1).

M.W. of Si	=	28.0855
M.W. of $\text{SiO}_2$	=	60.0843
Weight percent of $\text{SiO}_2$ in Sodium Silicate	=	28.5
M.W. of Al	=	26.9815
M.W. of $\text{AlCl}_3$	=	133.3405
Weight percent of $\text{AlCl}_3$	=	97

For example, to prepare ZSM-5 at Si/Al atomic ratio of 25.

Using Sodium Silicate 69 g. with 45 g. of water as B1 solution.

$$\begin{aligned}
 \text{Mole of Si used} &= \frac{\text{wt.(\%)} \times (\text{M.W. of Si}) \times (1 \text{ mole})}{100 (\text{M.W. of SiO}_2) (\text{M.W. of Si})} \\
 &= 69 \times (28.5/100) \times (1/60.0843) \\
 &= 0.3273
 \end{aligned}$$

Si/Al atomic ratio = 25

$$\begin{aligned}
 \text{Mole of AlCl}_3 \text{ required} &= 0.3273/25 \\
 &= 1.309 \times 10^{-2} \text{ mole}
 \end{aligned}$$

$$\begin{aligned}
 \text{Amount of AlCl}_3 &= 1.309 \times 10^{-2} \times 133.34 \times (100/97) \\
 &= 1.799 \text{ g.}
 \end{aligned}$$

Which used in A1 and A2 solutions.

## APPENDIX B

### CALCULATION OF GAS VELOCITY

The catalyst used = 0.2 g.

Packed catalyst into glass reactor (diameter = 6 mm.)

Determine the average high of catalyst bed = 25 mm.

So that, volume of catalyst bed =  $\pi \times (3)^2 \times 25$  (mm)<sup>3</sup>-catalyst

And, used volumetric flow rate = 50 ml/min

$$\begin{aligned} \text{GHSV (Gas Hourly Space Velocity)} &= \frac{\text{Volumetric flow rate}}{\text{Volume of catalyst}} \\ &= 4,244.131815 \text{ h}^{-1} \approx 4,250 \text{ h}^{-1} \end{aligned}$$

## APPENDIX C

### CALCULATION OF TEMPERATURE OF METHANOL

Set the partial vapor pressure of the reactants to the requirement by adjusting the temperature of saturator according to the Antoine equation;

$$\log P = A - \frac{B}{(T+C)}$$

When, P = vapor pressure of methanol, mmHg

T = temperature, °C

A = 7.89750

B = 1474.08

C = 229.13

And then, required 20% of methanol.

So that,  $\log [760 \times (20/100)] = 7.89750 - \frac{1474.08}{T + 229.13}$

$$T = 28.77 \approx 29 \text{ } ^\circ\text{C}$$

ศูนย์วิทยทรัพยากร  
จุฬาลงกรณ์มหาวิทยาลัย



## APPENDIX D

### CALCULATION OF Si/Al ATOMIC RATIO

Weight percent of SiO<sub>2</sub> = X

Weight percent of Al<sub>2</sub>O<sub>3</sub> = Y

So that, 
$$\text{Si/Al ratio} = \frac{(X/100) \times (\text{M.W. of Si}) \times (\text{M.W. of Al}_2\text{O}_3)}{(Y/100) \times (\text{M.W. of SiO}_2) \times (\text{M.W. of Al})}$$

M.W. of Si = 28.0855

M.W. of Al = 26.9815

M.W. of SiO<sub>2</sub> = 60.0843

M.W. of Al<sub>2</sub>O<sub>3</sub> = 74.9815

For example, to prepare ZSM-5 at Si/Al atomic ratio of 20.

From XRF, the result show that.

SiO<sub>2</sub> = 96.38 wt% concentration

Al<sub>2</sub>O<sub>3</sub> = 3.49 wt%

So, 
$$\text{Si/Al ratio} = \frac{(96.38/100) \times (28.0855) \times (74.9815)}{(3.49/100) \times (60.0843) \times (26.9815)}$$

$$= \frac{2029.659595}{56.57864246}$$

$$= 35.87$$

ศูนย์วิทยทรัพยากร  
จุฬาลงกรณ์มหาวิทยาลัย

**APPENDIX E****CALCULATION FOR CONVERSION OF METHANOL &  
SELECTIVITY OF DME**

$$\text{CH}_3\text{OH conversion (\%)} = \frac{100 \times [\text{mole of CH}_3\text{OH in feed} - \text{mole of CH}_3\text{OH in product}]}{\text{mole of CH}_3\text{OH in feed}}$$

$$\text{DME selectivity (\%)} = \frac{100 \times [\text{mole of DME occur}]}{[(\text{mole of CH}_3\text{OH in feed} - \text{mole of CH}_3\text{OH in product})/2]}$$



ศูนย์วิทยทรัพยากร  
จุฬาลงกรณ์มหาวิทยาลัย

## APPENDIX F

### CALCULATION OF % CRYSTALLINITY

$$\% \text{ Crystallinity} = \frac{\text{Area under XRD pattern of sample}}{\text{Area under XRD pattern of reference}} \times 100$$

Reference is the fresh commercial HZSM-5 catalyst.



ศูนย์วิทยทรัพยากร  
จุฬาลงกรณ์มหาวิทยาลัย

## APPENDIX G

### CALCULATION FOR PARTICLE SIZE

The photograph from SEM at 10 kv × 3500 in Figure 5.8(b) show that

$$5 \mu\text{m} = 33 \text{ mm.}$$

So that:

$$1 \mu\text{m} = 6.6 \text{ mm.}$$

And then, for example

HZSM-5(40) zeolite catalyst which it has 6 hours for crystallization.

$$\text{Particle size}(\mu\text{m}) = \frac{\text{particle size \#1} + \text{particle size \#2} + \dots + \text{particle size \#n}}{n \times 6.6}$$

$$= \frac{23+22+23+23+22+22+20+21+27+21}{10 \times 6.6}$$

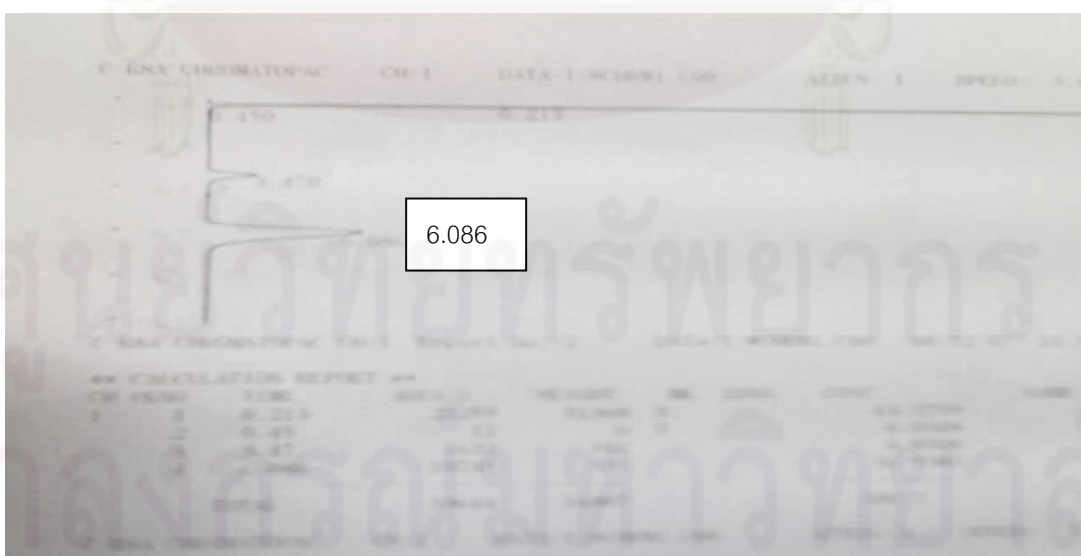
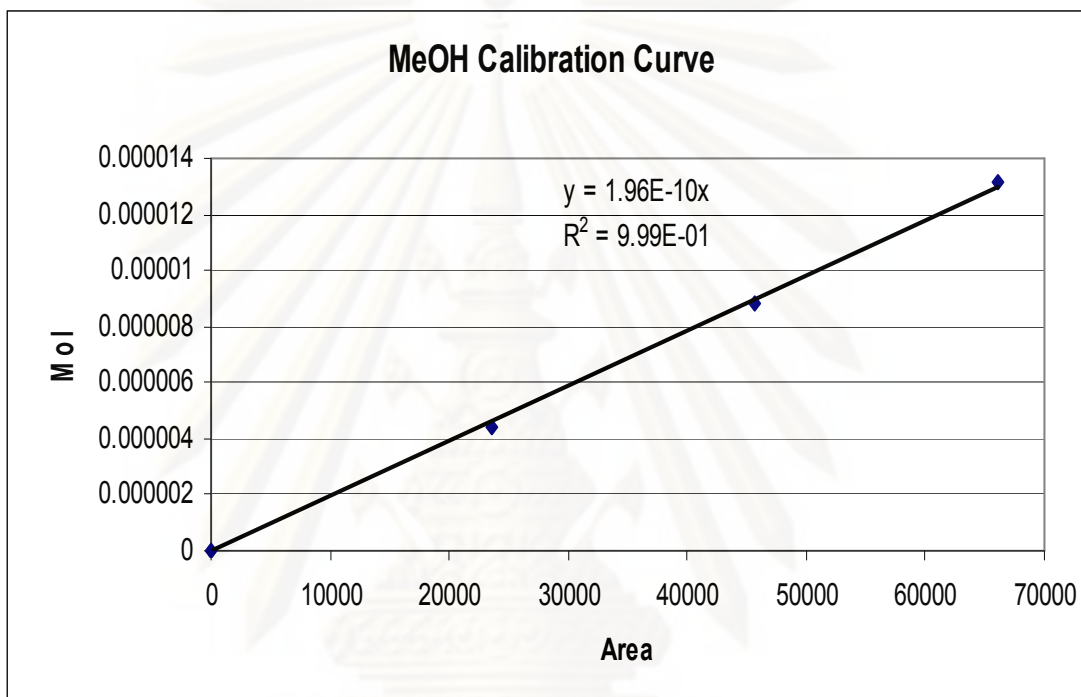
$$= 3.394 \mu\text{m}$$



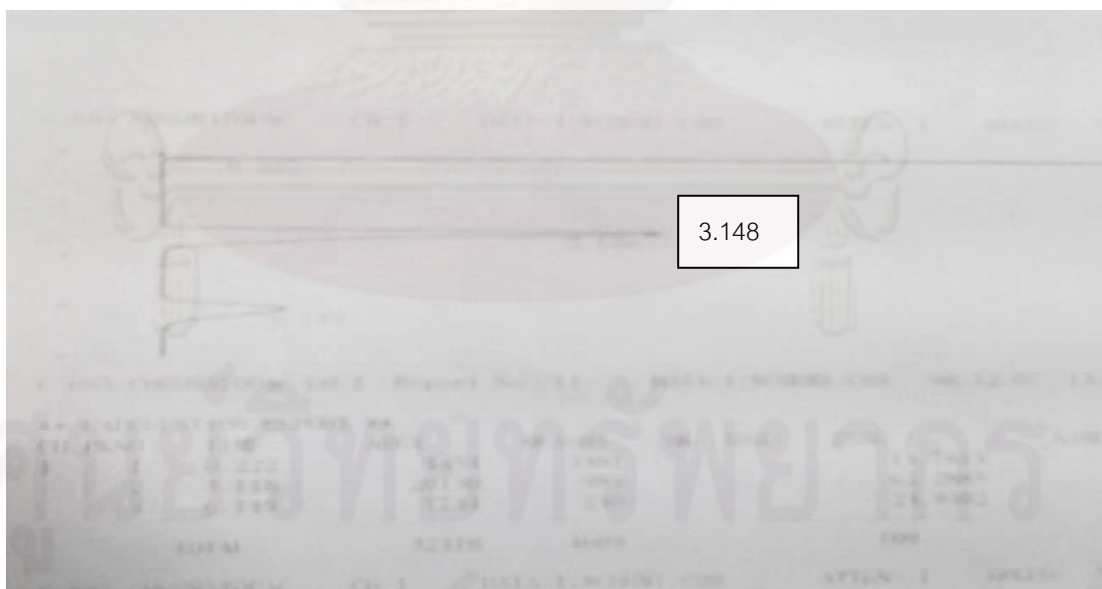
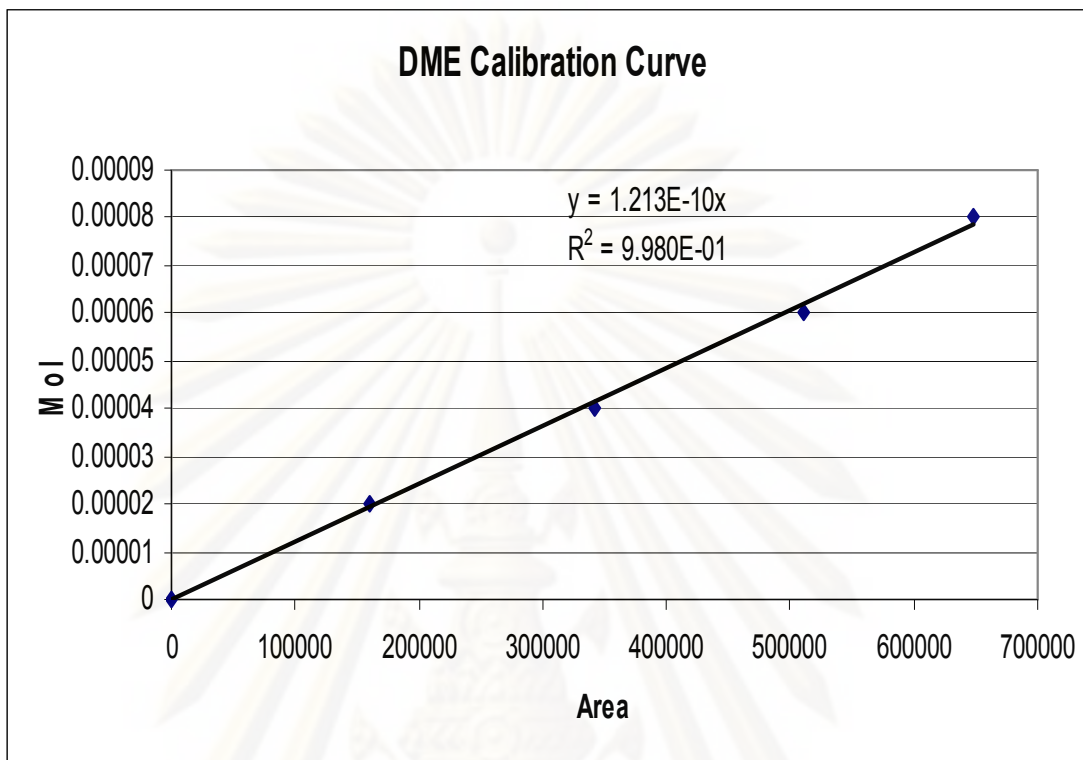
## APPENDIX H

## CALIBRATION CURVES

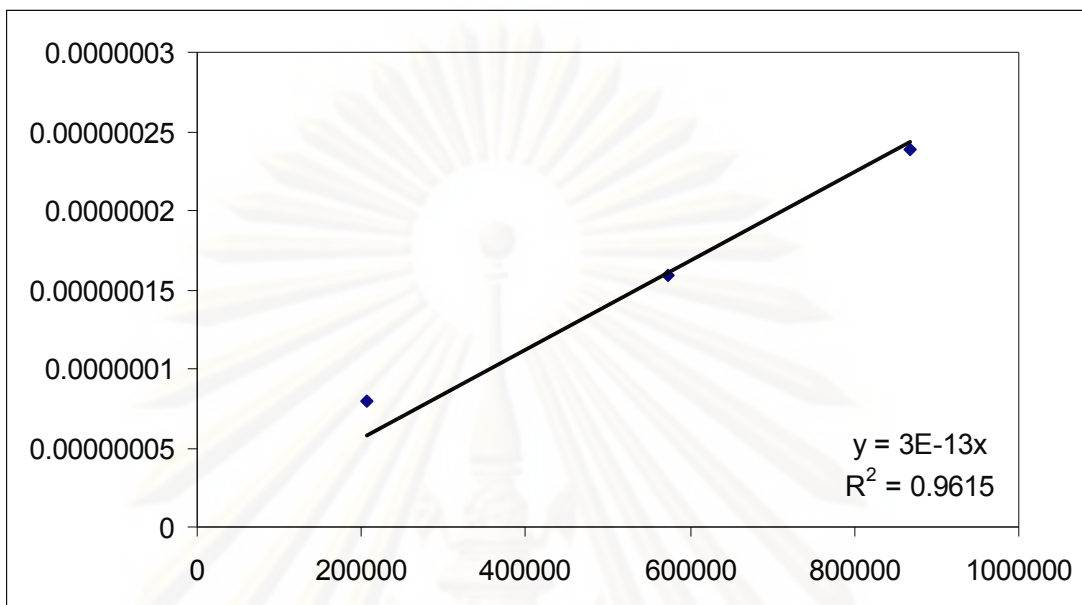
## H-1. METHANOL CALIBRATION CURVE AND GC PICTURE



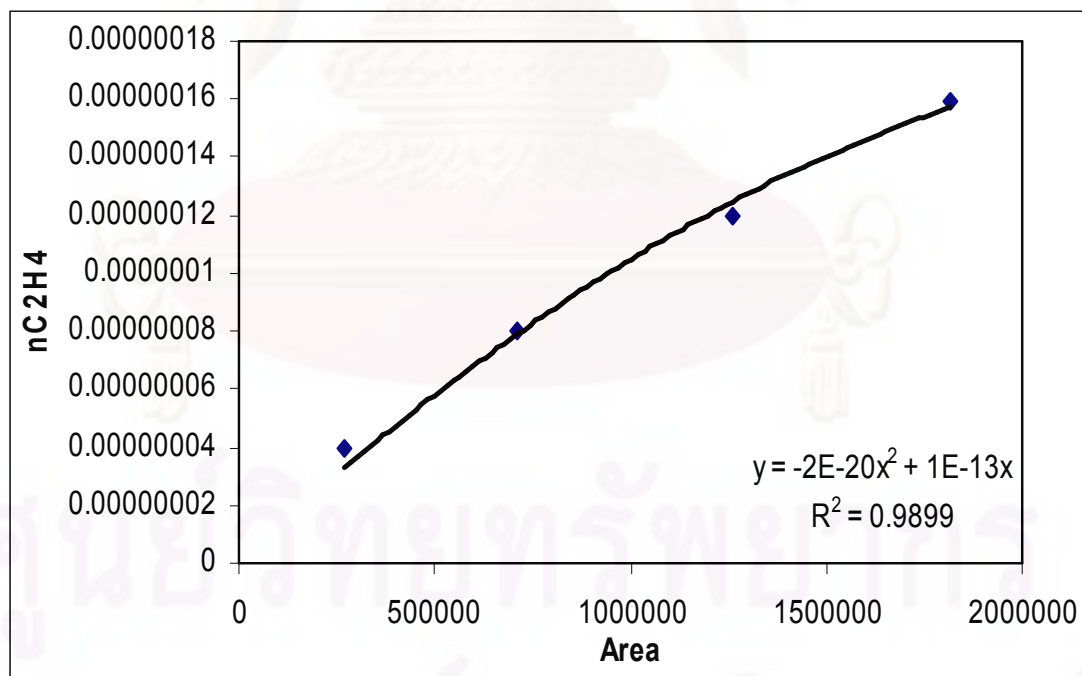
## H-2. DME CALIBRATION CURVE AND GC PICTURE



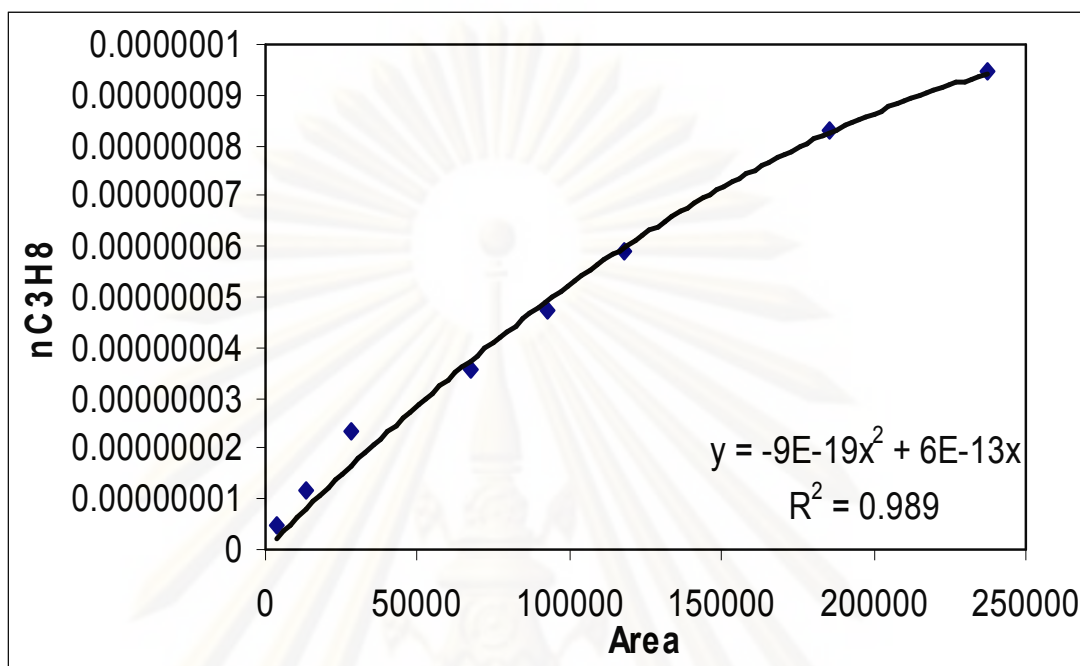
### H-3. METHANE CALIBRATION CURVE



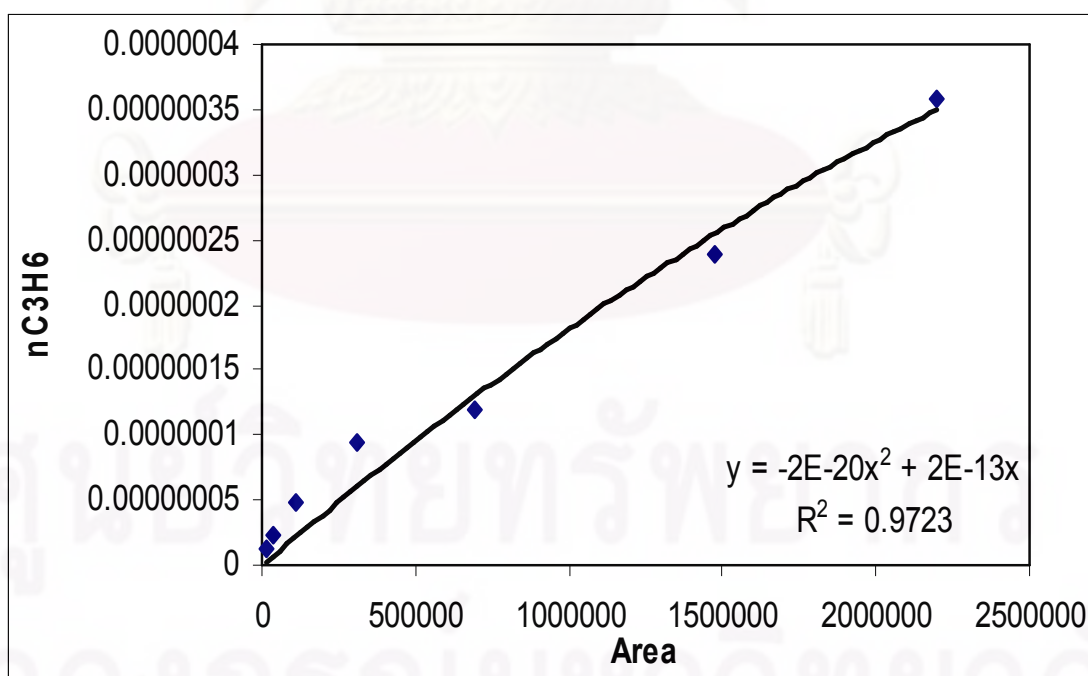
### H-4. ETHENE CALIBRATION CURVE



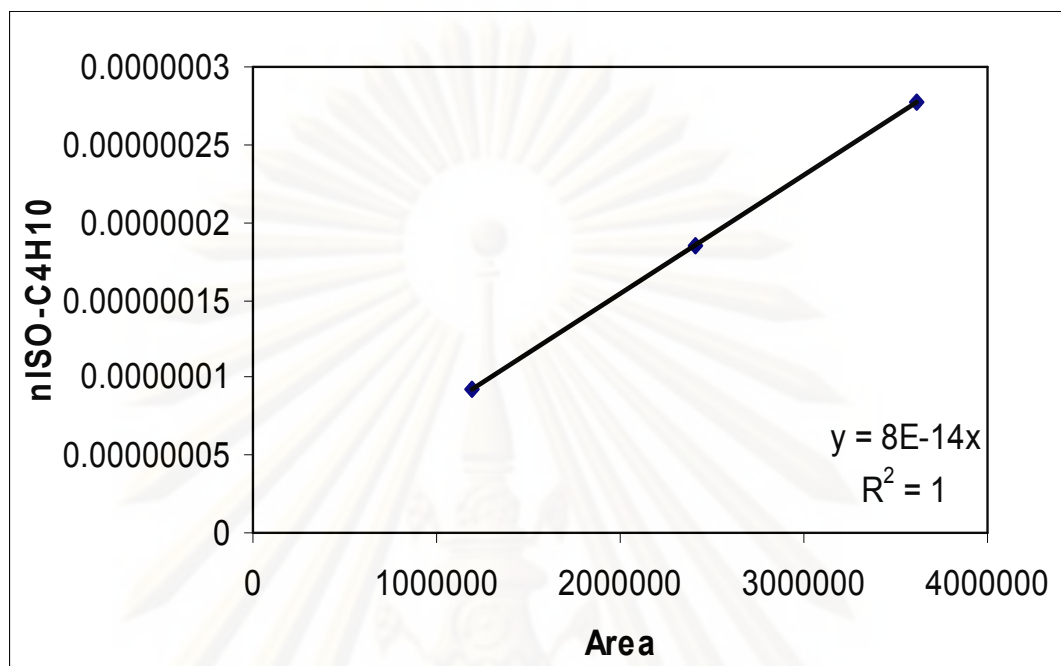
### H-5. PROPANE CALIBRATION CURVE



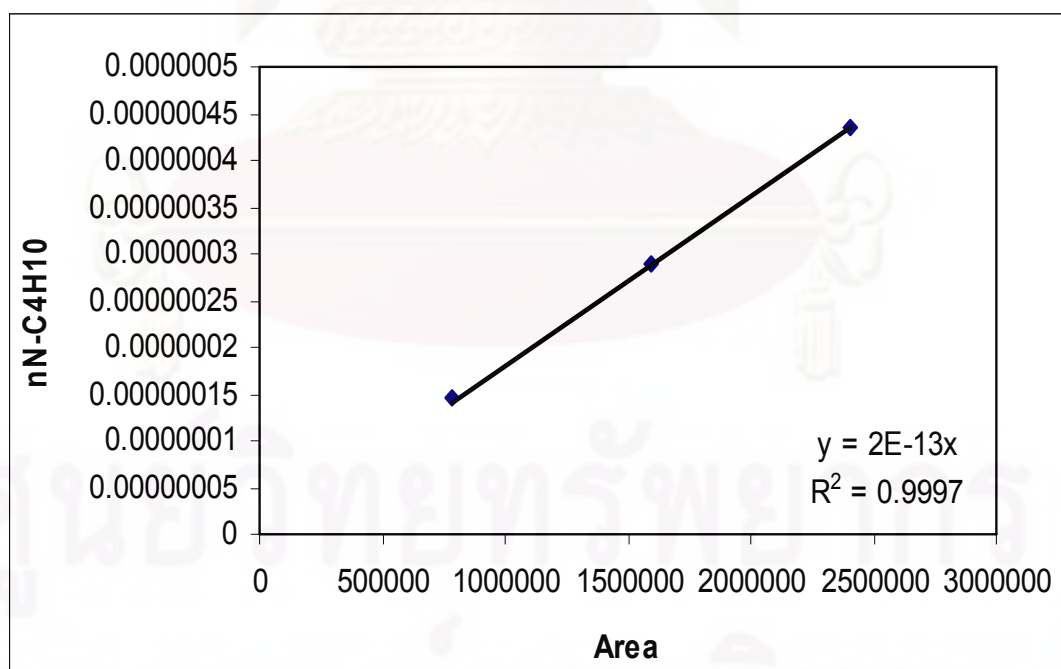
### H-6. PROPENE CALIBRATION CURVE



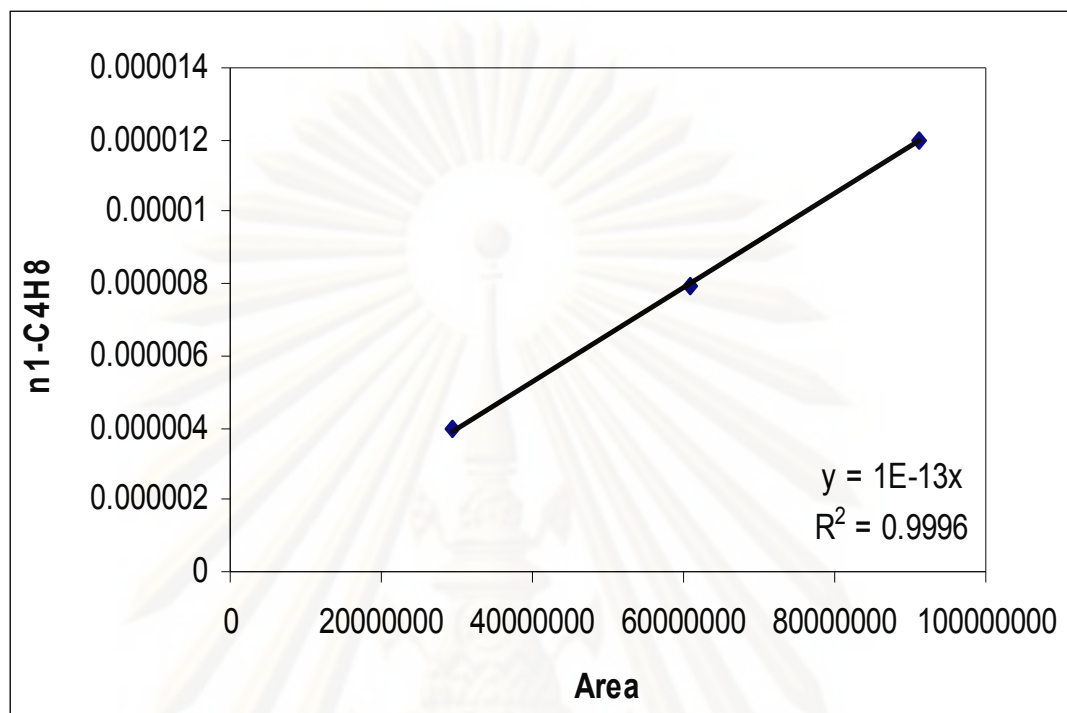
### H-7. ISO-BUTANE CALIBRATION CURVE



### H-8. N-BUTANE CALIBRATION CURVE





**H-9. BUTENE CALIBRATION CURVE**

ศูนย์วิทยทรัพยากร  
จุฬาลงกรณ์มหาวิทยาลัย

## APPENDIX I

### CALCULATION OF ACIDITY

Calculation of total acidity.

Total acidity is calculated from the NH<sub>3</sub>-TPD profiles as the following step.

The NH<sub>3</sub>-TPD profiles:

- Under area of the NH<sub>3</sub>-TPD profiles of the sample = A
- The mole of NH<sub>3</sub> was calculated from the calibration curve of NH<sub>3</sub> as formula:

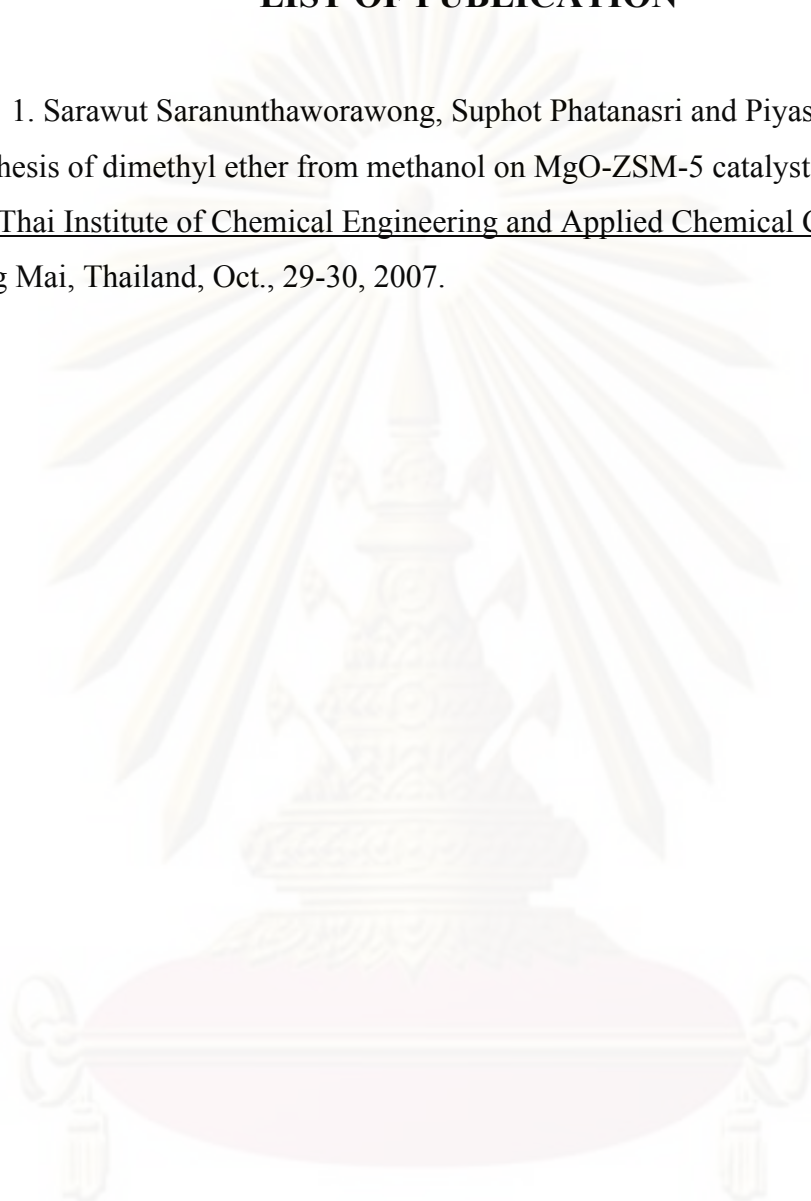
The mole of NH<sub>3</sub> of the sample = 0.0003×A mole.

- Amount of sample = B g.

The total acidity of sample =  $\frac{\text{The mole of NH}_3 \text{ of the sample}}{\text{Amount of dry catalyst}}$   
 $= \frac{0.0003 \times A}{B}$  mol NH<sub>3</sub>/g catalyst

**APPENDIX J****LIST OF PUBLICATION**

1. Sarawut Saranunthaworawong, Suphot Phatanasri and Piyasarn Prasertdam, “ Synthesis of dimethyl ether from methanol on MgO-ZSM-5 catalyst ”, Proceeding of the Thai Institute of Chemical Engineering and Applied Chemical Conference 17<sup>th</sup>, Chiang Mai, Thailand, Oct., 29-30, 2007.



ศูนย์วิทยทรัพยากร  
จุฬาลงกรณ์มหาวิทยาลัย

## VITA

Mr.Sarawut Saranunthaworawong was born on June 18, 1984 in Bangkok, Thailand. He received the Bachelor's Degree of Engineering from the Department of Chemical Engineering, King Mongkut's University of Technology Thonburi(KMUTT) in 2006, He continued his Master's study at Chulalongkorn University in 2006.



ศูนย์วิทยทรัพยากร  
จุฬาลงกรณ์มหาวิทยาลัย